KAISA YLÄNEN

Novel Imaging Methods and Biomarkers in the Screening of Late Cardiac Effects After Childhood Cancer

■

ACADEMIC DISSERTATION
To be presented, with the permission of
the Board of the School of Medicine of the University of Tampere,
for public discussion in the Jarmo Visakorpi Auditorium
of the Arvo Building, Lääkärinkatu 1, Tampere,
on May 29th, 2015, at 12 o'clock.

UNIVERSITY OF TAMPERE

KAISA YLÄNEN

Novel Imaging Methods and Biomarkers in the Screening of Late Cardiac Effects After Childhood Cancer

Acta Universitatis Tamperensis 2051
Tampere University Press
Tampere 2015

UNIVERSITY
OF TAMPERE

ACADEMIC DISSERTATION
University of Tampere, School of Medicine
Tampere University Hospital, Department of Pediatrics
National Graduate School of Clinical Investigation
Finland

Supervised by
Docent Kim Vettenranta
University of Helsinki
Finland
MD, PhD Tuija Poutanen
University of Tampere
Finland

Reviewed by
Docent Tiina Ojala
University of Helsinki
Finland
Docent Ulla Wartiovaara-Kautto
University of Helsinki
Finland

Cover design by
Mikko Reinikka

Distributor:
verkkokauppa@juvenesprint.fi
https://verkkokauppa.juvenes.fi

Acta Universitatis Tamperensis 2051
ISBN 978-951-44-9791-9 (print)
ISSN-L 1455-1616
ISSN 1455-1616

Acta Electronica Universitatis Tamperensis 1541
ISBN 978-951-44-9792-6 (pdf)
ISSN 1456-954X
http://tampub.uta.fi

Suomen Yliopistopaino Oy – Juvenes Print
Tampere 2015

A smooth sea never made a skilled mariner

Contents

List of original publications

This thesis is based on the following four original publications, referred to in the text by their Roman numerals I-IV. Some additional unpublished data are also presented.

I Ylänen K, Poutanen T, Savikurki-Heikkilä P, Rinta-Kiikka I, Eerola A, Vettenranta K. Cardiac magnetic resonance imaging in the evaluation of the late effects of anthracyclines among long-term survivors of childhood cancer. Journal of the American College of Cardiology 2013; 61(14):1539-1547. doi: 10.1016/j.jacc.2013.01.019.

II Ylänen K, Eerola A, Vettenranta K, Poutanen T. Three-dimensional echocardiography and cardiac magnetic resonance imaging in the screening of long-term survivors of childhood cancer after cardiotoxic therapy. American Journal of Cardiology 2014; 113(11):1886-1892. doi: 10.1016/j.amjcard.2014.03.019.

III Ylänen K, Poutanen T, Savukoski T, Eerola A, Vettenranta K. Cardiac biomarkers indicate a need for sensitive cardiac imaging among long-term childhood cancer survivors exposed to anthracyclines. Acta Paediatrica 2015; 104(3):313-319. doi: 10.1111/apa.12862.

IV Ylänen K, Eerola A, Vettenranta K, Poutanen T. Evaluation of the longitudinal cardiac function with speckle tracking echocardiography-based annular displacement in anthracycline-exposed survivors of childhood cancer. Submitted.

Abstract

Background: As a result of steady development over 80% of patients will survive childhood cancer. As these survivors have a long life expectancy, efforts are being made to minimize treatment-related long-term effects. Anthracycline-induced cardiomyopathy may not become symptomatic until years after exposure. Advances in cardiac imaging provide us with new, more sensitive methods for the necessary screening.

Aims: The aims of this study were, firstly, to evaluate the incidence and prevalence of treatment-related, and especially anthracycline-induced cardiotoxicity using modern cardiac imaging and biomarkers among childhood cancer survivors (CCSs) treated in the modern era, and secondly, to assess whether new cardiac diagnostic techniques offer any advantage over the conventional methods in screening for anthracycline-induced cardiotoxicity.

Subjects and methods: A total of 76 anthracycline-exposed CCSs comprising 42 females and 34 males, treated between 1993 and 2006, participated in this study. Their status was assessed at a mean age of 14.3 (range 7.2–20.0) years and after a median follow-up time of 7.1 (range 5.0–18.0) years after the end of the primary cancer therapy. Their median cumulative anthracycline dose was 224 (range 80–454) mg/m^2. Of the survivors, 10 (13%) had also been exposed to cardiac irradiation. Study **I** involved 62 survivors who underwent cardiac magnetic resonance (CMR) imaging. Study **II** evaluated 71 CCSs, who underwent left ventricular (LV) real-time three-dimensional echocardiography (RT-3DE), 58 of them also CMR. All subjects in Study **III** were analyzed for serum N-terminal pro-brain natriuretic peptide (NT-proBNP), cardiac troponin I, cardiac troponin T, high-sensitivity cardiac troponin T, and autoantibodies against cardiac troponin (cTnAAbs). In Study **IV**, longitudinal cardiac function was assessed by conventional echocardiography, tissue Doppler imaging (TDI), and speckle tracking echocardiography for tissue motion annular displacement (TMAD) analysis. Studies II and IV used gender-, age-, and body surface area (BSA) -matched healthy controls for the echocardiographic parameters.

Results: In Study **I**, 11/62 (18%) of the survivors had an abnormal left ventricular (LV) and 17/62 (27%) had an abnormal right ventricular (RV) ejection fraction (EF) in CMR. A subnormal LV EF was found in 38/62 (61%), and RV EF in 33/62 (53%). The survivors had a lower CMR-derived LV EF and larger BSA-

indexed LV volumes compared with the age- or gender-specific reference values. Their CMR-derived RV EF was lower and RV end-systolic volume (ESV) larger than the gender- and age-specific reference values. None of the 62 CCSs with CMR had late gadolinium enhancement as a sign of focal fibrosis. In Study **II**, those not exposed to cardiac irradiation had a lower RT3-DE derived LV EF (57% vs. 60%, p = 0.003) as well as a larger BSA-indexed LV ESV (31 vs. 28 ml/m^2, p = 0.001) than their controls. The eight exposed to cardiac irradiation had higher dyssynchrony indices for the 12 segments than their healthy controls (Tmsv12-SD: 1.76% vs. 1.11%, p = 0.008, Tmsv12-Dif: 5.92% vs. 3.85%, p = 0.007). In Study **II**, of the 58 CCSs with all imaging performed, none had abnormal fractional shortening by M-mode, but 6/58 (10%) had an abnormal LV EF by RT-3DE and 45/58 (78%) by CMR. In Study **III**, 4/76 (5%) had an abnormal NT-proBNP, associated with an abnormal LV EF and enlarged LV ESVs by CMR, and risk factors for anthracycline-induced cardiomyopathy. cTnAAbs were detected in 4/75 (5%) of those with low anhtracycline doses associated with an abnormal LV EF and enlarged LV ESVs by CMR. All CCSs had normal cardiac troponin levels by the three different methods used. Study **IV** showed a decreased systolic and diastolic longitudinal function in LV and RV by TDI and TMAD methods compared with the controls. TMAD values describing the LV and RV systolic longitudinal function (MAD mid% and TAD mid%, respectively) were lower among CCSs than controls (15.4% vs. 16.1%, p = 0.049 and 22.5% vs. 23.5%, p = 0.035, respectively). Those exposed to cardiac irradiation had the lowest MAD mid% values compared with the unexposed survivors (13.8% vs. 15.6%, p = 0.031, respectively) or matched controls (16.2%, p = 0.002). The mitral and tricuspid annular midpoint displacements correlated with the CMR- and RT-3DE-derived volumes.

Conclusion: A great proportion of CCSs exposed to anthracyclines with or without cardiac irradiation show signs of impaired systolic and diastolic function in LV and RV in modern imaging. In addition to conventional echocardiography, RT-3DE, TDI, TMAD analysis and NT-proBNP offer additional information on cardiac function and cardiotoxicity. CMR is a useful supplementary tool in cases with a suboptimal acoustic window, or if RV dysfunction is suspected on the basis of symptoms or echocardiography. The majority of CCSs demonstrate signs of cardiotoxicity under sensitive screening. Even while asymptomatic, CCSs remain in need of a regular cardiac follow-up and benefit from active life-style counseling.

Tiivistelmä

Taustaa: Lääketieteen kehityksen tuloksena lapsuusiän syöpien paranemisennuste on yli 80%. Lapsuusiän syövän sairastaneiden pitkästä elinajanodotteesta johtuen hoitojen aiheuttamia pitkäaikaisvaikutuksia pyritään minimoimaan. Antrasykliinin aiheuttama kardiomyopatia voi olla oireeton vuosien ajan. Sydänkuvantamisen kehitys tarjoaa uusia, herkempiä ja käyttökelpoisempia menetelmiä sydänseurantaan.

Tutkimuksen tarkoitus: Tarkoitus oli selvittää lapsuusiän syöpähoitojen aiheuttamien sydänhaittavaikutusten ilmaantuvuus ja esiintyminen nykyaikaisten hoito-ohjelmien mukaan hoidetuilla. Käytimme uusia sydänkuvantamismenetelmiä sekä plasman merkkiaineita ja kohdensimme huomion erityisesti antrasykliiniryhmän lääkkeiden vaikutuksiin. Lisäksi tutkimme, onko uusista menetelmistä hyötyä perinteisiin seulontamenetelmiin verrattuna.

Aineisto ja menetelmät: Tutkimukseen osallistui 76 (42 tyttöä, 34 poikaa) lapsuusiän syövän sairastanutta, joiden syöpä oli hoidettu vuosina 1993–2006, ja jotka olivat hoidoissaan saaneet antrasykliinejä. Osallistujien keski-ikä oli 14.3 (vaihteluväli 7.2–20.0) vuotta, mediaani seuranta-aika 7.1 (5.0–18.0) vuotta ja kumulatiivinen antrasykliini-annos 224 (80–454) mg/m^2. Heistä 10 (13%) oli lisäksi saanut sydämen alueelle kohdistunutta sädehoitoa. Osatyö **I** käsitti 62 henkilöä, joille tehtiin sydämen magneettikuvaus. Osatyössä **II** tehtiin vasemman kammion kolmiulotteinen sydämen ultraäänitutkimus 71 henkilölle, joista 58:lle tehtiin myös sydämen magneettitutkimus. Osatyössä **III** tutkittiin verikokeet B-tyypin N-terminaalisen propeptidin, troponiini T:n, I:n, herkän troponiini T:n ja troponiini-spesifisten autovasta-aineiden määrittämiseksi. Osatyössä **IV** tutkittiin sydämen pitkittäissuunnan toimintaa perinteisen ultraäänen, kudosdopplerin ja *speckle trackingiin* perustuvan, läppärenkaan pitkittäisliikettä kuvaavan *TMAD*-menetelmän avulla. Osatöissä **II** ja **IV** käytimme sukupuoli-, ikä- ja pinta-ala-vakioituja terveitä verrokkeja ultraäänitulosten vertailussa.

Tulokset: Osatyössä **I** todettiin poikkeava ejektiofraktio (EF) vasemmassa kammiossa 11/62 (18%):lla ja oikeassa kammiossa 17/62 (27%):lla. Raja-arvoinen EF todettiin vastaavasti 38/62 (61%):lla ja 33/62 (53%):lla. Tutkittavilla oli matalampi EF molemmissa kammioissa. Vasemman kammion pinta-alaan suhteutetut tilavuudet olivat normaalia suuremmat. Oikeassa kammiossa loppusystolinen tilavuus oli viitearvoihin verrattuna normaalia suurempi. Myöhäistä

gadolinium-tehostumista paikallisen fibroosin merkkinä ei todettu yhdelläkään. Osatyössä **II** todettiin 63:lla tutkittavalla, jotka eivät olleet saaneet sydämeen kohdistunutta sädehoitoa, matalampi vasemman kammion EF (57% vrt. 60%, p = 0.003) ja suurempi pinta-alaan suhteutettu loppu-systolinen tilavuus (31 vrt. 28 ml/m^2, p = 0.001) terveisiin verrattuna. Sydämeen kohdistunutta sädehoitoa saaneilla oli korkeammat dyssynkronia-indeksit 12 segmentin analyysissa terveisiin verrattuna (Tmsv12-SD: 1.76% vrt. 1.11%, p = 0.008, Tmsv12-Dif: 5.92% vrt. 3.85%, p = 0.007). Pitkäaikaisselviytyjistä 58:lle tehtiin kaikki kuvantamistutkimukset, eikä yhdelläkään heistä todettu poikkeavuutta vasemman kammion supistuvuudessa M-mode-menetelmällä tutkittuna. Sen sijaan 6/58 (10%):lla oli poikkeava vasemman kammion EF kolmiulotteisessa ultraäänessä ja 45/58 (78%):lla sydämen magneettitutkimuksessa. Osatyössä **III** 4/76 (5%):lla todettiin poikkeavan korkea B-tyypin N-terminaalinen propeptidin taso yhdistettynä poikkeavaan vasemman kammion EF:oon ja loppu-systoliseen tilavuuteen sekä antrasykliinikardiomyopatian riskitekijöihin. Troponiinispesifejä autovasta-aineita todettiin 4/75 (5%):lla, jotka olivat saaneet melko vähäisiä antrasykliini-määriä. Heillä todettiin kuitenkin poikkeavuutta vasemman kammion EF:ssa ja loppu-systolisissa tilavuuksissa. Kaikilla 76:lla tutkittavalla oli normaalit troponiini-pitoisuudet kolmella eri menetelmällä tutkittuna. Osatyössä **IV** todettiin lapsuusiän syövän sairastaneilla alentunut systolinen ja diastolinen pitkittäistoiminta sekä vasemmassa että oikeassa kammiossa mitraali- ja trikuspidaali-läppärenkaan pitkittäisliikettä kuvaavalla *TMAD*- sekä kudosdoppler-menetelmällä tutkittuna. Vasemman ja oikean kammion systolista pitkittäistoimintaa kuvaavat *TMAD*-arvot (MAD mid% ja TAD mid%) olivat matalammat syövän sairastaneilla terveisiin verrattuna (15.4% vrt. 16.1%, p = 0.049 ja 22.5% vrt. 23.5%, p = 0.035). Sydämeen kohdistunutta sädehoitoa saaneilla oli matalin MAD mid% verrattuna vain antrasykliiniä saaneisiin (13.8% vrt. 15.6% p = 0.031) tai terveisiin verrokkeihin (16.2% p = 0.002). Mitraali- ja trikuspidaali-läppärenkaan pitkittäisliikkeet korreloivat sydämen magneettitutkimuksella ja kolmiulotteisella ultraäänellä mitattujen kammiotilavuuksien kanssa.

Johtopäätökset: Suurella osalla antrasykliineille altistuneista lapsuusiän syövän pitkäaikaisselviytyjistä oli viitteitä sydämen alentuneesta systolisesta tai diastolisesta toiminnasta uusilla kuvantamismenetelmillä tutkittuna, myös ilman sydämeen kohdistunutta sädehoitovaikutusta. Kolmiulotteinen ultraääni, kudosdoppler, *TMAD*-analyysi ja B-tyypin N-terminaalinen propeptidi antoivat lisätietoa sydänhaittavaikutuksista pelkkään perinteiseen ultraäänitutkimukseen verrattuna. Sydämen magneettitutkimus on hyödyllinen lisä, jos ultraääninäkyvyys on riittämätön, tai jos herää epäily oikean kammion toiminnanhäiriöstä. Enemmistöllä pitkäaikaisselviytyjistä on viitteitä sydänhaittavaikutuksista herkillä menetelmillä tutkittuna, vaikka erityisesti sädehoidon käytön vähentäminen näkyy jo tässä

potilasryhmässä. Vaikka tutkitut lapsuusiän syövän sairastaneet olivatkin vähäoireisia, he tarvitsevat säännöllisen sydänseurannan ja hyötyvät sydänterveellisten elintapojen ohjauksesta.

Abbreviations

2DE	two-dimensional echocardiography
3DE	three-dimensional echocardiography
A	atrial peak flow velocity
A`	late diastolic myocardial velocity associated with atrial contraction
ALL	acute lymphoblastic leukemia
BNP	brain natriuretic peptide
BSA	body surface area
CCS	childhood cancer survivor
CMR	cardiac magnetic resonance
cTn	cardiac troponin
cTnAAb	autoantibodies to cardiac troponin
cTnI	cardiac troponin I
cTnT	cardiac troponin T
CW	continuous wave
E	early mitral/tricuspid peak flow velocity
E`	early diastolic myocardial relaxation velocity
ECG	electrocardiography
EDV	end-diastolic volume
EF	ejection fraction
ESV	end-systolic volume
FS	fractional shortening
Gd-CA	gadolinium-chelated contrast agent
hs-cTnT	high-sensitivity cardiac troponin T
LGE	late gadolinium enhancement
LV	left ventricle/ventricular
MAD	mitral annular displacement
MRI	magnetic resonance imaging
NOPHO	the Nordic Society of Pediatric Hematology and Oncology
NT-proBNP	N-terminal pro-brain natriuretic peptide
PSIR	phase-sensitive inversion recovery
PW	pulsed wave
RT-3DE	real-time three-dimensional echocardiography

RV	right ventricle/ventricular
S`	systolic myocardial velocity
SCT	stem cell transplantation
SD	standard deviation
SSFP	steady state free precession
STE	speckle tracking echocardiography
TAD	tricuspid annular displacement
TAPSE	tricuspid annular plane systolic excursion
TDI	tissue Doppler imaging
TMAD	tissue motion annular displacement
Tmsv12/16-Dif	maximum time difference to reach minimum systolic volume between the earliest and latest contracting segments for the 12/16 segments as a percentage of the RR interval
Tmsv12/16-SD	standard deviation of time to minimum systolic volume for the 12/16 segments as a percentage of the RR interval

1. Introduction

The 5-year survival rate in childhood cancer is nowadays over 80% in the USA and Europe [Howlader, N. et al. (eds) SEER Cancer Statistics Review, 1975-2011. National Cancer Institute. Bethesda, MD (online) http://seer.cancer.gov/csr/1975_2011/(2014)], this resulting in a substantial population of relatively young to early middle-aged adults previously exposed to anti-cancer therapy (Gatta et al. 2009). With increasing survival the late effects of pediatric cancer therapy have been the focus of increasing interest.

The dose-related cardiotoxicity of anthracyclines and radiotherapy was recognized decades ago. Anthracycline-induced cardiotoxicity can occur acutely, early or late. Late cardiotoxicity may manifest as subclinical left ventricular (LV) dysfunction or clinical heart failure years, even decades, after cancer therapy and is usually chronic and progressive in nature (Lipshultz et al. 1991).

Adult childhood cancer survivors (CCSs) carry an increased risk of heart failure and pericardial and valvular diseases compared with healthy siblings, and exposure to anthracyclines or radiation therapy to the chest even increases this risk (Mulrooney et al. 2009). Those exposed to both anthracyclines and radiotherapy have the highest risk of symptomatic cardiac events (van der Pal et al. 2012). As CCSs may also be liable to the well-established cardiovascular risk factors (i.e. obesity, hypertension, sedentary life style) the additional burden of cardiovascular morbidity and mortality they face at a younger age is greater than usual. Cardiac disease is the third most common cause of death among long-term CCSs, tailing cancer recurrence and secondary malignancies (Armstrong et al. 2009).

The incidence of subclinical LV dysfunction among long-term CCSs varies between 0% and 57% (Kremer et al. 2002c), and that of symptomatic heart failure between 0% and 16% (Kremer et al. 2002b), depending on the diagnostic method used. Conventional echocardiography remains insensitive in detecting early signs of cardiotoxicity. Many advances have recently been made in the field of cardiac imaging which provide us with more sensitive methods for screening. Three-dimensional echocardiography (3DE) enables an accurate assessment of LV volumes and ejection fraction (EF) (Poutanen et al. 2001; Thavendiranathan et al. 2013), and has become faster and easier to use during the last decade. Tissue Doppler imaging (TDI) measures myocardial tissue velocities and gives information on diastolic and systolic function of the heart (Gorcsan et al. 1996).

The novel speckle tracking echocardiography (STE)–based imaging mode enables the assessment of both left (DeCara et al. 2005) and right ventricular (RV) function (Ahmad et al. 2012). Cardiac magnetic resonance (CMR) is considered a reference method in cardiac imaging, also rendering the examination of RV (Fratz et al. 2009; Haddad et al. 2008) and myocardium (Ordovas and Higgins 2011; Wu et al. 2001) possible, and is independent of the acoustic window.

Serum cardiac biomarkers, including troponins (cTns) (Cardinale et al. 2000) and natriuretic peptides (Sandri et al. 2005) measured during or soon after cancer therapy have been associated with late cardiac events among adults. Nonetheless, their role in the screening of late cardiotoxicity after childhood cancer remains controversial. Also in the field of cardiac biomarkers advances have been made during the past decade. Modern, high-sensitivity cardiac troponin T (hs-cTnT) assays capable of measuring cTn concentrations more than ten-fold lower than those detected with the previous fourth generation assays, were introduced into clinical use during the past 5-6 years (Latini et al. 2007). The role of autoantibodies to cardiac troponin (cTnAAbs) in the pathogenesis of heart disease (Shmilovich et al. 2007) and their involvement in the detection of troponin leakage have also been studied (Eriksson et al. 2005a).

Especially children exposed to cancer therapy with potentially adverse cardiac effects warrant accurate and sensitive cardiac follow-up. Firstly, children are more prone than adults to the cardiotoxic effects of anthracyclines in that these reduce the number of cardiac stem cells playing a key role in myocardial growth (De Angelis et al. 2010). Secondly, CCSs have a longer life expectancy than adult survivors, and may be exposed to further cancer therapy involving additional cardiotoxic elements. Thirdly, CCSs may be exposed to additional, conventional or therapy-related cardiovascular risk factors such as obesity or hypertension at a younger age than normal. The risk of late cardiotoxicity incorporated in pediatric cancer care was already recognized a number of years ago and modifications in treatment protocols have ensued. The toxicity encountered today among long-term survivors reflects toxicity caused by treatment entities no longer in use.

The purpose of this study was to assess cardiac function among long-term survivors of pediatric cancer therapy over a broad spectrum by combining modern imaging with a comprehensive selection of cardiac biomarkers. We sought tools capable of detecting cardiac dysfunction at an early stage and employable in clinical practice for the cardiac follow-up of CCSs in the future.

2. Review of the literature

2.1 Childhood malignancies

Acute leukemia constitutes a quarter and brain tumors a quarter of childhood malignancies. The remaining conditions are solid tumors such as Hodgkin´s disease, non-Hodgkin lymphoma, neuroblastoma, Wilms tumor, osteosarcoma, rhabdomyosarcoma and other more rare malignancies. Acute lymphoblastic leukemia (ALL) is the most common of the childhood malignancies. Around 150 children receive a cancer diagnosis each year in Finland. Nowadays over 80% of these patients will survive (Gatta et al. 2009).

2.1.1 Treatment of childhood cancer

The treatment of childhood cancer may include chemotherapy, radiotherapy, surgery, and in some cases stem cell transplantation (SCT). The mechanism of action of most chemotherapeutic agents is based on the inhibition of cancer cell division. This inhibition is achieved through different pathways with different drugs. Thus, chemotherapy almost invariably involves a combination of drugs. Other mechanisms include the inhibition of angiogenesis. Whichever the primary mechanism, the damage caused by chemotherapeutic agents leads finally to apoptosis of the cancer cells. However, chemotherapeutic agents may also damage normal cells.

Anthracycline chemotherapeutic agents include doxorubicin, daunorubicin, epirubicin and idarubicin. Mitoxantrone belongs to the anthracenedione class of anti-tumor antibiotics, but is related to the anthracycline family. Anthracyclines have a high antineoplastic activity and thus are widely used in the chemotherapy of leukemias, lymphomas, breast cancer and many solid tumors. A majority of CCSs have been exposed to anthracyclines during their treatment.

ALL in children is treated in the Nordic countries according to the protocols of the Nordic Society of Pediatric Hematology and Oncology (NOPHO). The currently employed fifth generation is called the NOPHO ALL-2008 protocol with a cumulative dose of anthracyclines in the standard risk group 80 mg/m^2, in the intermediate risk group 120 mg/m^2 and in the high risk group 240 mg/m^2. Due to

their cardiotoxic effects, the anthracycline doses in the NOPHO ALL protocols have been markedly reduced during the development of the protocols: in the NOPHO ALL 1992 protocol the respective cumulative anthracycline doses were 120 mg/m^2, 240 mg/m^2 and 360 mg/m^2.

Other chemotherapeutic agents commonly used in pediatric oncology include cyclophosphamide, ifosfamide, vincristine, methothrexate, mercaptopurine, etoposide, asparaginase and platinum compounds.

Local radiotherapy is used in some cases in the treatment of solid tumors alongside surgery and chemotherapy. Total body irradiation may be used as pre-treatment before allogeneic SCT. Radiotherapy can also be used as a palliative therapy.

Allogeneic SCT is being used in the treatment of high risk or complicated leukemia or after leukemia relapse. Malignant cells in the bone marrow are destroyed with high-dose chemotherapy and, in some cases, with total body irradiation, and hematopoiesis is reconstituted using donor cells. Autologous stem cell rescue can be used in the treatment of solid tumors.

2.1.2 Cardiac side-effects of chemotherapy and radiotherapy

Anthracyclines

Anthracycline-induced cardiotoxicity is categorized into three classes according to the time of its manifestation (Lipshultz et al. 2013a). Acute cardiotoxicity occurs within the first week following anthracycline exposure, and is usually reversible in the absence of further exposure. Early-onset toxicity manifests within the first year after exposure and may be progressive. Late cardiotoxicity occurs later than one year after treatment and is of chronic and progressive nature. This classification is arbitrary, since these classes are assumed to be different stages of the same disease. The actual toxic insult, which causes the progressive cascade, occurs at the time of anthracycline exposure.

Signs of acute cardiotoxicity include electrocardiographic (ECG) abnormalities, arrhythmias, reversible decline in LV function and peri/myocarditis (Creutzig et al. 2007; Lipshultz et al. 2013a; Nakamae et al. 2005). Early and late cardiotoxicity are probably a continuum of acute toxicity, since cardiac troponin T (cTnT) release during cancer treatment has been associated with echocardiographic abnormalities years later (Lipshultz et al. 2012b).

Late cardiotoxicity manifests as asymptomatic LV dysfunction or resembles dilating or restrictive cardiomyopathy, and may lead to terminal cardiomyopathy (Levitt et al. 2009). Symptoms may develop gradually as non-specific fatigue or a minor decrease in tolerance of exercise, or manifest abruptly with additional stress such as severe infection or pregnancy.

The precise mechanism of anthracycline-induced cardiotoxicity remains uncertain, but oxidative stress is thought to be a major contributor to myocardial injury (Chen et al. 2006; Octavia et al. 2012; Sarvazyan 1996). The formation of anthracycline-iron complexes increases reactive oxygen species, causing lipid peroxidation and damage to cellular membranes. Due to limited antioxidant defences against reactive oxygen species, myocytes are more vulnerable to oxidative stress than other tissues and organs. Anthracyclines induce damage at multiple sites of cardiac metabolism, and also affect mitochondrial structure and function through several pathways (Octavia et al. 2012; Tokarska-Schlattner et al. 2006). The anthracyclines suppress the synthesis of some cardiac proteins (Jeyaseelan et al. 1997), induce proteolysis of titin (Lim et al. 2004), and cause intracellular calcium dysregulation, negatively affecting contractility (Holmberg and Williams 1990). The known cardiotoxic mechanisms of anthracyclines are illustrated in Figure 1.

Topoisomerase 2β enzyme was recently found to be a key mediator of anthracycline-induced cardiotoxicity Anthracyclines cause topoisomerase 2β inhibition, which leads to cardiomyocyte death through DNA damage. Anthracyclines also depress the defence mechanisms against oxidative stress and cause mitochondrial dysfunction through topoisomerase 2β inhibition. (Zhang et al. 2012)

Histologically anthracycline-induced, non-ischemic cellular degeneration shows vacuolization of the sarcoplasmic reticulum, loss and disorganization of myofibrils, swelling of the mitochondria, replacement fibrosis, and myocyte death (Mason et al. 1978; Torti et al. 1986). Anthracyclines also appear to reduce the number of cardiac stem cells participating in myocardial growth during adolescence and to interfere with the replacement of injured cells (De Angelis et al. 2010). Loss of myocytes leads to thinning of the heart walls. The heart can tolerate a mild degree of myocyte loss, but cardiac dysfunction ensues when the functional reserve capacity is exceeded.

The anthracyclines also cause impaired vascular endothelial function and increased aortic stiffness, risk factors for and early signs of cardiovascular disease (Jenei et al. 2013).

The frequency of anthracycline-induced subclinical cardiotoxicity after childhood cancer has varied between 0% and 57% (Kremer et al. 2002c), and that

of clinical heart failure between 0% and 16% (Kremer et al. 2002b) in different studies.

The frequency of anthracycline-induced cardiotoxicity increases with the cumulative anthracycline dose. The estimated cumulative percentage of adult cancer survivors with anthracycline-induced congestive heart failure has been reported to be 5% at a cumulative anthracycline dose of 400mg/m², 16% at 500 mg/m², 26% at 550 mg/m² and up to 48% at 700 mg/m² (Swain et al. 2003). Other risk factors for cardiotoxicity include young age at primary diagnosis (Lipshultz et al. 1991), female gender (Krischer et al. 1997), length of follow-up (Lipshultz et al. 1991; van Dalen et al. 2006), trisomy 21 (Krischer et al. 1997), high-dose cyclophosphamide (Zver et al. 2007), African-American ancestry (Krischer et al. 1997), pharmacogenomics (Blanco et al. 2012; Visscher et al. 2012), hemochromatosis (Lipshultz et al. 2013c), and cranial irradiation (Landy et al. 2013).

No unambiguous diagnostic test exists for the cardiotoxic effects of anthracyclines. Right ventricular endomyocardial biopsy was previously a more commonly used diagnostic approach (Lipshultz et al. 1991; Steinherz et al. 1995), but due to its invasive nature and advances in modern imaging techniques, it is nowadays performed rather seldom and at a late phase of the disease in children with anthracycline-induced cardiomyopathy (Lipshultz et al. 2013a). Despite the high specificity of the endomyocardial biopsy, it is prone to sampling errors and complications and samples present only the local tissue. CMR has replaced endomyocardial biopsy in the diagnosis of many heart diseases during recent years (Yoshida et al. 2013).

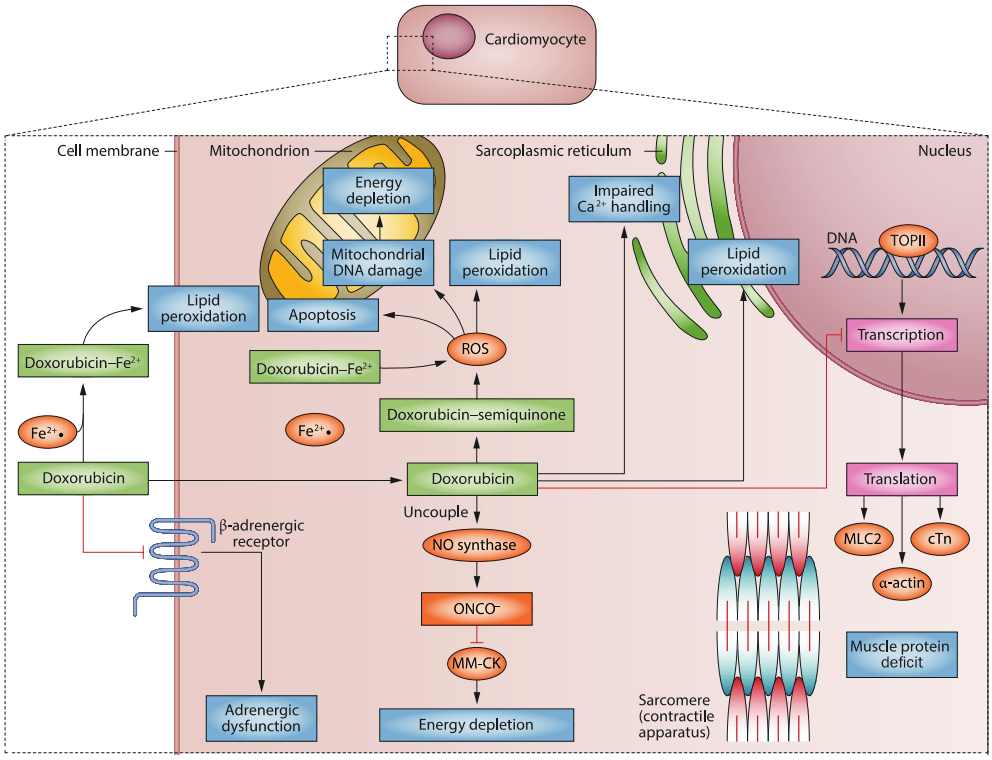

Figure 1. Anthracycline has a range of effects on cardiomyocytes. It induces lipid peroxidation at the cell and mitochondrial membranes, induces apoptosis, mitochondrial DNA damage and energy depletion. Furthermore, it impairs Ca^{2+} processing in the sarcoplasmic reticulum and inhibits the transcription of important muscle elements, weakening the heart muscle. It also downregulates adrenergic receptors and interrupts cell signaling. Abbreviations: cTn, cardiac troponin; MLC2, myosin light chain 2; MM-CK, myofibrillar isoform of the CK enzyme; ROS, reactive oxygen species; TOPII, topoisomerase 2. Reprinted with permission from Macmillan Publishers Ltd [Nat. Rev. Clin. Oncol] (Lipshultz SE et al. 2013b), copyright (2013).

Other chemotherapeutic agents

Of the other chemotherapeutic agents used in children, alkylators (e.g. cyclophosphamide, ifosfamide), cytarabine and cisplatin have also been associated with myocarditis, arrhythmias, LV dysfunction, heart failure and myocardial ischemia (Lipshultz et al. 2013a).

Radiotherapy

Radiotherapy involving the heart can cause a number of complications, including cardiomyopathy, congestive heart failure, pericarditis, myo- and pericardial fibrosis, coronary artery disease, valve abnormalities, conduction disturbances and vascular changes (Lipshultz et al. 2013a). Radiation damage begins with inflammation leading to diffuse interstitial fibrosis through microcirculatory damage (Stewart and Fajardo 1971; Stewart et al. 1995). Increased fibrosis causes myocardial stiffness and a typical cardiomyopathy of restrictive nature (Adams et al. 2004). Diastolic cardiac function appears to be more vulnerable to radiation than systolic (Christiansen et al. 2014).

Cardiac radiation exposure of 15 Gy or more among CCSs has increased the risk of heart failure, myocardial infarction, pericardial disease and valve disease two- to six-fold compared with non-exposed survivors (Mulrooney et al. 2009). Guidelines from the Children`s Oncology Group attach the highest risk to those with doses exceeding 30 Gy with or 40 Gy without anthracyclines. However, even average radiation doses 5 to 20 Gy combined with anthracyclines during childhood increase the relative risk of cardiac failure (Pein et al. 2004). Modern radiotherapy techniques have enabled the fractioning of doses, reduction of the total dose, and a reduction in the volume of the heart being exposed, all resulting in a decline in the incidence of radiation-induced cardiac disease (Schellong et al. 2010). Especially among children the modern cancer treatment protocols aim at diminishing cardiac radiation exposure.

2.2 Cardiac pump function

The heart consists of two separate pumps, LV and RV. Cardiac pump function depends on its ability to fill (diastolic function) and empty (systolic function). Factors influencing pump function include the contractility of sarcomeres, ventricular geometry, function of the valves, loading conditions and heart rate (Fukuta and Little 2008).

The left heart receives blood from the pulmonary veins and pumps well-oxygenated blood to the peripheral organs. The LV has a higher pressure and thicker walls and thus a better response to pressure overload than the RV. Myofibers are arranged in a complex three-dimensional network. The LV walls consist of subepicardial myofibers predominantly left-handedly and longitudinally oriented, mid-wall myofibers oriented circumferentially and subendocardial myofibers mainly right-handedly and longitudinally oriented (Sengupta et al. 2006). The contraction of sarcomeres causes a longitudinal shortening, radial thickening,

circumferential shortening, and apical torsion of the LV resulting in blood ejection (Garcia 2008).

The right compartment receives systemic venous blood from the caval veins and ejects it to the lungs. The RV has a low pressure and thin walls and thus a better response to volume overload than the LV. The RV wall consists of superficial, mainly circumferentially arranged and deep longitudinally oriented myofibers (Haddad et al. 2008). RV contraction consists of a bellows effect produced by inward movement of the free wall and the contraction of the longitudinal fibers (Haddad et al. 2008). LV contraction markedly affects the RV function through a mechanical ventricular interdependence (Santamore and Dell'Italia 1998). In the absence of intracardial shunts LV output equals RV output.

2.2.1 Systolic function

The systole is a period of ventricular contraction when the ventricles empty. It is initiated by an electrical signal delivered into the myocardium. The shortening of the myofibers and sarcomeres leads to the generation of pressure. As a consequence, the intraventricular pressure rises rapidly until it exceeds the atrial pressure, leading to the closure of the mitral and tricuspid valves. When the ventricular pressure exceeds the aortic and pulmonary pressures, the aortic and pulmonary valves open and blood is ejected into the systemic and pulmonary circulations. After the ejection, the pressure of the ventricles falls below that in the aorta and pulmonary artery, leading to the closure of the aortic and pulmonary valves and the end of the systole (Fukuta and Little 2008).

The cardiac output comprises the blood volume ejected during each heartbeat, stroke volume (SV), and heart rate. It is affected by preload, afterload, myocardial contractility, synchrony, and heart rate (Figure 2). Preload depends mainly on the amount of venous blood returning into the heart and the capacity of the ventricle to fill. Afterload is the resistance against which the ventricle contracts (Fukuta and Little 2008) [www.vascularconcepts.com/content/pages.php?pg=patients_cardio_system&page=cardiac_cycle (2015)].

The systolic function of LV and RV can be estimated by EF, which is a ratio of SV to end-diastolic volume. EF can be calculated using volumes derived from two-dimensional echocardiography (2DE), 3DE or CMR. LV systolic function can also be estimated by fractional shortening (FS) with the M-mode (the ratio of the difference of LV end-diastolic and -systolic dimensions to the LV end-diastolic dimension). Due to the shape and geometry of RV, it is difficult to measure the volumes by other than three-dimensional methods. Therefore, change in area is

used for the assessment of RV systolic function. The RV fractional area change is a ratio of the RV systolic area change over the diastolic RV area.

The systolic function of the RV differs from the LV for anatomical reasons. RV is more after-load dependent due to its thinner walls and lower elasticity (Haddad et al. 2008). Furthermore, the RV can better tolerate volume overload due to its higher diastolic compliance (Haddad et al. 2008). The contraction of the RV is sequential, starting from the inflow region and trabeculated apical component and ending in the outflow region (Walker and Buttrick 2013). The most common cause for RV failure is LV failure, again through ventricular interaction (Walker and Buttrick 2013).

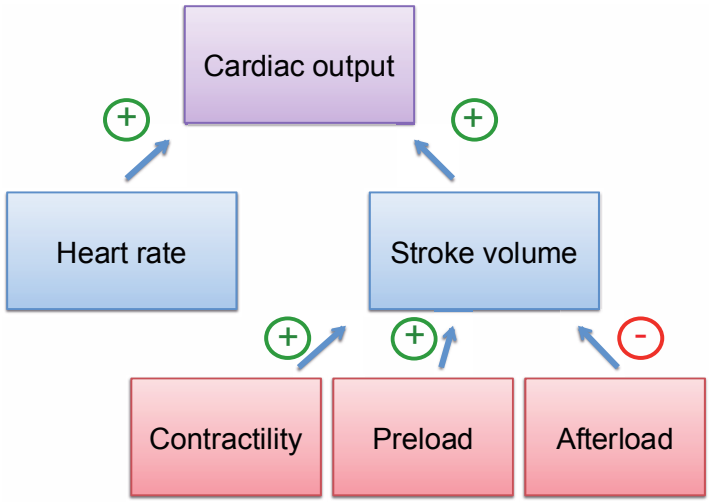

Figure 2. Factors affecting cardiac output.

2.2.2 *Diastolic function*

The diastole is a period of ventricular relaxation when the ventricles fill with blood. It begins when the aortic and pulmonary valves close. When the ventricular pressure falls below the atrial pressure, mitral and tricuspid valves open. Blood flows initially fast from the atria to the respective ventricles, but in mid-diastole only a little blood flow occurs since atrial and ventricular pressure equalize. Finally, the atrial contraction propels the remainig blood into the ventricles. Following atrial relaxation the atrial pressure decreases below the ventricular and the atrio-ventricular valves close. (Fukuta and Little 2008)

Ventricular filling contributes to myocardial relaxation, atrioventricular compliance, atrial systolic function, and pericardial constraint. LV relaxation is an active, energy-dependent process with the myocardium returning to its initial length and tension (Garcia 2008). LV compliance is determined by cellular, extracellular and geometric properties (Garcia 2008). The left atrial contribution to LV filling increases greatly in the case of impaired LV relaxation.

The filling velocities of RV are lower than in the LV. In addition, changes in intra-thoracic pressure during the normal respiratory cycle cause wide variability in RV preload and the respective inflow patterns.

2.2.3 *Ventricular synchrony*

In the normal heart, the ventricular contraction and relaxation are coordinated and homogenous, as a result of electrical and mechanical synchrony. Electrical dyssynchrony is uncommon among children. It is caused by prolonged or inhomogeneous electrical activation of the heart, due to bundle branch block or pacing, and can be diagnosed with prolonged QRS duration in ECG (Friedberg and Mertens 2013).

Mechanical synchrony consists of coordinated function at atrioventricular, interventricular and intraventricular levels (Friedberg and Mertens 2013). Intraventricular dyssynchrony refers to incoordinated contraction between the different segments of the ventricle. It leads to a reduced SV with blood moving around the ventricle from segments activated early to those activated late, resulting in impaired systolic function. Intraventricular dyssynchrony has been detected in children with dilated cardiomyopathy (Chen CA et al. 2009), LV hypertrophy in end-stage renal disease (Kobayashi et al. 2012), and in congenital heart diseases (Ho et al. 2012).

Intraventricular dyssynchrony can be evaluated with echocardiography. M-mode may reveal local septal-posterior wall delay. Color TDI enables the assessment of dyssynchrony data from multiple myocardial segments simultaneously. The RT-3DE method for the evaluation of dyssynchrony is based on the time-volume data derived from full-volume data sets (Kapetanakis et al. 2005).

2.3 Myocardium

Increased LV mass is associated with poor prognosis in many heart diseases. However, a recent study on anthracycline-exposed adults demonstrated a low body

surface area (BSA) -indexed LV mass in CMR to be a predictor of adverse cardiac effects (Neilan et al. 2012). Some echocardiographic studies have shown decreased LV mass and wall thickness among long-term CCSs (Lipshultz et al. 2005; Poutanen et al. 2003b; Rathe et al. 2007). LV mass can be estimated by M-mode (Devereux et al. 1986; Lang et al. 2005), two-dimensional echocardiography (2DE) with area-length method (Schiller et al. 1989; Wyatt et al. 1979), truncated ellipsoid model (Schiller et al. 1983; Schiller et al. 1989), or with the Simpson biplane method (Lang et al. 2005; Vogel et al. 1992), by 3DE (Ojala et al. 2014; Poutanen et al. 2001), or CMR (Katz et al. 1988; McDonald et al. 1992). Three-dimensional imaging methods do not make assumptions regarding LV geometry, and are thus considered to give a more accurate estimate of LV mass than M-mode or 2DE. There are different methods for LV mass indexation for body size related to weight, height or BSA, which cannot be used interchangeably (Simpson et al. 2010). LV mass/(height in meters)$^{2.7}$ has been proposed to be the indexation method most closely approximated to lean body mass (de Simone et al. 1992). However, many CMR reference data for children still use LV mass indexation to BSA (Buechel et al. 2009; Robbers-Visser et al. 2009).

Several pathophysiological mechanisms lead to myocardial fibrosis, a significant increase in the collagen volume fraction of myocardial tissue first affecting the diastolic, and later systolic cardiac function. Myocardial fibrosis is seen in many heart diseases, including cardiomyopathies, myocardial infarction, and heart disease with pressure overload. Three subtypes of fibrosis exist: reactive interstitial, infiltrative interstitial and replacement/scarring fibrosis. Replacement fibrosis develops after myocyte damage or necrosis, and it may have either a localized or a diffuse distribution. Interstitial and infiltrative fibrosis leads to replacement fibrosis at later stages of disease (Mewton et al. 2011). Myocardial fibrosis is associated with an adverse outcome in dilating (Assomull et al. 2006) and hypertrophic cardiomyopathies (Rubinshtein et al. 2010). Interstitial and replacement fibrosis have also been detected histologically in patients with anthracycline-induced cardiomyopathy (Cascales et al. 2013; Lipshultz et al. 1991; Steinherz et al. 1995).

2.4 Echocardiography in the evaluation of cardiac function

Echocardiographic imaging is based on the reflection of ultrasonic waves at the interface between different types of tissues with different acoustic characteristics, for example blood and myocardium. Transthoracic echocardiography is a useful, safe and non-invasive method to evaluate the cardiac structure and function. An

inadequate acoustic window may cause limitations with echocardiography. A variety of echocardiographic modalities exist: 2DE, M-mode, Doppler, TDI, STE and 3DE. With a combination of these modalities it is possible to obtain more and different kinds of information on the heart.

Table 1. Imaging methods used for the evaluation of cardiac function and signs of cardiotoxicity in this thesis.

Method	Abbreviation	Applications	Strengths	Weaknesses	Study
M-mode echocardiography	M-mode	Chamber dimensions, myocardial thickness, FS and LV mass TAPSE	Fast Good temporal resolution	One-dimensional Dependent on LV geometry Does not take into account regional wall motion abnormalities	II, III, IV
Doppler echocardiography	Doppler	Velocities of the atrio-ventricular valve inflows	Fast Assesses diastolic function in LV and RV	One-dimensional Angle- and load-dependent Values vary greatly	IV
Pulsed wave tissue Doppler imaging	PW TDI	Velocities of the myocardium in LV and RV	Fast Assesses diastolic and systolic function in LV and RV	One-dimensional Angle-dependent	IV
Speckle tracking echocardiography – based tissue motion annular displacement	STE (TMAD)	Longitudinal shortening of the LV and RV	Fast Angle-independent Two-dimensional Can also be used in RV	Need for post-processing	IV
Real-time three-dimensional echocardiography	RT-3DE	LV volumes and EF LV dyssynchrony	Good temporal resolution Independent of LV geometry Three-dimensional method Faster than CMR	Dependent on acoustic window Need for post-processing	II, III, IV
Cardiac magnetic resonance imaging	CMR	LV and RV volumes and EF	Independent of acoustic window Good spatial resolution Best method for the RV Assessment of myocardium Three-dimensional method	Expensive Long imaging time (need for sedation) Contrast agent Need for post-processing	I-IV

CMR, cardiac magnetic resonance; EF, ejection fraction; FS, fractional shortening; LV, left ventricle/ventricular; RV, right ventricle/ventricular; TAPSE, tricuspid annular plane systolic excursion.

2.4.1 Two-dimensional echocardiography

2DE enables the assessment of cardiac morphology and function, chamber sizes and spatial relationships in cardiovascular structures. 2DE is one of the main methods to exclude structural abnormalities of the heart.

LV volumes can be measured by the biplane Simpson method of discs derived from apical four- and two-chamber views. The height of the discs is obtained by dividing the total length of the LV cavity (L) by the number of discs (n, usually 20). The volume of the discs is calculated from the radius of discs (ai and bi) obtained from four- and two-chamber views. The LV volumes in the end-diastole and –systole are calculated from the sum of the volumes of the individual discs as follows: $[(\pi/4\ \Sigma(a\text{i} \times b\text{i}) \times L/n]$. In the area-length method, ventricular volumes are calculated from the formula: [5/6 x mid-LV short-axis area x LV length] (Lopez et al. 2010). The EF is calculated from the LV end-diastolic (EDV) and end-systolic (ESV) volumes following [(LV EDV – LV ESV)/LV EDV x 100]. Most children have an excellent acoustic window, and thus LV volumes and EF are easily obtained by 2DE. Measurement of LV volumes and EF by 2DE is included in the complete pediatric echocardiographic evaluation (Lopez et al. 2010).

It is often challenging to obtain optimal views of the RV with 2DE, due to its complex geometry. The systolic function of the RV can be assessed with 2DE by calculating the fractional area change in the apical four-chamber views [(end-diastolic area – end-systolic area)/end-diastolic area] (Lopez et al. 2010).

In the assessment of the global ventricular function, the 2DE-derived EF takes into account a regional dysfunction better than the M-mode, but is dependent on the ventricular geometry and visualization of the blood-endocardium borders. Reference values of the 2DE-derived ventricular volumes for children are available (Franklin et al. 1990; Lytrivi et al. 2011; Vogel et al. 1991). Reference values of RV fractional area change are available for adults but not children (Lang et al. 2005).

2.4.2 M-mode echocardiography

The M-mode echocardiography shows cardiac motion against time, enabling the measurement of dimensions and timing. It is used for the measurement of chamber dimensions and myocardial thickness, assessment of the LV function and the longitudinal motion of the tricuspid valve annulus (TAPSE, tricuspid annular plane systolic excursion), assessment of valve motion, inferior vena cava collapse

and pericardial fluid. The LV internal diameters for fractional shortening (FS) calculation can be obtained from M-mode recordings of either the parasternal long- or short-axis views (Figure 3) (Lopez et al. 2010). BSA–indexed reference values for the M-mode–derived dimensions for infants and children are available (Kampmann et al. 2000). The LV mass can be calculated from the LV dimensions derived from the M-mode (Devereux et al. 1986; Lang et al. 2005). M-mode assumes the LV mass to be symmetric and thus cannot be used in the case of asymmetric mass accumulation. TAPSE measures tricuspid valve lateral annulus longitudinal excursion from the end-diastole to peak excursion. TAPSE is reduced in abnormal RV function.

A disadvantage of the M-mode is its one-dimensional nature. FS does not present the global LV function in that it reflects only the circumferential fiber shortening and does not take into account regional wall motion abnormalities. As the FS is dependent on the LV geometry, M-mode is unreliable with ventricles of abnormal shape (Lang et al. 2005).

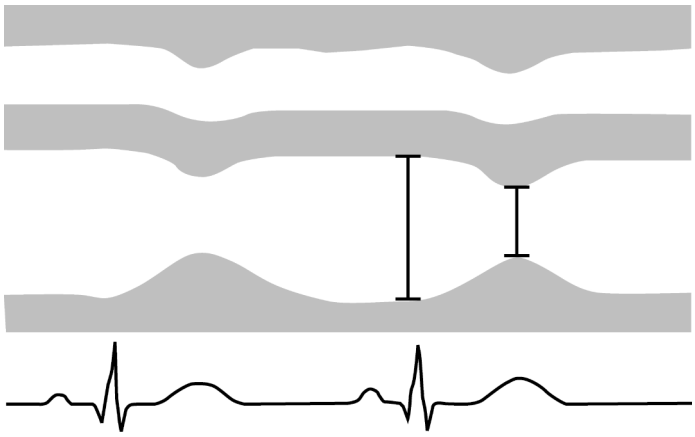

Figure 3. M-mode image of the LV. The longest diameter at the onset of the QRS-complex represents the LV end-diastolic dimension, and the shortest diameter at the maximum downward excursion of interventricular septum represents the LV end-systolic dimension. FS is calculated as follows: [(LV end-diastolic dimension – LV end-systolic dimension)/LV end-diastolic dimension] x 100.

2.4.3 Doppler echocardiography

Doppler echocardiography is based on the detection of the shift in frequency of ultrasound signals reflected from moving objects. It enables the assessment of directions, disturbances and velocities of blood flow. Shunts and valvular lesions can be visualized by the color flow mapping mode. Estimation of pressure gradients and prediction of intracardiac or intravascular pressure can be accomplished using the blood flow velocities obtained with Doppler echocardiography. The pulsed wave (PW) Doppler measures velocities at a specific location within a sample volume, but the maximal detectable velocity is limited. Continuous wave (CW) Doppler is used to detect the highest flow velocities available, but it cannot localize the site of the sampling (Quinones et al. 2002).

PW Doppler analyses of the atrio-ventricular valve inflows are used to assess LV and RV diastolic function, ventricular preload, and atrial and valvular functions. The sample volume is positioned distal to the valve annulus near the tips of the atrio-ventricular valve leaflets in the apical four-chamber view (Quinones et al. 2002). The E wave represents passive filling during early diastole and the A wave that during atrial contraction. Reference values for children are available (Eidem et al. 2004). In normal hearts the E wave is typically higher than A (Lopez et al. 2010). In the early phase of diastolic dysfunction, the mitral inflow tracing represents an abnormal relaxation pattern where the E/A ratio decreases below normal. As the diastolic dysfunction progresses, the mitral inflow tracing shifts to a restrictive pattern with an increasing E and decreasing A wave, and an abnormally high E/A ratio (Quinones et al. 2002). The E wave increases with increasing preload, and Doppler images of the tricuspid inflow vary greatly during normal breathing.

2.4.4 Tissue Doppler echocardiography

TDI uses the same principles as conventional Doppler, but measures the higher-amplitude, lower-velocity signals of the myocardial tissue motion instead of the high-frequency, low-amplitude signals from fast-moving blood cells (Ho and Solomon 2006; Isaaz et al. 1989). TDI gives information on both systolic and diastolic cardiac function. It remains angle-dependent in measuring only motion parallel to the ultrasound beam. It is thus mostly used for assessment of the longitudinal function of the heart. The myocardial velocities are higher at the heart base and decrease to the apex and higher in the lateral ventricular walls than in the interventricular septum (Eidem et al. 2004).

TDI is not able to distinguish passive from active motion and thus the movement of the heart within the thorax cannot be discriminated from the

myocardial movement. The motion of the adjacent myocardial segments affects the myocardial velocities. Also age and ventricular geometry influence the myocardial motion (Eidem et al. 2004). Even though TDI is less load-dependent than the conventional Doppler indices, load changes still affect the myocardial velocities (Abali et al. 2005; Eidem et al. 2005).

Two different TDI methods can be used (Mor-Avi et al. 2011). The PW TDI measures peak myocardial velocities in a specific myocardial segment at a given time and has high temporal resolution. The sample volume is placed within the myocardium of interest parallel to the ultrasound beam. The cardiac cycle consists of three major TDI waveforms: the systolic myocardial peak (S`); early diastolic myocardial relaxation peak (E`); and late diastolic myocardial peak associated with atrial contraction (A`) (Figure 4) (Ho and Solomon 2006). S` is a positive wave above the baseline, E` and A` negative waves below it.

Color TDI measures mean myocardial velocities lower than the peak velocities measured by PW TDI (Mor-Avi et al. 2011). The images need to be post-processed after acquisition. Color TDI combines good temporal resolution with high spatial resolution in the axial direction, enabling measurement of velocity gradients between the myocardial segments. The rate of regional myocardial deformation (strain rate) can be calculated by dividing the difference in the myocardial velocities between two points by the distance between them. Regional strain is the amount of deformation and can be calculated by integrating the strain rate curve over time during the cardiac cycle. Assessment of the synchrony of ventricular contraction is also possible with color TDI, the velocity recordings being made simultaneously in multiple segments (Mor-Avi et al. 2011).

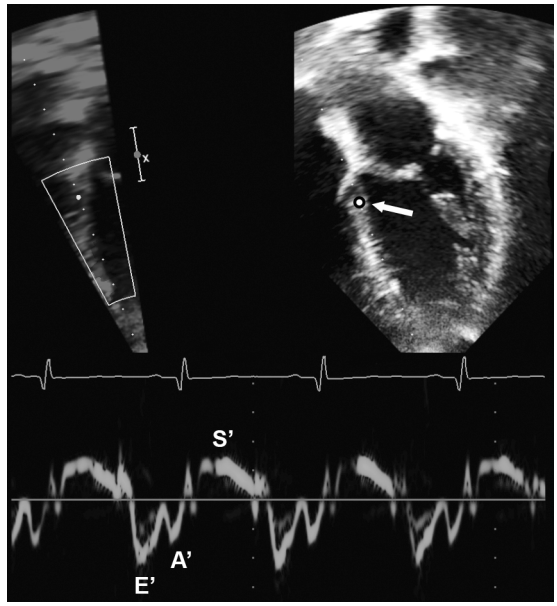

Figure 4. A typical PW TDI tracing from the septal mitral annulus (lower part of the figure). The upper sector represents the site of PW TDI sample volume during measurement (arrow).

2.4.5 Speckle tracking echocardiography

Two-dimensional STE is a fairly new method for assessing myocardial function (Bohs and Trahey 1991). It is an offline technique applied on previously acquired two-dimensional images. The speckles seen in the 2DE images are created by the interference of different ultrasound waves in the myocardium. Each piece of the myocardium scatters the ultrasound waves generating speckles unique for that piece. Blocks of speckles can be tracked from frame to frame, providing displacement information simultaneously from multiple regions (Mor-Avi et al. 2011). Parameters describing myocardial function, such as velocity, strain (describes myocardial deformation) and strain rate (the rate of change in strain) can be derived from this data. Due to the two-dimensional nature of STE, radial and longitudinal strain can be measured simultaneously from the long-axis images and radial and circumferential strain from the short-axis images (Edvardsen et al. 2006).

Assessment of two-dimensional strain by STE is a semi-automatic method. The regions of interest have to be placed and the definition of the myocardium has to be checked manually. STE-based strain analyses are performed on vendor-specific

software packages employing different post-processing algorithms. Thus, for most STE measurements, it is advisable to use consistently the same ultrasound machine and analysis software, until industry standards for these measurements have been established (Koopman et al. 2010a). However, the longitudinal strain has low intra- and inter-observer variability and seems to be reliably measured using different machines and software (Koopman et al. 2010a). Age-specific normative values also for children are available (Marcus et al. 2011), but the system-specific reference values should be used whenever possible.

With the measurement of global longitudinal and/or circumferential strain being time-intensive, several STE-based modalities for an easy assessment of regional strain, annular displacement and LV EF are being marketed (DeCara et al. 2005). The STE-based method for assessing tissue motion annular displacement (TMAD) is a fast and easy means of measuring LV (DeCara et al. 2005) and RV longitudinal function (Ahmad et al. 2012) and TMAD has been shown to correlate with CMR (Ahmad et al. 2012; Tsang et al. 2010).

2.4.6 *Real-time three-dimensional echocardiography*

3DE was developed to overcome the limitations of the M-mode and 2DE related to the LV geometry. Instead of a mental reconstruction using 2DE images, 3DE allows direct visualization of the three-dimensional relationships of complex heart structures and defects.

Efforts to construct a three-dimensional model of the heart date back to the seventies (Dekker et al. 1974). Early three-dimensional datasets were created by merging serial two-dimensional cross-sectional echocardiographic images obtained at different levels or from different angles (Ghosh et al. 1982). The cut planes were obtained using a predetermined linear, fanlike or rotational transducer motion (Vettukattil 2012). The early three-dimensional techniques were both labor-intensive and prone to artifacts caused by the long acquisition time, images acquired during several cardiac cycles, and motion of the patient or probe.

Real-time three-dimensional echocardiography (RT-3DE) was developed in the early 1990s (von Ramm and Smith 1990). Advances in the technology of the transducers, ultrasound systems and computers have enabled processing of the sizeable amounts of data created. Currently used, fully sampled matrix array transducers have almost 3000 active piezoelectric elements to produce true, real-time three-dimensional echo images (Lang et al. 2012). Modern RT-3DE further renders fast acquisition of high-resolution pyramidal volume datasets possible during a single breath-hold, displaying multiple image planes (Mor-Avi et al. 2008).

Image analysis can be performed online or offline with commercially available analysis softwares (Vettukattil 2012).

RT-3DE is used in the clinic for reconstruction of the cardiac morphology and quantification of chamber volume changes (Lang et al. 2012; Mor-Avi and Lang 2009; Vettukattil 2012). It also yields important information on the valves and complex structural heart diseases (Lang et al. 2012; Takahashi et al. 2010; Vettukattil 2012). The time-volume data obtained from RT-3DE full-volume data sets enables the assessment of LV synchronity (Kapetanakis et al. 2005). The standard deviations of times to the minimal volumes in 12 and 16 subvolumes are used as dyssynchrony indices, the latter however being considered the most repeatable index (Ojala et al. 2014).

The term "RT-3DE" is usually, as in this thesis, applied broadly to cover all the modern applications to distinguish them from the reconstructed 3DE images of earlier generations (Yang et al. 2008). A true real-time 3DE produces a narrow sector with a simultaneous ECG recording. This sector is not large enough to cover the whole LV or RV cavity. Thus, a full-volume RT-3DE uses ECG gating to synchronize image portions accumulated over sequential cardiac cycles and is near real-time, the full volume image being available only when the final recorded cycle is complete (Yang et al. 2008). The advantages of ECG gating include larger imaging sectors, higher frame rates and better line density, making it optimal for the volumetric quantification and visualization of larger structures such as the mitral valve. A disadvantage of ECG gating is a stitching artifact caused by an irregular heart rhythm or respiratory variability (Yang et al. 2008).

RT-3DE has been validated against CMR among adults in the assessment of LV mass and volumes with or without wall motion abnormalities (Pouleur et al. 2008). Validation has also been undertaken among healthy children (Bu et al. 2005), those with congenital heart disease (Friedberg et al. 2010), or with a functional single ventricle (Soriano et al. 2008). RT-3DE systematically underestimates ventricular volumes compared with CMR (Bell et al. 2014; Dorosz et al. 2012; Pouleur et al. 2008). Age- and gender-specific RT-3DE reference values for LV volumes and EF are available for adults (Chahal et al. 2012), but for healthy children are still based on an older 3DE technique (Poutanen et al. 2003a). Among children, RT-3DE has been demonstrated to be superior to M-mode and 2DE for the measurement of the LV parameters with CMR as reference (Lu et al. 2008). Normal reference data for RT-3DE dyssynchrony parameters are available for adolescents (Cui et al. 2010; Ten Harkel et al. 2009).

2.5 Cardiac magnetic resonance imaging in the evaluation of cardiac function and fibrosis

CMR is a non-invasive, radiation-free imaging technique with good spatial and temporal resolution enabling visualization of the heart in any plane. It makes possible accurate assessment of the cardiac morphology and dimensions, myocardial function and metabolism, blood flow, myocardial perfusion and tissue characterization (American College of Cardiology Foundation Task Force on Expert Consensus, Documents et al. 2010). Echocardiography is excellent for the visualization of intracardiac anatomy, but CMR is especially useful in the imaging of a congenital heart disease with complex vascular anatomy (e.g. aortic arch anomalies), cardiomyopathies and RV dimensions and function (American College of Cardiology Foundation Task Force on Expert Consensus, Documents et al. 2010; Belloni et al. 2008; Haddad et al. 2008; Helbing et al. 1995).

To avoid movement artifacts the patient should lie still during imaging. Children under school age usually need sedation for CMR. Contraindications for CMR include claustrophobia and magnetic resonance imaging (MRI) incompatible, iron-containing devices. Previously cardiac pacemakers were also a contraindication, but recently MRI-compatible pacemakers have been introduced (American College of Cardiology Foundation Task Force on Expert Consensus, Documents et al. 2010).

2.5.1 Volumes, mass and ejection fraction

Cine images for cardiac volume and mass assessment are currently acquired using a steady state in free precession (SSFP) sequence instead of the previously used gradient echo technique (American College of Cardiology Foundation Task Force on Expert Consensus, Documents et al. 2010). The SSFP technique gives a better distinction between blood and myocardium and yields larger ventricular volumes and lower EF than older methods (Alfakih et al. 2003b; Plein et al. 2001). CMR is usually performed in a magnetic field of 1.5 Tesla. For the measurement of the ventricular volumes and mass, ECG-gated SSFP cine images are acquired during breath-holding or free breathing in several cardiac cycles and the final image is derived from the data thus acquired (Keenan and Pennell 2007). Ten to twelve consecutive slices of 4 to 8 mm thickness covering the ventricles from base to apex in the short-axis view are obtained. The ventricular volumes can also be measured from axial slices (American College of Cardiology Foundation Task Force on

Expert Consensus, Documents et al. 2010; Sarikouch et al. 2010). The RV volumes derived form the axial slices have a better reproducibility than those from short axis slices (Alfakih et al. 2003a; Fratz et al. 2009). The summation of discs method is applied to calculate the ventricular volumes. The EF is calculated from the EDV and ESV derived. The LV mass is calculated as the difference between the LV EVD and ESV multiplied by a specific myocardial density of 1.05 g/ml (Schulz-Menger et al. 2013).

CMR ensures very good accuracy and reproducibility for the measurement of the LV (Cranney et al. 1990; Danilouchkine et al. 2005; Rehr et al. 1985) and RV volumes, mass and EF (Catalano et al. 2007; Jauhiainen et al. 1998; Walsh et al. 2011). It is therefore used as a reference method against which other cardiac imaging modalities are validated (Higgins 1992). However, a semiautomated volume analysis by software often requires manual correction according to endo- and epicardial borders. Reference values for the ventricular volumes, mass and EF obtained with SSFP method are available for both adults (Alfakih et al. 2003b) and children (Buechel et al. 2009; Robbers-Visser et al. 2009; Sarikouch et al. 2010).

2.5.2 *Late gadolinium enhancement*

Myocardial replacement fibrosis can be detected non-invasively with the late gadolinium enhancement (LGE) CMR technique (Kim et al. 1999; Mewton et al. 2011; Wu et al. 2001). Intravenously administered gadolinium-chelated contrast agent (Gd-CA) shortens the tissue T1 relaxation time in proportion to its local concentration, making areas with high gadolinium concentrations brighter in T1-weighted images (American College of Cardiology Foundation Task Force on Expert Consensus, Documents et al. 2010). The typical Gd-CA dose administered is 0.1-0.2 mmol/kg. During the very early phase after administration, Gd-CA penetrates myocardial segments with a normal blood supply, making them hyperenhanced, while segments with an impaired blood supply appear hypoenhanced. During the next phase, Gd-CA washes out from the normal myocardium. A late steady-state phase is reached by 10-15 minutes, when Gd-CA accumulates in the areas of replacement/scarring fibrosis with only little Gd-CA present in the healthy myocardium. Focused T1-weighted inversion recovery scans acquired at this phase show the LGE bright and the normal myocardium black (Assomull et al. 2007b). LGE has been detected in patients with hypertrophic (Moon et al. 2003) and dilating cardiomyopathy (Assomull et al. 2006), acute and chronic myocardial infarction, myocarditis, and severe aortic valve disease (Ordovas and Higgins 2011).

Nephrogenic systemic fibrosis is an extremely rare complication of Gd-CA administration, and thus Gd-CA is contraindicated in renal failure, and seldom used with infants under three months of age (American College of Cardiology Foundation Task Force on Expert Consensus, Documents et al. 2010).

2.5.3 Detection of diffuse fibrosis

The difference in signal intensity between fibrotic and normal myocardium creates the image contrast in LGE CMR. LGE is not applicable in diffuse fibrosis with no normal myocardium as reference (Mewton et al. 2011). The optimal technique for the detection of diffuse fibrosis remains endomyocardial biopsy, invasive and prone to sampling errors (Sado et al. 2011). The CMR methods available for the assessment of diffuse fibrosis are T1 mapping (Messroghli et al. 2003) and equilibrium contrast CMR (Flett et al. 2010).

In the T1 mapping method, T1 is measured at a fixed time after contrast injection. A shorter post-contrast T1 time reflects a greater contrast volume distribution indicative of diffuse fibrosis. The post-contrast T1 times have been demonstrated to correlate histologically with fibrosis (Iles et al. 2008). Limitations to T1 mapping include differences in hematocrit and renal function, both affecting the Gd-CA kinetics (Mewton et al. 2011). Imaging protocols remain to be standardized for Gd-CA doses, acquisition sequences and the time between Gd-CA administration and imaging to ensure comparable studies (Mewton et al. 2011). Age- and gender-specific reference values for T1 mapping are also lacking.

Equilibrium-contrast CMR is a novel method to measure diffuse fibrosis (Flett et al. 2010). A bolus of Gd-CA is followed by a continuous infusion for 45 to 80 minutes to achieve blood-myocardium equilibrium. The hematocrit is taken to measure the blood volume of distribution (1-hematocrit). CMR images are acquired to measure the pre- and post-equilibrium T1. The myocardial volume of distribution calculated from these data reflects diffuse myocardial fibrosis. Equilibrium-contrast CMR has been tentatively validated histologically in patients with aortic stenosis and hypertrophic cardiomyopathy (Flett et al. 2010). The complex imaging protocol makes this method time-consuming and thus challenging.

2.6 Natriuretic peptides

Natriuretic peptides are hormones secreted by the heart and impacting the renal, cardiovascular and endocrine systems. They include atrial natriuretic peptide, brain

natriuretic peptide (BNP) and C-type natriuretic peptide. Under normal conditions BNP is secreted by the atrial myocytes, but upon heart failure the synthesis is shifted to the LV. BNP secretion is stimulated by an increased wall stress caused by volume or pressure overload (Magga et al. 1994), neurohumoral activation (Harada et al. 1998) and hypoxia (Hopkins et al. 2004). A pro-peptide of BNP is cleaved into the biologically active BNP and an inactive split product called N-terminal proBNP (NT-proBNP). The latter is more suitable as a biomarker due to its higher plasma concentration and longer half-life (Pemberton et al. 2000). BNP causes diuresis, natriuresis and vasodilatation, it inhibits fibroblast activation and sympathetic tone, and antagonizes the renin-angiotensin-aldosterone system (Omland and Hagve 2009; Tsuruda et al. 2002).

Normal NT-proBNP levels among children are age-dependent. Neonates have very high NT-proBNP levels, decreasing rapidly within the first few days of life followed by a gradual decline until school age (Nir et al. 2009). The decline in levels is small between the ages 6 to 18 years (Nir et al. 2009). Among the pediatric population no significant gender difference in NT-proBNP values has been reported (Koerbin et al. 2012; Nir et al. 2009).

Plasma BNP and NT-proBNP levels are increased in cardiac pathologies with a pressure or volume overload, but also in renal failure. Increased NT-proBNP levels have been documented in congenital heart disease (Eerola et al. 2010; Eindhoven et al. 2012), dilating (Kim et al. 2013) or hypertrophic cardiomyopathy (Coats et al. 2013), and acute or chronic heart failure (Berin et al. 2014; Hollander et al. 2014), the levels being prognostic (Berin et al. 2014; Coats et al. 2013; Eerola et al. 2010; Kim et al. 2013).

Among adult cancer patients persistently elevated NT-proBNP during chemotherapy has been associated with an impaired LV EF (Romano et al. 2011; Sandri et al. 2005). Concordant findings have been reported for pediatric cancer patients, increased NT-proBNP values during the first three months of chemotherapy being related to abnormal echocardiographic findings four years later (Table 2) (Lipshultz et al. 2012b). In some studies, an increased NT-proBNP measured at late follow-up in childhood cancer survivors has not been associated with abnormal echocardiographic parameters, whereas in others, increased levels have correlated with unfavorable echocardiographic parameters (Table 3). Thus the usefulness of NT-proBNP in the screening of late cardiotoxicity after childhood cancer remains to be established.

Table 2. Studies on NT-proBNP measured during anthracycline therapy in relation to echocardiography among children. Note the differences in the cut-off values and the timing of echocardiography.

Study	n	Age	Cum. ANT dose (mg/m^2)	Cut-off /reference	NT-proBNP	Echocardiography
Ekstein et al. 2007	23, ctrls 54	8 months-23 yrs, median 8 yrs	30-300, median 180	95th percentile of ctrls, 350 pg/ml	NT-proBNP increased only after the first ANT-dose (from 150±112 to 327±321 pg/ml). At least one abnormal value in 16/23	All had normal LV systolic function[a] at 1 to 9 months after therapy
Lipshultz et al. 2012b	75 in doxo-alone and 81 in doxo-dexra group	Mean age doxo-alone 7.7 yrs, doxo-dexra 8.2 yrs	Median 300	<1v. 150 pg/ml, ≥1 v. 100 pg/ml	Any increased levels of NT-proBNP during therapy had 100% in doxo-alone and 86% in doxo-dexra group	Increased NT-proBNP values during the first 90 days of therapy were associated with changes in LV thickness-to-dimension ratio[a] 4 yrs later
Ruggiero et al. 2013	19	14-169 months, mean 6 yrs	240	Age-dependent reference values (Albers et al. 2006)	Reversible increase in NT-proBNP following hyperhydration. Median levels did not change during treatment	All had normal LV systolic[a,b] and diastolic[c] function after ANT-doses, but MPI increased during therapy. All had an abnormal MPI at 20-month follow-up

ANT, anthracycline; ctrl, control; dexra, dexrazoxane; doxo, doxorubicin; LV, left ventricular; MPI, myocardial performance index; NT-proBNP, N-terminal pro-brain natriuretic peptide.
[a]M-mode; [b]two-dimensional echocardiography; [c]Doppler echocardiography

Table 3. Cross-sectional studies on NT-proBNP and echocardiography after anthracycline therapy completion among children. Note the contradiction in respect of the link between abnormal NT-proBNP levels and LV dysfunction by echocardiography.

Study	N	Age	Cum. ANT dose (mg/m²)	Follow-up	Cut-off /reference	NT-proBNP	Echocardiography
Soker and Kervancioglu 2005	31	4-15 yrs, median 8.2 yrs	30-600, median 240	1-42 months	30 healthy ctrls: 47±19 pg/ml	Pts with LV dysfunction 299±265, with normal function 108±132 pg/ml	LV systolic dysfunction[a] in 4/31
Mavinkurve-Groothuis et al. 2009	122	5.0-39.4 yrs, median 21 yrs	50-542, median 180	5.0-28.7 yrs, median 13.8 yrs	Males 85, females 152 pg/ml[b]. Children 97.5th percentile from age-dependent reference values (Albers et al. 2006)	Abnormal in 16/122. All with ANT-dose <120 mg/m² had a normal NT-proBNP. Of pts with ANT-dose ≥300 mg/m², 11/31 had an abnormal level	LV systolic dysfunction in 4/122 [a] and 9/122 [c]. LV dysfunction was not related to abnormal NT-proBNP levels
Mavinkurve-Groothuis et al. 2010	96 of 111 pts had NT-proBNP analyzed	5.6-37.4 yrs, median 20 yrs	50-600, median 180	5.0-29.2 yrs, median 13.2 yrs	Same as above	Abnormal in 16/96, but abnormal NT-proBNP values were not related to lower strain values	Pts had lower two-dimensional strain values and LV systolic function[a,c] than ctrls
Sherief et al. 2012	50	8-16 yrs, mean 11.6 yrs	>300 mg/m² in 64%, <300 mg/m² in 36%	1.5-6 yrs, mean 3.8 yrs	Age-dependent reference values (Albers et al. 2006)	Abnormal in 10/50	Pts with abnormal NT-proBNP had lower FS[a] and larger LV[a] than those with normal NT-proBNP
Lipshultz et al. 2012a	201 (ANT/radiation-exposed 156, unexposed 45)	Exposed 5.9-39.7 yrs, median 17.4 yrs, unexposed 8.0-32.8 yrs, median 23 yrs	Not available	3-32 yrs, median 11 yrs	76 healthy ctrls: 39 pg/ml	Exposed (82 pg/ml) and unexposed pts (69 pg/ml) had higher NT-proBNP than ctrls	Pts had below normal LV mass and wall thickness[a]. Exposed pts had lower LV systolic function[a] and load-dependent contractility than unexposed or ctrls

ANT, anthracycline; ctrl, control; FS, fractional shortening; LV, left ventricular; NT-proBNP, N-terminal pro-brain natriuretic peptide; pt, patient.
[a]M-mode; [b]unit conversion performed 1 pmol/l = 8.475 pg/ml; [c]two-dimensional echocardiography

2.7 Cardiac troponins

The cTn complex consisting of cardiac troponin C, cardiac troponin I (cTnI), and cTnT, is a component of the contractile apparatus of myocardial cells. cTns have an important role in cardiac contraction via regulating the interaction between actin and myosin filaments. cTnI and cTnT are expressed almost exclusively in the heart and have high cardiac specificity.

Cardiomyocyte damage causes cTn release into the circulation, where it appears after 3 to 4 hrs following damage and persists for up to 5 to 14 days (Katus et al. 1989; Katus et al. 1991). In the heart, cTn has an easily accessible cytosolic pool released early after myocardial damage. However, the major part of cTn is located in a structurally bound pool whence it is released later with remodeling of the damaged area (Katus et al. 1991).

A common cause for elevated cTn levels is myocardial infarction, and cTn release is regarded as one of the diagnostic criteria. The universal definition of myocardial infarction defines increased cTn as a level value exceeding that of the 99th percentile of a normal reference population determined for each specific assay (Thygesen et al. 2012). In addition to primary myocardial ischemia, cTn release may be caused by supply-demand imbalance in myocardial ischemia (arrhythmias, cardiomyopathy, hypertension, severe anemia) (Bukkapatnam et al. 2010; Sato et al. 2001), non-ischemic myocardial injury (myocarditis or toxic agents) (Assomull et al. 2007; Lauer et al. 1997; Lipshultz et al. 1997), or by indeterminate myocardial injury (sepsis, heart failure, pulmonary embolus) (ver Elst et al. 2000). Increased cTn in heart failure is associated with an adverse outcome regardless of etiology (Latini et al. 2007; Sato et al. 2001).

One single assay is available for cTnT, but a multitude for cTnI, which are neither standardized nor harmonized, making comparison between assays challenging (Apple 2009). Recently introduced hs-cTn assays allow for the detection of cTn in over half of a normal reference population, thus detecting very minute troponin amounts (Apple et al. 2010; Omland et al. 2009).

Early cTnI release after chemotherapy has predicted further depression in the LV EF among adult cancer patients (Cardinale et al. 2000). The utility of cTns in the detection of anthracycline-induced cardiotoxicity during and after childhood cancer has been extensively investigated. Increased cTn levels during chemotherapy have been associated with later echocardiographic abnormalities (Table 4), but that measured later during follow-up does not seem to add information on the late cardiotoxicity of anthracyclines (Table 5). Despite detectable hs-cTnT levels among adult survivors of childhood cancer having been

associated with poorer LV myocardial function, the role of hs-cTnT in the screening of cardiotoxicity among pediatric age groups remains unestablished (Cheung et al. 2013).

Table 4. Studies on cardiac troponins measured during anthracycline therapy in relation to echocardiography among children. Note that cTn release during therapy was linked to abnormalities in echocardiography at later follow-up.

Study	n	Age	Cum. ANT-dose (mg/m^2)	cTn-method and cut-off	cTn	Echocardiography
Fink et al. 1995	22	1-17 yrs, mean 6.7 yrs	60-460, median 180	cTnT: 0.14 µg/l	Stayed normal	LV systolic function[a] stayed normal
Lipshultz et al. 1997	15	Median 4.4 yrs	45-222, median 60	cTnT: 0.03 µg/l	Low level cTnT elevations during therapy in 6/10. cTnT was normal after therapy	LV systolic function[a] normal after therapy, but peak cTnT predicted LV dilatation and wall thinning 9 months later
Mathew et al. 2001	15	15 months-15.5 yrs, median 5.8 yrs	11.7 mg/kg-375 mg/m^2	cTnI: 0.5 µg/l	One pt had one abnormal cTnI value	LV systolic function[a,b] showed mild decline after malignancy therapy
Kremer et al. 2002a	38	Mean 9.9 yrs	Mean ANT 255 and mitoxantrone 106	cTnT: 0.01 µg/l	An abnormal cTnT in 3/38	LV systolic dysfunction[a] developed in 7/38 after the last ANT-dose, but only 1/7 of them had an abnormal cTnT
Lipshultz et al. 2004	76 in doxo-alone and 82 in doxo-dexra group	Median age doxo-alone 7.3 yrs, doxo-dexra 7.5 yrs	Median 300	cTnT: 0.01 µg/l	More elevated cTnT in doxo-alone group (50%) than in doxo-dexra treated (21%) pts	LV systolic function[a] was depressed in both groups during and after ANT therapy
Clark et al. 2007	30	0.3-16 yrs, median 10 yrs	Doses during study 15-60, median 25. Previous exposure 0-300, median 150	cTnT: 0.01 µg/l	None had detectable cTnT	Was not performed
Lipshultz et al. 2012b	75 in doxo-alone and 81 in doxo-dexra group	Mean age doxo-alone 7.7 yrs, doxo-dexra 8.2 yrs	Median 300	cTnT: 0.0 µg/l cTnI (18 pts): 0.0002 µg/l	This study describes long-term results of previous study (Lipshultz et al. 2004)	Increases in cTnT during the first 90 days of therapy were associated with low LV mass[a] and LV end-diastolic posterior wall thickness[a] 4 yrs later

ANT, anthracyline; cTn, cardiac troponin; cTnI, cardiac troponin I; cTnT, cardiac troponin T; dexra, dexrazoxane; doxo, doxorubicin; LV, left ventricular; pt, patient. [a]M-mode; [b]two-dimensional echocardiography

Table 5. Studies on cardiac troponins and echocardiography after anthracycline therapy among children. Note the normal cTn levels at late follow-up, despite the large anthracycline doses received during therapy.

Study	n	Age	Cum. ANT-dose (mg/m²)	cTn-method and cut-off	Time of sampling	cTn	Echocardiography
Kismet et al. 2004	24	3-31 yrs, median 14 yrs	400-840, median 480	cTnT: 0.01 µg/l detection limit, 0.10 µg/l clinical threshold limit	1-168 months, median 12 months after therapy	3/24 had cTnT ≥ detection limit, but all had it below clinical threshold limit	LV systolic dysfunction[a,b] in 2/24 and diastolic dysfunction[c] in 7/24, not correlating with cTnT
Soker and Kervancioglu 2005	Pts 31, ctrls 30	4-15 yrs, median 8.2 yrs	30-600, median 240	cTnI: 0.5 µg/l	1-42 months after therapy	All pts and ctrls had normal cTnI	LV systolic dysfunction[a] in 4/31
Mavinkurve-Groothuis et al. 2009	122	5.0-39.4 yrs, median 21 yrs	50-542, median 180	cTnT: 0.01 µg/l	5.0-28.7 yrs, median 13.8 yrs after therapy	None had an abnormal cTnT	LV systolic dysfunction in 4/122[a] and 9/122[b]
Sherief et al. 2012	50	8-16 yrs, mean 11.6 yrs	ANT-dose >300 mg/m² in 64% and <300 mg/m² in 36%	cTnT: 0.01 µg/l	1.5-6 yrs, mean 3.8 yrs after therapy	None had an abnormal cTnT	LV systolic dysfunction[a] in 8/50 and abnormal tissue Doppler imaging in 13/50

ANT, anthracyline; cTn, cardiac troponin; cTnI, cardiac troponin I; cTnT, cardiac troponin T; ctrl, control; LV, left ventricular; pt, patient.
[a]M-mode; [b]two-dimensional echocardiography; [c]Doppler echocardiography

2.7 Autoantibodies to cardiac troponins

Autoimmunity is defined as a state in which the immune system erroneously recognizes self-antigens and promotes activation against them, eventually resulting in tissue damage. Factors resulting in the release of cTn may also trigger the formation of cTnAAbs. Autoimmune responses and inflammation are involved in the pathogenesis of many cardiovascular diseases.

Animal models have demonstrated that the induction of an autoimmune response to cTnI induces myocardial inflammation leading to heart failure, and the autoantibodies against cTnI are involved in the development of a dilating cardiomyopathy (Goser et al. 2006; Okazaki et al. 2003). The current consensus on myocarditis holds that in individuals with genetic susceptibility, microbial or non-infectious (toxins, unknown antigens) pathogens cause the primary myocardial damage, which exposes the normally hidden cardiac antigens (including cTns) to the immune system (Caforio et al. 2013). Individuals generating cardiac autoantibodies also develop autoreactive cardiac damage leading to chronic myocarditis with dilating cardiomyopathy or chronic autoreactive cardiomyopathy. However, cardiac autoantibody formation is not always implicated in the pathogenesis of myocarditis.

cTnAAbs have been detected in the serum or plasma of individuals with dilating or ischemic cardiomyopathy (Shmilovich et al. 2007), non-compaction cardiomyopathy (Erer et al. 2013), congestive heart failure (Dungen et al. 2010), and acute coronary syndrome (Pettersson et al. 2009). Adults without known heart disease have also been shown to have low levels of cTnAAbs (Adamczyk et al 2009; Dungen et al. 2010). One study on cTnAAbs in children has been reported, and none of the healthy subjects had cTnAAbs (Eerola et al. 2014). The presence of cTnAAbs has been associated with a poorer outcome after acute myocardial infarction (Leuschner et al. 2008), longer cTnI release after acute coronary syndrome without impact on long-term prognosis (Lindahl et al. 2010), and with improved survival in patients with chronic dilating but not ischemic cardiomyopathy (Doesch et al. 2011). Despite these seemingly conflicting results it is obvious that cTnAAbs may be involved in the pathogenesis of many cardiac diseases. However, their role in anthracycline-induced cardiotoxicity has not thus far been studied.

The presence of circulating cTnAAbs may result in false negative results in the evaluation of cTn levels, thus potentially delaying the diagnosis of myocardial damage (Eriksson et al. 2005a). Consequently, a special cTnI assay has been developed with minimal interference by cTnAAbs (Eriksson et al. 2005b). Several

techniques are used in detecting cTnAAbs, some detecting anti-cTnI and others anti-cTnT autoantibodies, but a gold standard is still lacking (Nussinovitch and Shoenfeld 2010).

2.8 Screening for cardiotoxicity after childhood cancer

Because anthracycline-induced cardiomyopathy may develop years after treatment, and is often preceded by asymptomatic LV dysfunction, screening for cardiotoxicity is recommended for CCSs exposed to potentially cardiotoxic therapy. Evidence-based guidelines for the timing and frequency of cardiac screening among CCSs are still lacking. Long-term follow-up screening guidelines from the Children`s Oncology Group are applied in many centers [http://www.survivorshipguidelines.org/ (2015)] (Landier et al. 2004). The group recommends a more frequent follow-up for those with higher cumulative anthracycline or mediastinal irradiation doses, and/or younger age at exposure. This notwithstanding, even CCSs with a low risk for anthracycline-induced cardiomyopathy should be screened at least every five years. Echocardiography is method-of-choice, but there is no recommendation as to echocardiographic modality (Landier et al. 2004). In the previous era, 2DE and M-mode were the routine methods for the screening, and even radionuclide angiography was utilized (Steinherz et al. 1992). A recent Dutch guideline recommends using FS and/or EF by echocardiography, and radionuclide angiogram as an alternative test, to screen for asymptomatic cardiac dysfunction (Sieswerda et al. 2012). On the other hand, a recent expert consensus for the screening of adult cancer patients recommends RT-3DE and two-dimensional strain imaging in addition to standard transthoracic echocardiography (Plana et al. 2014).

A great number of studies have been published on the incidences of anthracycline-induced cardiotoxicity among CCSs using the older echocardiographic techniques or other imaging. The incidences of asymptomatic LV dysfunction and clinical heart failure have varied greatly, depending on diagnostic method, treatment protocols and follow-up time (Kremer et al. 2002a; Kremer et al. 2002b). In addition to the direct cardiotoxicity of cancer therapy, CCSs may be subjected to additional cardiovascular risk factors including obesity, hypertension or suboptimal physical performance (Hovi et al. 2010), further increasing the risk of cardiovascular disease at a relatively young age. Continuing investigational vigilance is required to elucidate the late effects of the modern

treatment protocols. In addition, information is needed on the utility of new imaging methods in screening for cardiotoxicity.

3. Aims of the study

The aims of the present study were firstly to evaluate the incidence of anthracycline-induced cardiotoxicity using modern diagnostic techniques, and secondly, to evaluate whether the new imaging modalities and biomarkers offer any advantage over conventional methods in the screening of cardiotoxicity among childhood cancer survivors.

The specific aims were as follows:

1. to examine the LV and RV function and signs of focal fibrosis by CMR imaging among long-term survivors of childhood cancer (I)
2. to evaluate the LV function and possible dyssynchrony by RT-3DE (II)
3. to evaluate the suitability of cardiac biomarkers (cTnT, cTnI, hs-cTnT, cTnAAb and NT-proBNP) in the screening of anthracycline-induced cardiotoxicity (III)
4. to assess the putative long-term impact of anthracyclines and radiotherapy on cardiac longitudinal function (IV)

4. Patients and methods

4.1 Patients

4.1.1 Long-term survivors of childhood cancer

CCSs were recruited from the population-based pediatric hematology-oncology service of Tampere University Hospital in Finland between February 2010 and June 2011. Inclusion criteria required anthracyclines (doxorubicin, daunorubicin, epirubicin, idarubicin, mitoxantrone) as a part of cancer therapy, a minimum follow-up of five years and CCS to be in remission. Patients with a hemodynamically significant congenital heart disease were excluded.

Seventy-six out of 86 potentially eligible patients (88%) agreed to participate in the study, 42 (55%) females and 34 (45%) males. Their mean age at study commencement was 14.3 ± 3.1 (range 7.2–20.0) years, median follow-up time from the end of primary therapy 7.1 (5.0–18.0) years, median cumulative anthracycline dose 224 (80–454) mg/m^2 and a mean BSA 1.55 ± 0.31 m^2. Their cancer had been treated between January 1993 and June 2006.

All CCSs were offered a chance to undergo echocardiographic examination and CMR imaging, and to give a blood sample for biomarker analysis. Clinical data on the cancer treatment and medical history were collected from the medical records. The total cumulative anthracycline dose was calculated and dose conversion to doxorubicin isotoxic equivalents made according to the Children`s Oncology Group recommendations using the BSA measured at diagnosis.

4.1.2 Reference children for echocardiography

Altogether 76 healthy children and adolescents were recruited as gender-, age- and BSA–matched controls for the echocardiographic examination. The cohort consisted mainly of the children of hospital personnel or their acquaintances. The reference children had no other heart diseases, but bicuspid aortic valve with normal function was allowed. Their mean age was 14.2 ± 3.2 (range 5.9–20.4) years

and BSA 1.55 ± 0.3 m². CMR imaging or biomarker analyses were not performed on the controls.

4.2 Methods

4.2.1 Clinical examination

Both the CCSs and healthy controls underwent a clinical examination immediately prior to echocardiography. Height and weight were measured and BSA calculated. Examination included assessment of pubertal status, femoral pulses and size of liver, and auscultation of heart and lungs. Blood pressure was measured oscillometrically (Dinamap) from the right arm.

4.2.2 Echocardiographic examination

The study patients lay supine or in left lateral semirecumbent position during the echocardiographic examination. Imaging was done without sedation. One investigator (K.Y.) performed nearly all examinations, while another (A.E.) examined six control children.

Transthoracic echocardiographic examination was made on an iE33 ultrasound machine (Royal Philips Electronics, Philips Healthcare, Bothell, Washington), using an S8-3, S5-1, X3-1 or X5-1 transducer depending on the patient`s size. The two-dimensional, Doppler, M-mode and TDI examinations were made from the standard subcostal, apical and parasternal views according to current recommendations (Lang et al. 2005; Lopez et al. 2010; Mor-Avi et al. 2011). The transducer position was optimized to avoid foreshortening and minimize angulation. The whole LV/RV cavity, walls and apex were meticulously included within two-dimensional echocardiogram cine loops. Three consecutive cardiac cycles were acquired and stored digitally for off-line analysis.

RT-3DE used either an X3-1 or X5-1 matrix-array transducers. The image was optimized to obtain the whole LV in the full-volume data set. The RT-3DE full-volume data sets were acquired from the apical four-chamber views during four consecutive cardiac cycles and normal breathing. At least three data sets were acquired and stored digitally and the set with the highest quality selected for analysis for each patient.

4.2.3 Echocardiographic analysis

A single investigator (K.Y.) performed all the echocardiographic analyses. An average of three cardiac cycles was used in all analyses.

Two-dimensional echocardiography

2DE images were analyzed visually to exclude pericardial fluid and structural abnormalities.

M-mode analysis

Images for M-mode analysis were acquired from the parasternal long axis view. The end-diastolic and -systolic dimensions of the LV, and the end-diastolic and -systolic dimensions of the interventricular septum and posterior wall were measured according to the recommendations of the American Society of Echocardiography (Lang et al. 2005). The parameters derived from the M-mode analysis were expressed as absolute values or standard deviations from BSA-indexed reference values (Kampmann et al. 2000). The FS was calculated from the LV dimensions derived by M-mode.

The M-mode-derived LV mass was calculated according to the American Society of Echocardiography recommendation using the formula: [LV mass = 0.8 x {1.04 [(LV end-diastolic dimension + posterior wall diastolic thickness + septal wall diastolic thickness)^3 – (LV end-diastolic dimension)^3]} + 0.6 g] (Devereux et al. 1986; Lang et al. 2005).

The LV mass/volume ratio was calculated using the LV end-diastolic volume derived from the formula of Teichholz: [LV volume = {7.0/(2.4 + LV end-diastolic dimension) x (LV end-diastolic dimension)^3}] (Teichholz et al. 1976).

The TAPSE was measured from the M-mode tracing acquired from the apical four-chamber view (Kaul et al. 1984; Koestenberger et al. 2009). The total excursion of the junction of the tricuspid valve lateral annulus and the free wall of the RV during systole was measured from leading edge to leading edge.

Doppler echocardiography

The PW and/or CW Doppler recordings and color flow mapping images were analyzed visually to exclude stenosis and regurgitation of valves and intracardiac

shunts. The transmitral and –tricuspid flow velocities were recorded by positioning the sample volume of the PW Doppler between the tips of the mitral/tricuspid leaflets in the apical four-chamber views. The peak velocities of the early (E) and late (A) filling of the mitral and tricuspid inflow were measured from the PW Doppler recordings.

Tissue Doppler echocardiography

TDI was done from the apical four-chamber view with a PW Doppler mode. A narrow angle sector was used to achieve a frame rate exceeding 150/sec, and in most cases, a frame rate over 200/sec was easily achieved. A sample volume of 4 mm was placed at the basal septal and lateral annulus of the mitral valve, at the midventricular septum, as well as at the basal lateral annulus of the tricuspid valve (Mor-Avi et al. 2011). Care was taken to ensure that the sample volume position remained within the region of interest inside the myocardium throughout the cardiac cycle, and the ultrasound beam was aligned as parallel as possible to the corresponding myocardial wall segment. Furthermore, gain, scale, baseline and sweep speed were optimized.

The peak velocities of systolic (S`), early diastolic (E`) and late diastolic motion (A`) were measured directly on the spectral display. The recognition of each peak velocity was based on the direction and timing (ECG) of the wave.

Tissue motion annular displacement analysis

The STE-based TMAD analysis was made from the 2DE cine loops of the LV and RV obtained from the apical four-chamber view (Ahmad et al. 2012; DeCara et al. 2005). A data set was analyzed off-line using the Q-lab workstation (Philips Q-lab, version 9.0; 3DQA; Philips Healthcare, Bothell, Washington, USA). For the LV, three points were placed in a diastolic frame: the basal septal, lateral mitral annulus, and the LV apex. The software automatically tracked the two mitral valve annular points and calculated their absolute displacement towards the LV apex throughout the cardiac cycle. Displacement of annular points (MAD septal and lateral) as well as that of the midpoint of the two (MAD mid) was expressed in millimeters (Figure 5). In order to normalize for LV length, the total midpoint displacement was also expressed as a ratio of the longitudinal ventricle length at the end-diastole (MAD mid%). For the RV, another three points were placed at the septal and lateral tricuspid annulus and the apex and the respective parameters (TAD septal, lateral,

mid and mid%) obtained. The tracking was checked visually and repeated if necessary.

Five LV and one RV study were excluded from the analysis due to inadequate image quality or missing images.

Two investigators (K.Y. and T.P.) measured independently 20 randomly selected data sets for inter-observer and the former independently 20 data sets twice for intra-observer variability.

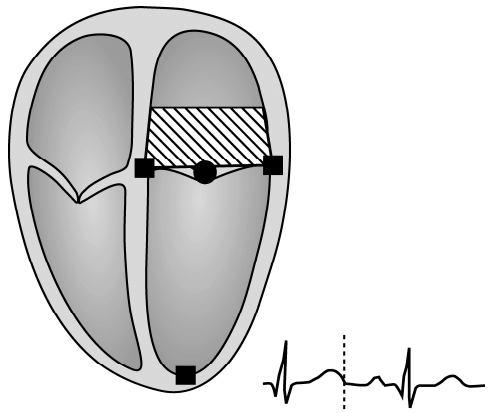

Figure 5. TMAD analyses of the LV. Black squares represent the LV apex (down), basal septal (on the left) and lateral (on the right) mitral annulus. The black circle represents the midpoint of the latter two. The area with oblique lines demonstrates the mitral annular displacement during the cardiac cycle.

Three-dimensional echocardiography analysis

The highest quality RT-3DE data set was selected for analysis. A single investigator (K.Y.) carried out the off-line analysis on a Q-lab workstation (Philips Q-lab, version 8.1; 3DQA; Philips Healthcare, Bothell, Washington, USA). The optimal image planes were adjusted by defining the proper four-chamber view, adjusting three orthogonal views to avoid foreshortening and checking that the intersection of the displayed vertical and horizontal lines lay in the middle of the LV cavity. The frame immediately before the full closure of the mitral valve and with the largest cavity size was selected as end-diastole, and the frame with the smallest cavity size with the mitral valve still closed, as end-systole. Five anatomical landmarks were set in both the end-diastolic and –systolic frames: the septal and lateral mitral annuli in the four-chamber, the anterior and inferior mitral annuli in the two-chamber view, and the LV apex in either of the two. Semiautomated endocardial border detection

was used to track the LV endocardium throughout the entire cardiac cycle. The accuracy of the endocardial border detection was checked and manually corrected if necessary. The software created a three-dimensional dynamic model representing the cardiac cycle in the whole LV cavity and divided it into 16 segments excluding the apex as defined by the American Society of Echocardiography (Cerqueira et al. 2002). The software displayed the LV EDV and ESV, EF, and time-volume data for each segment (Figure 6).

The time to reach the minimum systolic volume for each of the 16 segments was calculated. The dyssynchrony index for the 16 segments (Tmsv16-SD) was defined as the SD of this time as a percentage of the RR interval to correct for differences in heart rate between the subjects (Kapetanakis et al. 2005). The maximum time difference in reaching the minimum regional volume between the segments reaching the volume earliest and latest was calculated as a percentage of the RR interval (Tmsv16-Dif). Corresponding measurements (Tmsv12-SD and Tmsv12-Dif) were also made for the 12 segments (6 basal and 6 middle). The more synchronous the ventricular contraction, the lower the dyssynchrony index obtained.

One RT-3DE study was excluded from the analysis due to inadequate image quality. A stitch artifact in another data set caused its exclusion from dyssynchrony analysis.

Two investigators (K.Y. and A.E.) independently measured 20 randomly selected data sets for inter-observer and the former independently 20 data sets twice for intra-observer variability.

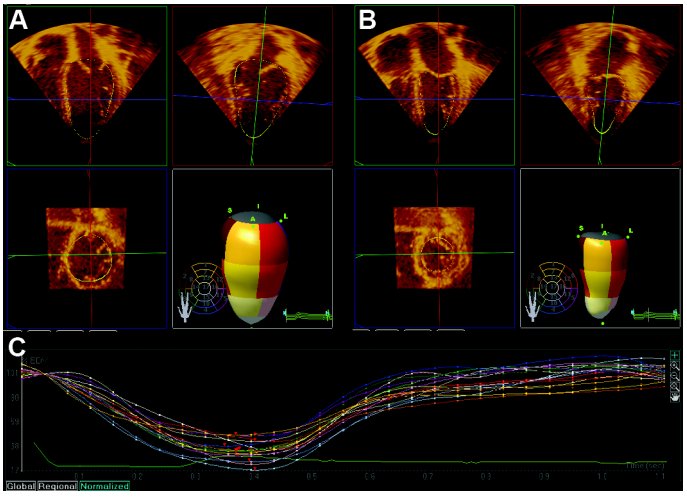

Figure 6. LV volume at end-diastole (A) and end-systole (B) by RT-3DE. Time-volume curves to show the synchronity for 16 cardiac segments (C).

4.2.4 Cardiac magnetic resonance imaging

CMR imaging was performed without sedation in all but one case. Images were acquired during short breath holdings whenever possible, but otherwise during normal breathing.

All examinations were made on a 1.5-T scanner (Siemens Magnetom Avanto; Siemens Healthcare, Enlargen, Germany) according to contemporary recommendations (Kramer et al. 2008). A 6-channel body array coil with a spine coil and ECG-gating were used. Cine TrueFISP slices of 8 mm without any gap from heart apex to valves were obtained in the short-axis plane to analyze the LV and in the axial plane to analyze the RV volumes and function. After injection of gadoterate meglumine (0.1 mmol/kg, Dotarem [Guerbet, Roissy, France]), a five-minute delay was used before obtaining a segmented inversion recovery cine TrueFISP pulse sequence at the midventricular short-axis level for determination of the inversion time (T1) value for nullification of the impact of the normal myocardium. Within the next five minutes, the LGE images were obtained using a TrueFISP gradient echo sequence with a determined T1 (range: 280 to 330 ms) with a slice thickness of 8 mm in the short axis, two-chamber view (vertical long axis), four-chamber view (horizontal long axis), and axial stacks covering the heart from apex to valves. Thereafter, the corresponding views were recovered using a phase-sensitive inversion recovery (PSIR) technique with a constant T1 value of 300 ms. Late-enhancement imaging was performed within 15 min from the beginning of the gadoterate injection.

The analysis was made according to the principles of the current recommendations (Schulz-Menger et al. 2013). In the analysis, ARGUS software (Siemens AG, Munich, Germany) was used. All measurements were done manually. An assessment of the ventricular blood-pool areas was made to identify the end-systolic and -diastolic frames. The LV volumes were calculated from the short axis cine views (Figure 7). The RV volumes were calculated from the axial cine views, the axial slices covering the cavity better than the short axis slices (Figure 7). The aortic outflow track below the valve and the LV portion of the slice in the basal region near the left atrium were included in the LV volume measurements. The same principles were used for the RV. The free papillary muscles were included for both ventricular volumes. The ventricular volumes were calculated as the sum of the ventricular cavity areas multiplied by the slice thickness. The LV and RV SVs and EFs were calculated from the respective end-diastolic EDV and ESVs. The LV mass was calculated as the difference between the epi- and endocardial contours multiplied by slice thickness and using the specific gravity of a ventricular mass of 1.05 g/ml.

Two radiologists (P.S-H. and I.R-K.) independently analyzed the LGE in the TrueFISP and PSIR sequences. They also independently analyzed 15 randomly selected data sets to evaluate the inter-observer variability of the ventricular volumes. One investigator (P.S-H) measured 15 data sets twice to assess the intra-observer variability.

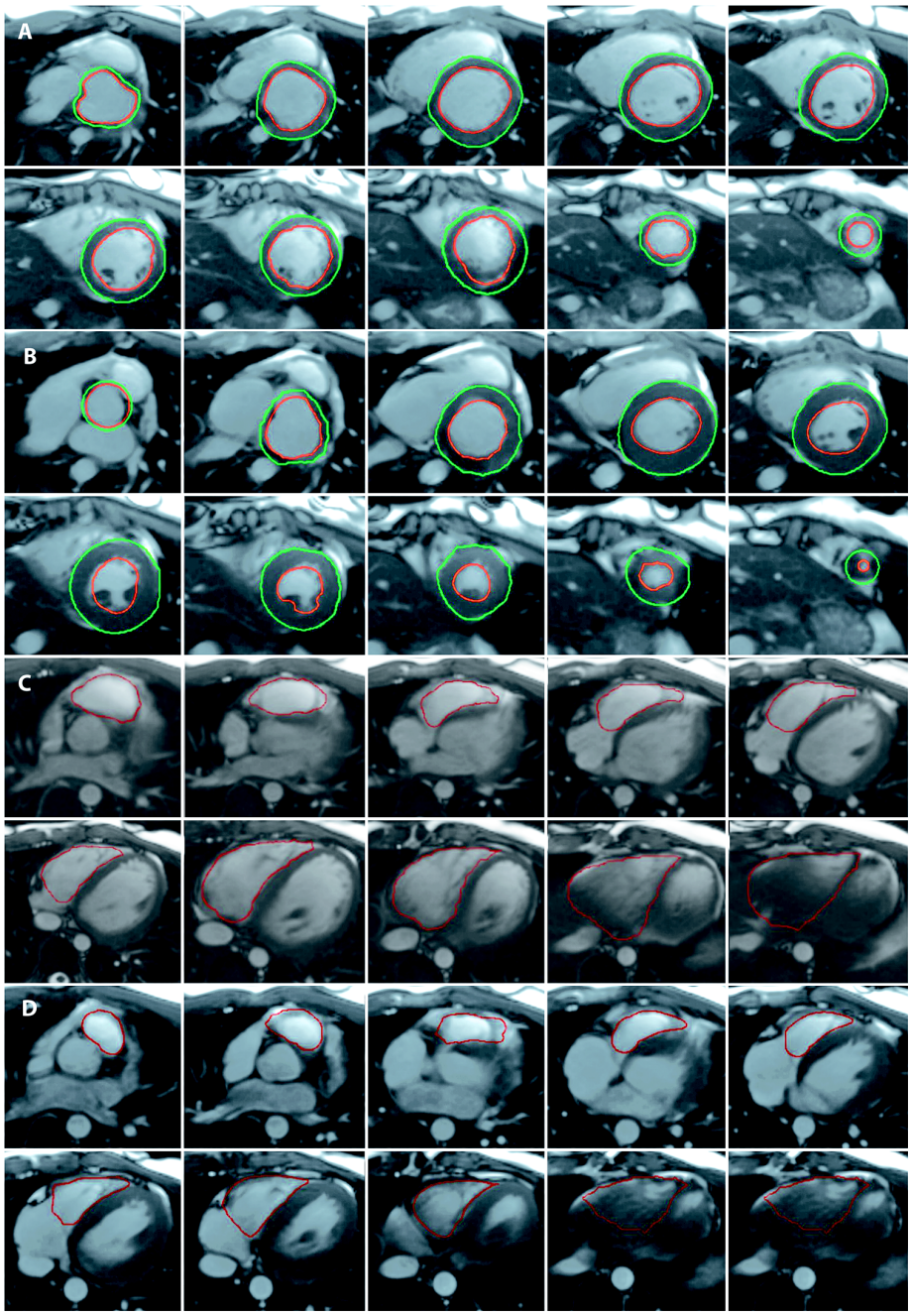

Figure 7. CMR images of LV EVD (A), LV ESV (B), RV EDV (C) and RV ESV (D). Republished with permission from Elsevier Inc., from J Am Coll Cardiol, Ylänen K et al., 61 (14), copyright 2013; permission conveyed through Copyright Clearance Center, Inc.

4.2.5 Biomarkers

Blood samples were obtained by venous puncture. For NT-proBNP and cTnT the samples were taken into a lithium heparin tube with gel, centrifuged at 3000 rpm for 5 minutes and analyzed directly. The samples for other biomarkers were taken into serum tubes, the blood allowed to coagulate for 30 minutes before centrifugation at 2000 G for 10 minutes for serum, subsequently frozen at -70° and analyzed later.

N-terminal pro-B-type natriuretic peptide

Plasma NT-proBNP was determined using an electrochemiluminescence immunoassay method with a Cobas 6000 immunoanalyzer, an e601 module (Roche) and the proBNP II kit (Roche Diagnostics, Mannheim, Germany) with a detection limit of 5 pg/ml. Age-related reference values were used for those younger than 19 years and those <160 pg/ml between ages 6 to 18 years were considered normal (Nir et al. 2009). For patients ≥ 19 years normal values were different for males (< 63 pg/ml) and females (< 116 pg/ml), as suggested by the manufacturer.

Cardiac troponins

Fourth-generation cTnT analysis was made using an electrochemiluminescence immunoassay method with a Cobas 6000 immunoanalyzer, an e601 module (Roche) and the Elecsys Troponin T Cardiac T kit (Roche Diagnostics, Mannheim, Germany). The detection limit was 0.01μg/l and upper normal limit 0.03 μg/l.

Concentrations of cTnI were determined with the Innotrac Aio!™ immunoanalyzer (Radiometer/Innotrac Diagnostics, Turku, Finland) using the Radiometer TnI Test minimally susceptible to interference by the cTnI-specific cTnAAbs known to cause negative interference in many commercial assays (Eriksson et al. 2005a; Savukoski et al. 2012; Tang et al. 2012). The detection limit was 0.0095 μg/l and the measuring range of the assay up to 100 μg/l. All samples were analyzed in duplicate and the results calculated using MultiCalc Software (Perkin-Elmer/Wallac, Turku, Finland).

The fifth-generation hs-cTnT assay was undertaken on an Elecsys 2010 immunoanalyzer (Roche) using the Elecsys Troponin T hs kit (Rohe Diagnostics, Mannheim, Germany) with a detection limit of 5 ng/l and upper normal limit of 14

ng/l. At time of study, the laboratory where the analyses were performed, reported normal hs-cTnT values only as below 14 ng/l, but not the exact values.

Autoantibodies to cardiac troponin

Measurement of human cTnAAbs was made as previously described (Eriksson et al. 2005a; Pettersson et al. 2009). In brief, serum samples were first diluted five-fold with Insulating Layer II (Innotrac Diagnostics Oy, Turku, Finland) and the fluorescence signal subsequently measured from each sample with and without ternary troponin complex (ITC) addition (HyTest Ltd, Turku, Finland), corresponding to a final concentration of 30 μg/l cTnI.

Samples with an ITC-specific signal of 100 counts or higher were regarded as cTnAAb-positive if the p value was <0.05 by t-test when comparing signals from the same serum with and without added ITC.

4.2.6 Statistical methods

The IBM® SPSS® Statistics version 21 (IBM Corp., Armonk, NY, USA) software was used for statistical analysis. The normal distribution of continuous variables was assessed using the Kolmogorov-Smirnov test, visual assessment of the histogram of distribution, and also taking into account the skewness, kurtosis and the similarity of mean and median. Categorical data are presented as frequencies and percentages, normally distributed data as mean ± SD and non-normally distributed data as median and range. The one-sample Student t test was used to compare CMR parameters with published data. Group means were compared between the CCSs and their matched controls by the paired-samples t test. The Mann-Whitney U test was employed for the medians and the independent samples t test for the means among the CCSs. Correlations were assessed with Pearson`s correlation coefficients with data normally distributed and Spearman`s rho test in cases of non-normality. Linear regression analysis was used to establish the predictors for Tmsv16-SD. Univariate analysis of variance was used to study the effect of cardiac irradiation and gender on the NT-proBNP levels. All tests were 2-sided and p values <0.05 considered significant. Intra- and inter-observer variability was assessed by calculating intra-class correlation coefficients or using Bland-Altman analysis (Bland and Altman 1986).

4.2.7 Ethics

This study complied with the Declaration of Helsinki. The institutional review board of Tampere University Hospital approved the study protocol. All study patients, control children and their legal guardians gave their written informed consent.

5. Results

5.1 Characteristics of the study patients

Seventy-six survivors and their gender-, age- and BSA-matched healthy controls constituted the study population. Four survivors had a prior diagnosis of anthracycline-induced cardiomyopathy and were on enalapril, and one in addition was on carvedilol. One survivor had a long QT-syndrome, one an asymptomatic patent ductus arteriosus and one had had a thrombus in the right atrium during primary therapy, but all were asymptomatic. None of the survivors had renal failure. Of the survivors 6 (8%) thought their exercise tolerance to be compromised when compared to peers. Echocardiography revealed a functionally normal bicuspid aortic valve in four controls and a silent ductus in one. The cardiac irradiation dose of those who received local radiotherapy was derived from the radiotherapy planning charts, whereas the dose among those with total body irradiation was estimated to equal the total radiation dose. Of the cardiac irradiation-exposed CCSs, three had received local radiotherapy and ten total body irradiation.

Survivors in studies I-IV all came from the study population of 76 CCSs. Subpopulations in studies I-IV constituted different numbers of study patients, depending on the imaging method or blood test performed and the inclusion criteria of the particular study.

5.1.1 Survivors imaged with CMR (Study I)

Sixty-two survivors agreed to undergo CMR imaging. Their clinical details are presented in Table 6. Three (5%) of them had a prior diagnosis of anthracycline-induced cardiomyopathy. The median average cumulative cardiac irradiation dose of the seven (11%) exposed to cardiac irradiation was 10.0 Gy (3.6–12.0 Gy).

Table 6. The clinical characteristics of the survivors imaged with cardiac magnetic resonance imaging by gender (Study I).

Variable	Females (n = 34)	Males (n = 28)	p value*
Age at study (years)	14.4 ± 3.4	14.9 ± 2.9	0.565
Age at diagnosis (years)	3.8 (0.5–12.6)	4.7 (0.0–13.8)	0.756
Follow-up (years)	7.7 (4.9–13.6)	7.8 (5.0–18.0)	0.804
Cumulative anthracycline dose (mg/m^2)	224 (108–419)	184 (80–416)	0.365
Height (cm)	156.4 ± 14.1	164.2 ± 16.7	0.051
Weight (kg)	51.9 ± 15.2	58.5 ± 18.7	0.133
Body surface area (m^2)	1.49 ± 0.28	1.63 ± 0.34	0.094
Diagnosis			
Leukemia	23 (68)	12 (43)	
Solid tumor	11 (32)	16 (57)	
Type of anthracycline			
Doxorubicin	32 (94)	27 (96)	
Daunorubicin	14 (41)	3 (11)	
Mitoxantrone	6 (18)	1 (4)	
Idarubicin	3 (9)	1 (4)	
Radiotherapy involving heart	6 (18)	1 (4)	
History of relapse	1 (3)	2 (7)	
History of stem cell transplantation			
Allogeneic	3 (9)	1 (4)	
Autologous	2 (6)	2 (7)	

Data are n (%), mean ± SD or median (range).
*Independent samples t test for the means and Mann-Whitney U test for the medians were used in the comparison between genders.

5.1.2 Survivors and controls imaged with RT-3DE (Study II)

Study II comprised seventy-one survivors and their matched controls. Their clinical characteristics are presented in Table 7. Four survivors with anthracycline-induced cardiomyopathy were excluded from this study group, since the focus was on the CCSs without known cardiotoxicity. Echocardiography was not possible in one case with an inadequate acoustic window, and this patient was also excluded from the analysis. For the analysis the survivors were divided into two groups according to cardiac non-exposure (group I)/exposure (group II) to irradiation. Of the survivors, six had received total body irradiation and two local radiotherapy including the cardiac region. Their median average cumulative cardiac radiation dose was 10.0 Gy (range 3.6–12.0). The CCSs in group II had received a greater

cumulative anthracycline dose than those in group I, ($p = 0.001$) (Table 7). Age at diagnosis and follow-up time did not differ between groups I and II (Table 7).

Table 7. Clinical characteristics of the survivors and controls imaged with real-time three-dimensional echocardiography (Study II).

Variable	Group I (n = 63)	Controls II (n = 63)	p value*	Group II (n = 8)	Controls II (n = 8)	p value*	p value**
Gender							
Female	31 (49)	31 (49)		6 (75)	6 (75)		
Male	32 (51)	32 (51)		2 (25)	2 (25)		
Age at study (years)	14.4 ± 3.0	14.2 ± 3.2	0.099	13.2 ± 3.5	13.8 ± 3.4	0.020	0.289
Height (cm)	160.5 ± 15.8	162.3 ± 16.9	0.012	152.4 ± 15.0	153.8 ± 13.0	0.585	0.171
Weight (kg)	55.2 ± 17.4	54.3 ± 16.5	0.147	46.2 ± 13.3	47.3 ± 11.2	0.376	0.164
Body surface area (m^2)	1.56 ± 0.31	1.57 ± 0.31	0.573	1.40 ± 0.27	1.42 ± 0.23	0.435	0.161
Body mass index (kg/m^2)	20.8 ± 3.7	20.1 ± 3.2	0.049	19.4 ± 2.3	19.7 ± 2.1	0.605	0.308
Age at diagnosis (years)	3.8 (0.0–13.8)			5.0 (0.2–12.6)			0.573
Follow-up (years)	7.1 (5.0–18.0)			5.8 (5.0–11.9)			0.178
Cumulative anthracycline dose (mg/m^2)	218 (80–386)			382 (163–454)			0.001
Diagnosis							
Leukemia	34 (54)			6 (75)			
Solid tumor	29 (46)			2 (25)			
Type of anthracycline							
Doxorubicin	63 (100)			5 (63)			
Daunorubicin	21 (33)			2 (25)			
Mitoxantrone	3 (5)			6 (75)			
Idarubicin	0			3 (38)			
Radiotherapy involving heart	0			8 (100)			
History of relapse	1 (2)			3 (38)			
History of stem cell transplantation							
Allogeneic	0			6 (75)			
Autologous	6 (10)			0			

Group I = no cardiac irradiation. Group II = cardiac irradiation. Data are n (%), mean ± SD or median (range).
*Paired samples t test was used for the comparison between survivors and their matched controls; **Independent samples t test for the means and Mann-Whitney U test for the medians were used in the comparison between group I and group II.

5.1.3 Survivors with biomarker analyses performed (Study III)

Blood marker data were obtained from all 76 survivors. The clinical characteristics of these survivors are presented in Table 8. The age at malignancy diagnosis, follow-up time and cumulative anthracycline dose did not differ between female and male survivors (Table 8). Of the females 8 (19%) and of the males 2 (6%) had been exposed to cardiac irradiation.

Table 8. Clinical characteristics of the survivors with biomarker analyses (Study III).

Variable	Survivors (n = 76)	Females (n = 42)	Males (n =34)	p value*
Age at study (years)	14.3 ± 3.1	14.1± 3.2	14.6 ± 3.1	0.542
Height (cm)	159.7 ± 15.6	156.1 ± 14.0	164.1 ± 16.4	0.024
Weight (kg)	54.6 ± 16.9	51.2 ± 14.9	58.8 ± 18.6	0.050
Body surface area (m^2)	1.55 ± 0.31	1.48 ± 0.27	1.63 ± 0.33	0.035
Age at primary diagnosis (years)	3.8 (0.0–13.8)	3.7 (0.2–12.6)	4.7 (0.0–13.8)	0.810
Time from primary diagnosis (years)	9.0 (5.4–18.4)	8.8 (5.4–15.1)	9.1 (5.4–18.4)	0.843
Time from end of primary therapy (years)	7.1 (5.0–18.0)	7.1 (5.0–13.4)	7.8 (5.0–18.0)	0.594
Cum. anthracycline dose (mg/m^2)	224 (80–454)	226 (108–454)	196 (80–416)	0.363
Diagnosis				
Acute lymphoblastic leukemia	33 (43)	21 (50)	12 (35)	
Acute myeloid leukemia	9 (12)	7 (17)	2 (6)	
Neuroblastoma	9 (12)	4 (10)	5 (15)	
Hodgkin disease	8 (11)	4 (10)	4 (12)	
Non-Hodgkin lymphoma	8 (11)	1 (2)	7 (21)	
Rhabdomyosarcoma	2 (3)	0	2 (6)	
Osteosarcoma	1 (1)	1 (2)	0	
Wilms tumor	1 (1)	1 (2)	0	
Ewing	1 (1)	0	1 (3)	
Other	4 (5)	3 (7)	1 (3)	
Type of anthracycline				
Doxorubicin	73 (96)	40 (95)	33 (97)	
Daunorubicin	24 (32)	18 (43)	6 (18)	
Mitoxantrone	9 (12)	7 (17)	2 (6)	
Idarubicin	4 (5)	3 (7)	1 (3)	
Radiotherapy involving heart	10 (13)	8 (19)	2 (6)	
History of relapse	6 (8)	3 (7)	3 (9)	
History of SCT				
Allogeneic	7 (9)	5 (12)	2 (6)	
Autologous	7 (9)	2 (5)	5 (15)	

Data are n (%), mean ± SD or median (range).
SCT, stem cell transplantation.
*Independent samples t test for the means and Mann-Whitney U test for the medians were used in the comparison between genders.

5.1.4 Survivors and controls with analyses on cardiac longitudinal function (Study IV)

Analyses of cardiac longitudinal function were made on 75 survivors and their matched controls. Their clinical characteristics are presented in Table 9. One survivor and her control were excluded from the study group as yielding suboptimal images due to an inadequate acoustic window.

The CCSs were shorter than the controls, but weight and BSA did not differ significantly (Table 9). However, the CCSs had a higher body mass index (BMI) and systolic blood pressure as metabolic risk factors (Table 9).

Table 9. The clinical characteristics of the survivors and controls with cardiac longitudinal function analyzed (Study IV).

Variable	Survivors (n = 75)	Controls (n = 75)	p value*
Female	41 (55)	41 (55)	
Male	34 (45)	34 (45)	
Age at study (years)	14.3 ± 3.1	14.2 ± 3.2	0.875
Height (cm)	159.5 ± 15.6	161.4 ± 16.2	0.004
Weight (kg)	54.5 ± 17.0	53.7 ± 16.0	0.163
Body surface area (m^2)	1.55 ± 0.31	1.55 ± 0.30	0.309
Body mass index (kg/m^2)	20.8 ± 3.7	20.1 ± 3.2	0.028
Systolic blood pressure (mmHg)	118 ± 13	110 ± 16	<0.001
Diastolic blood pressure (mmHg)	64 ± 8	63 ± 7	0.153
Prepubertal	14 (19)	17 (23)	
Diagnosis			
Leukemia	42 (56)		
Solid tumor	33 (44)		
Age at primary diagnosis (years)	3.8 (0.0–13.8)		
Time from end of primary therapy (years)	7.1 (5.0–18.0)		
Cumulative anthracycline dose (mg/m^2)	224 (80–454)		
Radiotherapy involving heart	9 (12)		
History of relapse	6 (8)		
History of stem cell transplantation			
Allogeneic	7 (9)		
Autologous	7 (9)		

Data are n (%), mean ± SD or median (range).
*Paired samples t test was used for the comparison between survivors and their matched controls.

5.2 Cardiac function of childhood cancer survivors measured by cardiac magnetic resonance imaging (Study I)

Due to ethical reasons and resource limitations we were not able to obtain controls for the CMR. We therefore compared the LV and RV volumes and function with reference values deduced from published data. The reference data employed were obtained using the same SSFP imaging method as here. We defined abnormally large ventricular volumes as those exceeding the published mean volumes by at least 2 SD. In accordance with normal clinical practice, we categorized EF as normal (≥ 55%), subnormal (45 ≤ EF <55%) and abnormal (<45%).

5.2.1 Left ventricular volumes, mass and function by cardiac magnetic resonance

For the LV analysis, the data of Robbers-Visser and associates on 60 healthy children aged 8 to 17 years, obtained from short axis slices, were used (Robbers-Visser et al. 2009). We compared the LV parameters in three age groups (8 to 11, 12 to 14, and 15 to 17 years) with the reference data (Table 10) (Robbers-Visser et al. 2009). We also compared the parameters of all females and males with their gender-specific reference values. There were no reference data available for the short-axis LV parameters for children, taking both age and gender simultaneously into account.

The EDVs and ESVs were significantly larger among CCSs in all age groups and both genders compared with reference values. Female CCSs had a higher LV mass compared with reference data, but when comparison was made in the age groups, the LV mass of CCSs did not differ significantly from the reference values. The proportion of abnormally large LV volumes was greater in end-systole than in -diastole (90% vs 29%) (Table 11).

The LV EFs were significantly lower in all age groups and both genders compared with the reference values used. One-fifth had a normal, another fifth an abnormal LV EF and the majority remained within the subnormal range (Table 12).

No objective measurement of physical exercise tolerance was undertaken, but 5/62 (8%) of the CCSs considered their exercise tolerance to be compromised when comparing with peers and had an LV EF <55%. The cumulative anthracycline dose ($r = 0.07$, $p = 0.569$), age at diagnosis ($r = -0.17$, $p = 0.191$) and follow-up time ($r = 0.03$, $p = 0.807$) did not correlate with the LV EF. Nor did the

LV parameters differ significantly between those exposed (n = 7) or unexposed (n = 55) to cardiac irradiation, though the number of study patients is too small for any further conclusions (Table 13).

Table 10. The body surface area-indexed left ventricular parameters per age group or gender by cardiac magnetic resonance compared with reference values by one-sample t-test (Study I). Note low ejection fractions and abnormally large end-diastolic and –systolic volumes of the survivors compared with the reference values.

Variable	Age group	Mean ± SD	Range	Mean ± SD from reference values*	Range from reference values*	p value
LV EF (%)	8 to 11 years *(n = 14)*	52.1 ± 5.2	44.0–61.8	69 ± 5	NA	<0.001
	12 to 14 years *(n = 15)*	51.1 ± 4.3	43.5–58.6	69 ± 5	NA	<0.001
	15 to 17 years *(n = 33)*	49.0 ± 6.0	33.7–61.7	69 ± 5	NA	<0.001
	All girls *(n = 34)*	50.8 ± 4.7	43.5–61.8	69 ± 5	NA	<0.001
	All boys *(n = 28)*	49.5 ± 6.4	33.7–61.7	69 ± 5	NA	<0.001
LV EDV (ml/m²)	8 to 11 years	84.1 ± 13.4	69.4–118.8	71 ± 8	58–87	0.003
	12 to 14 years	89.5 ±11.0	71.4–117.8	78 ± 9	66–97	0.001
	15 to 17 years	91.1 ± 15.8	58.7–131.3	77 ± 12	62–102	<0.001
	All girls	85.5 ± 13.5	58.7–118.8	71 ± 8	58–87	<0.001
	All boys	93.6 ± 14.2	71.4–131.3	79 ± 11	64–102	<0.001
LV ESV (ml/m²)	8 to 11 years	40.3 ± 8.0	29.6–60.5	22 ± 5	15–33	<0.001
	12 to 14 years	43.8 ± 6.2	36.0–52.8	24 ± 5	16–34	<0.001
	15 to 17 years	46.3 ± 9.5	28.9–71.9	25 ± 6	18–39	<0.001
	All girls	41.9 ± 7.3	28.9–60.5	22 ± 4	15–33	<0.001
	All boys	47.3 ± 9.6	33.0–71.9	25 ± 6	16–39	<0.001
LV SV (ml/m²)	8 to 11 years	43.8 ±7.9	31.6–58.2	NA	NA	ND
	12 to 14 years	45.8 ± 7.2	34.8–65.1	NA	NA	ND
	15 to 17 years	44.7 ± 10.2	27.3–71.0	NA	NA	ND
	All girls	43.5 ± 8.4	27.3–65.1	NA	NA	ND
	All boys	46.3 ± 9.5	31.0–71.0	NA	NA	ND
LV mass (g/m²)	8 to 11 years	64.4 ± 13.3	44.0–92.5	59 ± 8	44–84	0.153
	12 to 14 years	68.7 ± 10.1	53.6–91.2	66 ± 11	54–87	0.310
	15 to 17 years	68.2 ± 12.8	50.4–90.9	70 ± 17	42–98	0.417
	All girls	62.7 ± 11.7	44.0–92.5	58 ± 9	42–84	0.024
	All boys	73.2 ± 10.4	53.3–90.0	72 ± 13	52–98	0.555

EDV, end-diastolic volume; EF, ejection fraction; ESV, end-systolic volume; LV, left ventricular; NA, not available; ND, not determined; SD, standard deviation; SV, stroke volume.

*Robber-Visser *et al.* 2009.

Table 11. The proportions of the abnormal ventricular volumes by cardiac magnetic resonance (Study I).

	Females (n = 34)	**Males (n = 28)**
LV EDV[a, c]	18% (6/34)	43% (12/28)
LV ESV[a, c]	82% (28/34)	100% (28/28)
RV EDV[b, c]	15% (5/34)	21% (6/28)
RV ESV[b, c]	41% (14/34)	64% (18/28)
RV SV[b, d]	35% (12/34)	32% (9/28)

EDV, end-diastolic volume; ESV, end-systolic volume; LV, left ventricular; SV, stroke volume; RV, right ventricular. [a]Robbers-Visser 2009. [b]Sarikouch et al 2010. [c]> 2 SD from reference values. [d]< 2 SD from reference values.

Table 12. The proportions of the ejection fractions by cardiac magnetic resonance (Study I).

	Abnormal EF < 45%	**Subnormal 45% ≤ EF ≤ 55%**	**Normal EF > 55%**
Left ventricle	18% (11/62)	61% (38/62)	21% (13/62)
Right ventricle	27% (17/62)	53% (33/62)	19% (12/62)

EF, ejection fraction.

Table 13. Comparison of the ventricular parameters by cardiac magnetic resonance between the survivors exposed or unexposed to cardiac irradiation (Study I).

Variable	Survivors with cardiac irradiation (n = 7)	Survivors without cardiac irradiation (n = 55)	p value*
LV EF (%)	50.6 ± 5.6	50.2 ± 5.6	0.856
LV EDV (ml/m²)	83.6 ± 19.0	89.8 ± 13.6	0.278
LV ESV (ml/m²)	41.1 ± 9.9	44.8 ± 8.6	0.300
LV SV (ml/m²)	42.5 ± 11.2	45.1 ± 8.7	0.474
LV mass (g/m²)	61.7 ± 14.4	68.2 ± 11.9	0.190
RV EF (%)	55.6 ± 9.7	47.1 ± 8.1	0.013
RV EDV (ml/m²)	77.6 ± 15.4	89.2 ± 19.0	0.128
RV ESV (ml/m²)	35.2 ± 13.9	47.4 ± 13.3	0.027
RV SV (ml/m²)	42.4 ± 7.9	41.8 ± 11.2	0.900

EDV, end-diastolic volume; EF, ejection fraction; ESV, end-systolic volume; LV, left ventricular; RV, right ventricular; SD, standard deviation; SV, stroke volume. Values are presented as mean ± SD.
*Independent samples t test was used for the comparison between the groups.

5.2.2 Right ventricular volumes and function by cardiac magnetic resonance

The RV parameters were compared with the data of Sarikouch and associates describing the axial slices from 99 healthy children aged 8 to 20 years (Sarikouch et al. 2010). The comparison with reference values was made in two age groups (8 to 15 and 16 to 20 years) and separately for girls and boys (Table 14). Both genders had larger RV ESVs and smaller SVs compared with the age- and gender-specific reference values. In contrast, only boys aged 16 to 20 years had significantly larger RV EDVs compared with the reference values. The number of abnormally large ventricular volumes was smaller in RV than in LV (Table 11). The proportion of abnormally large RV volumes was greater in end-systole than in -diastole (52% vs 18%) (Table 11). About one-third of both females and males had an abnormally small RV SV (Table 11).

Both genders in both age groups had a significantly lower RV EF compared with reference values. Of the CCSs, 27% had an abnormal RV EF, 53% subnormal, and 19% a normal RV EF (Table 12).

The RV EF did not correlate with cumulative anthracycline dose ($r = 0.01$, $p = 0.963$), age at diagnosis ($r = -0.06$, $p = 0.627$), or follow-up time ($r = -0.21$, $p = 0.108$). CCSs exposed to cardiac irradiation had a higher RV EF and smaller ESV compared with those unexposed, but the number of cardiac irradiation-exposed CCSs was somewhat small (Table 13).

Table 14. The body surface area -indexed right ventricular parameters per gender and age group by cardiac magnetic resonance compared with reference values by one-sample t-test (Study I). Note low ejection fractions and stroke volumes, and abnormally large end-systolic volumes among survivors compared with the reference values.

Variable	Age group	Mean ± SD	Range	Mean ± SD from reference values*	p value
Females	*8 to 15 years (n = 23)*				
(n = 34)	*16 to 20 years (n = 11)*				
RV EF (%)	8 to 15 years	51.2 ± 8.4	26.5–65.4	62.6 ± 3.6	<0.001
	16 to 20 years	47.8 ± 8.9	30.6–64.5	62.1 ± 6.0	<0.001
	All girls	50.1 ± 8.6	26.5–65.4	62.8 ± 4.3	<0.001
RV EDV (ml/m²)	8 to 15 years	84.6 ± 16.3	56.6–113.0	78.3 ± 9.7	0.076
	16 to 20 years	77.8 ± 12.3	56.3–100.2	79.7 ± 10.3	0.629
	All girls	82.4 ± 15.3	56.3–113.0	76.9 ± 12.7	0.043
RV ESV (ml/m²)	8 to 15 years	41.5 ± 11.8	26.0–67.1	29.2 ± 4.6	<0.001
	16 to 20 years	41.2 ± 11.7	20.0–64.0	30.4 ± 6.9	0.012
	All girls	41.4 ± 11.6	20.0–67.1	28.6 ± 5.4	<0.001
RV SV (ml/m²)	8 to 15 years	43.1 ± 10.2	24.3–55.4	49.1 ± 6.8	0.010
	16 to 20 years	36.6 ± 5.6	23.3–43.6	49.3 ± 6.3	<0.001
	All girls	41.0 ±9.4	23.3–55.4	48.2 ± 6.8	<0.001
Males	*8 to 15 years (n = 17)*				
(n = 28)	*16 to 20 years (n = 11)*				
RV EF (%)	8 to 15 years	48.8 ± 6.7	38.0–61.5	62.3 ± 4.3	<0.001
	16 to 20 years	40.6 ± 8.3	28.8–54.7	60.0 ± 4.4	<0.001
	All boys	45.6 ± 8.3	28.8–61.5	61.6 ± 4.5	<0.001
RV EDV (ml/m²)	8 to 15 years	89.6 ± 23.5	60.5–142.3	82.9 ± 12.6	0.256
	16 to 20 years	102.0 ± 14.2	81.8–128.7	90.2 ± 10.9	0.020
	All boys	94.5 ± 21.0	60.5–142.3	84.5 ± 12.7	0.018
RV ESV (ml/m²)	8 to 15 years	45.7 ± 12.4	26.9–66.0	31.3 ± 6.1	<0.001
	16 to 20 years	60.7 ± 12.8	41.8–85.3	36.1 ± 6.3	<0.001
	All boys	51.6 ± 14.4	26.9–85.3	32.5 ± 6.4	<0.001
RV SV (ml/m²)	8 to 15 years	43.9 ± 14.3	28.0–80.6	51.6 ± 8.4	0.042
	16 to 20 years	41.3 ± 9.4	27.0–59.8	54.1 ± 7.3	0.001
	All boys	42.9 ± 12.5	27.0–80.6	52.0 ± 8.4	0.001

EDV, end-diastolic volume; EF, ejection fraction; ESV, end-systolic volume; RV, right ventricular; SV, stroke volume. *Sarikouch *et al.* 2010.

5.2.3 Intra- and inter-observer variability of ventricular volumes measured by CMR

The intra- and inter-observer data for CMR-derived ventricular volumes are presented in Table 15.

Table 15. The inter-observer and intra-observer variability for the ventricular volumes measured by cardiac magnetic resonance.

Variable	Intra-observer variability		Inter-observer variability	
	Mean difference (LOA)	ICC (95% CI)	Mean difference (LOA)	ICC (95% CI)
LV EDV (ml)	4.9 (-20.0/29.8)	0.94 (0.83, 0.98)	-14.7 (-38.0/8.6)	0.98 (0.93, 0.99)
LV ESV (ml)	5.3 (-13.6/24.3)	0.90 (0.72, 0.96)	3.1 (-34.1/40.3)	0.86 (0.63, 0.95)
RV EDV (ml)	0.3 (-35.0/35.6)	0.92 (0.77, 0.97)	-36.3 (-94.3/21.7)	0.72 (0.34, 0.90)
RV ESV (ml)	-4.5 (-21.4/12.4)	0.94 (0.83, 0.98)	-17.5 (-48.3/13.3)	0.75 (0.40, 0.91)

EDV, end-diastolic volume; EF, ejection fraction; ESV, end-systolic volume; ICC, intra-class correlation coefficient; LOA, limits of agreement; LV, left ventricular; RV, right ventricular.

5.2.4 Late gadolinium enhancement

None of the CCSs showed LGE either by the method using changing T1 time or the PSIR method using a constant T1 time.

5.3 Left ventricular function of childhood cancer survivors measured by three-dimensional echocardiography (Study II)

5.3.1 Left ventricular volumes and function

The conventional and RT-DE data on the cardiac irradiation-unexposed (group I) and -exposed (group II) CCSs and their matched controls are presented in Table 16. None of these survivors had a prior diagnosis of anthracycline-induced cardiomyopathy.

CCSs in group I had larger LV end-systolic dimensions and a smaller FS than their matched controls. They also had a larger LV ESV and smaller LV EF in RT-3DE analysis than their controls.

Survivors in group II had a lower LV mass/volume ratio and smaller FS in M-mode and a smaller LV SV in RT-3DE analysis than their controls.

None of the controls had an FS <28% or an RT-3DE LV EF <50%. Among our healthy controls, -2 SD for RT-3DE LV EF was 51%. We thus took 50% to be the appropriate lower normal limit by RT-3DE, which is in accord with published reference values for children (Poutanen et al. 2003a; Ten Harkel et al. 2009).

None of the survivors had an FS <28%. M-mode classified 7/71 (10%) of the survivors with an abnormal LV EF by RT-3DE as having a normal LV function with M-mode. Figure 8 shows box-plots for LV EF by RT-3DE and CMR of those 58 survivors with all imaging methods employed. Of those imaged with both RT-3DE and CMR, 6/58 (10%) had an RT-3DE LV EF <50%, and 45/58 (78%) had a CMR LV EF <55%. All six who had an abnormal LV EF by RT-3DE also had it abnormal by CMR. In group I, 5/63 (8%) of CCSs had an abnormal LV EF by RT-3DE and 40/52 (77%) by CMR. Of the group II survivors, 2/8 (25%) had an abnormal LV EF by RT-3DE and 5/6 (83%) by CMR.

No significant correlation was found between the RT-3DE LV EF and cumulative anthracycline dose ($r = -0.18$, $p = 0.138$), age at diagnosis ($r = -0.13$, $p = 0.27$) or follow-up time ($r = -0.08$, $p = 0.519$).

The Bland-Altman plots for intra- and inter-observer variability in the context of LV volumes are shown in Figure 9. Among those 58 assessed by both imaging methods, LV EDV and ESV were larger as measured by CMR than by RT-3DE (89 ± 14 vs. 73 ± 11 ml/m^2 and 44 ± 9 vs. 31 ± 7 ml/m^2, $p < 0.001$, for both). The variability in LV parameters by RT-3DE and CMR is presented in Table 17. The biases and limits of agreement for LV volume measurements by RT-3DE and CMR were acceptable and in line with previously published studies and the volumes correlated closely (Dorosz et al. 2012). The variability in LV EF measurements was larger and correlation lower.

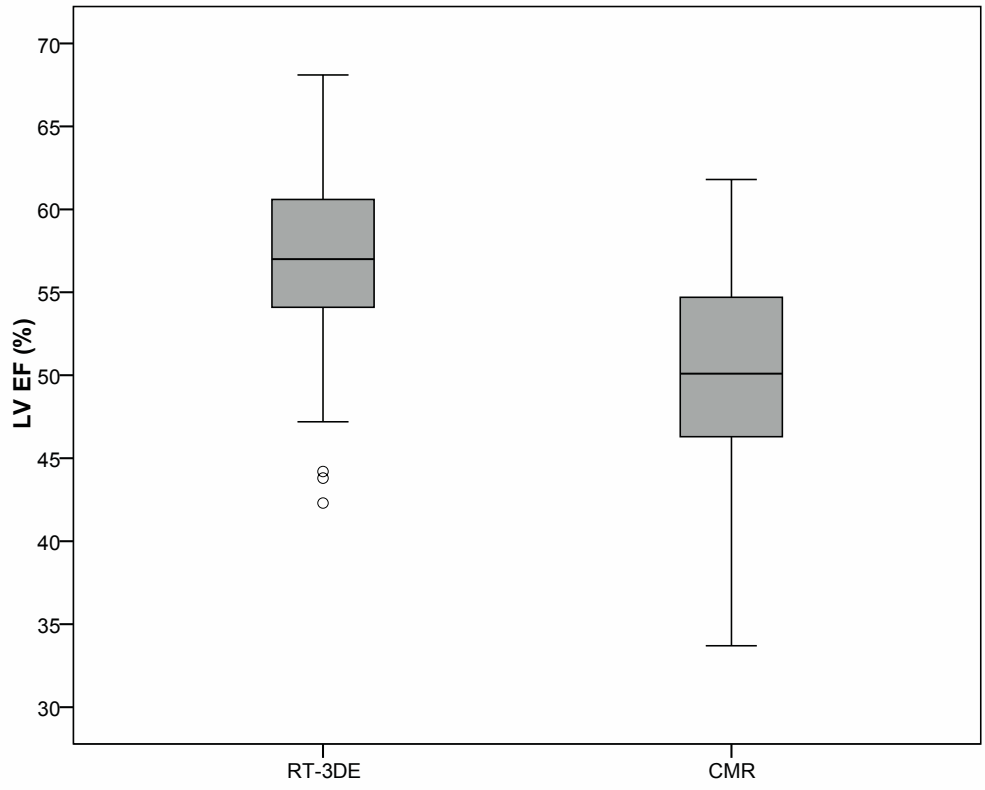

Figure 8. Box-plots for LV EF by RT-3DE and CMR of the 58 survivors with both imaging modes performed.

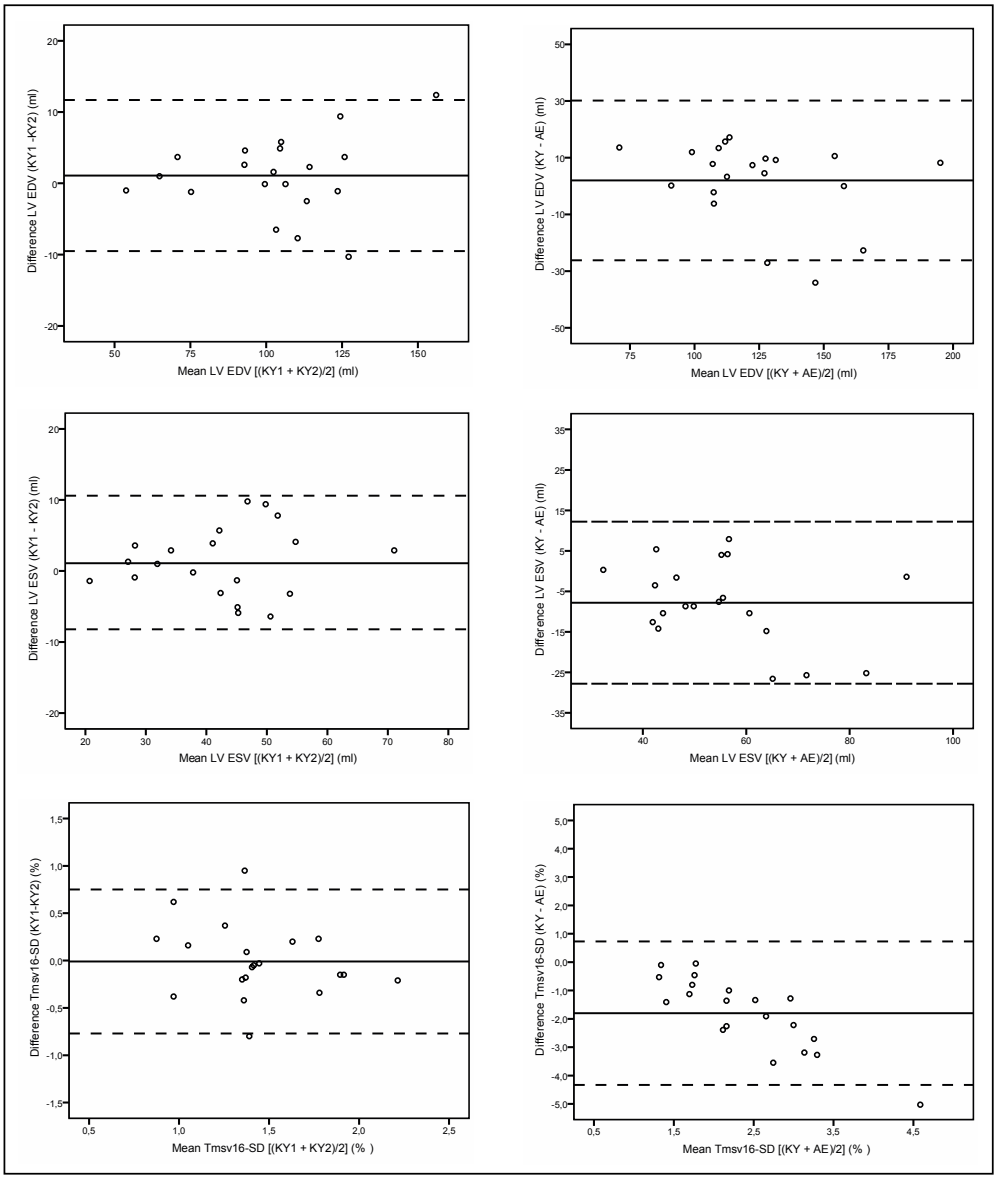

Figure 9. The Bland-Altman plots for intra-observer (on the left) and inter-observer (on the right) variability for LV EDV, LV ESV and Tmsv16-SD. The horizontal line represents the mean difference, and the dashed lines represent ± 1.96 SD from the mean between the two measurements.

Table 16. Conventional and real-time three-dimensional echocardiographic parameters of cardiac irradiation-unexposed and -exposed survivors and their matched controls (Study II).

Variable	Group I (n = 63)	Control I (n = 63)	p value*	Group II (n = 8)	Control II (n = 8)	p value*
M-mode						
LV end-diastolic dimension**	0.8 ± 0.8	0.7 ± 0.9	0.282	0.3 ± 0.8	0.4 ± 1.1	0.831
LV end-systolic dimension**	1.1 ± 0.7	0.7 ± 0.8	0.003	0.8 ± 0.6	0.4 ± 0.8	0.289
Interventricular septum diastolic dimension**	0.4 ± 0.8	0.5 ± 1.0	0.535	0.4 ± 1.0	1.0 ± 0.8	0.220
LV posterior wall diastolic dimension**	-0.2 ± 0.7	-0.2 ± 0.6	0.950	-0.5 ± 0.4	0.1 ± 0.6	0.089
LV mass (g/m^2)	75 ± 13	75 ± 16	0.975	63 ± 9	74 ± 13	0.119
LV mass/volume ratio (g/ml)	1.1 ± 0.2	1.1 ± 0.2	0.558	1.0 ± 0.1	1.2 ± 0.1	0.039
Fractional shortening (%)	33 ± 3	35 ± 3	0.003	33 ± 2	35 ± 3	0.045
RT-3DE						
LV end-diastolic volume (ml/m^2)	73 ± 10	70 ± 9	0.060	67 ± 7	72 ± 8	0.218
LV end-systolic volume (ml/m^2)	31 ± 6	28 ± 5	0.001	30 ± 5	30 ± 6	0.963
LV stroke volume (ml/m^2)	41 ± 7	42 ± 6	0.890	38 ± 6	43 ± 3	0.039
LV ejection fraction (%)	57 ± 6	60 ± 4	0.003	56 ± 7	59 ± 5	0.131
Tmsv16-SD (%)	1.39 ± 0.43	1.49 ± 0.40	0.164	1.93 ± 0.72	1.37 ± 0.24	0.098
Tmsv16-Dif (%)	5.13 ± 1.60	5.48 ± 1.57	0.208	6.92 ± 2.01	5.56 ± 1.19	0.192
Tmsv12-SD (%)	1.19 ± 0.44	1.30 ± 0.43	0.207	1.76 ± 0.48	1.11 ± 0.35	0.008
Tmsv12-Dif (%)	3.95 ± 1.51	4.33 ± 1.50	0.178	5.92 ± 1.64	3.85 ± 1.43	0.007

Group I = no cardiac irradiation. Group II = cardiac irradiation. Values are presented as mean ± SD. LV, left ventricular; RT-3DE, real-time three-dimensional echocardiography; Tmsv12-Dif/Tmsv16-Dif, the maximum time difference to reach the minimum systolic volume between the earliest and latest contracting segments for the 12/16 segments as a percentage of the RR interval; Tmsv12-SD/Tmsv16-SD, standard deviation of the time to minimum systolic volume for the 12/16 segments as a percentage of the RR interval.

*Paired samples t test was used for the comparison between survivors and their matched controls.

**Z score

Table 17. Comparison of real-time three-dimensional echocardiography versus cardiac magnetic resonance imaging (Study II).

Variable	Mean difference (limits of agreement)	Intra-class correlation coefficient (95% CI)	r
LV EDV (ml)	-26.2 (-64.2/11.7)	0.87 (0.79, 0.92)	0.88
LV ESV (ml)	-20.7 (-47.0/5.7)	0.80 (0.69, 0.88)	0.83
LV SV (ml)	-5.5 (-35.3/24.3)	0.72 (0.56, 0.82)	0.72
LV EF (%)	6.7 (-7.6/21.0)	0.19 (-0.07, 0.43)	0.19

CI, confidence interval; EDV, end-diastolic volume; EF, ejection fraction; ESV, end-systolic volume; LV, left ventricular; SV, stroke volume.

5.3.2 Left ventricular dyssynchrony indices

One case-control pair was omitted from the dyssynchrony analysis due to a stitch artifact. The +2 SD derived from our healthy controls was 2.26% for Tmsv16-SD and 2.11% for Tmsv12-SD, in line with previously published data (Cui et al. 2010; Ten Harkel et al. 2009).

The dyssynchrony indices of the CCSs unexposed (group I) or exposed to cardiac irradiation (group II) and their matched controls are presented in Table 16. The dyssynchrony indices did not differ between the group I survivors and their matched controls. In contrast, the survivors in group II had a higher Tmsv12-SD and Tmsv12-Dif than their controls.

Even though FS, LV EF (RT-3DE and CMR-derived) and RT-3DE-derived BSA-indexed LV volumes did not differ between the group I and II, all dyssynchrony indices were higher in group II survivors: Tmsv16-SD ($p = 0.003$), Tmsv16-Dif ($p = 0.005$), Tmsv12-SD ($p = 0.001$), and Tmsv12-Dif ($p = 0.001$), respectively (Table 16). Regardless of the fact that 3/70 (4%) of the survivors had an abnormally high Tmsv16-SD and 4/70 (6%) Tmsv12-SD, all had a normal QRS-duration in electrocardiogram.

Among the CCSs, the correlations of dyssynchrony indices with RT-3D LV EF or LV volumes were not particularly strong. RT-3DE LV EF correlated negatively with the Tmsv16-SD ($r = -0.44$, $p < 0.001$), Tmsv16-Dif ($r = -0.43$, $p < 0.001$), Tmsv12-SD ($r = -0.34$, $p = 0.005$) and Tmsv12-Dif ($r = -0.27$, $p = 0.024$). Tmv16-SD correlated positively with BSA-indexed LV ESV ($r = 0.32$, $p = 0.007$). Tmsv-16SD did not appear to correlate with anthracycline dose ($r = 0.03$, $p = 0.838$), age at diagnosis ($r = 0.02$, $p = 0.902$) or follow-up time ($r = 0.05$, $p = 0.664$).

In the linear regression analysis the Tmsv16-SD was predicted by the equation: [(3.47 - 0.04 x RT-3DE LV EF) + (0.50 if cardiac irradiation)], $p < 0.001$ for RT-3DE LV EF and $p = 0.002$ for cardiac irradiation, R square 0.30. Bland-Altman

plots for the intra- and inter-observer variability of the Tmsv16-SD are presented in Figure 9. Intra-observer variability was lower than inter-observer.

5.4 Cardiac biomarkers in the detection of cardiotoxicity among childhood cancer survivors (Study III)

Due to the limited number of CCSs with abnormal biomarkers, we were not able to compare echocardiographic and CMR parameters between those with normal and abnormal biomarker levels.

5.4.1 N-terminal pro-brain natriuretic peptide

None of the 76 survivors had renal failure or any other established extra-cardiac reason for their elevated NT-proBNP levels. Four (5%) were on medication for late-onset anthracycline-induced cardiomyopathy. None had had their NT-proBNP measured during malignancy treatment, biomarker measurements not being part of the clinical follow-up routine at the time. Cumulative anthracycline dose did not correlate with NT-proBNP ($r = 0.11$, $p = 0.346$).

The female survivors exposed to cardiac irradiation ($n = 8$) had higher NT-proBNP than unexposed females ($n = 34$) (median 108 vs. 62 pg/ml, $p = 0.012$). On the other hand, the NT-proBNP of the male survivors exposed ($n = 2$) or unexposed to cardiac irradiation ($n = 32$) showed no statistically significant difference (median 120 vs. 35 pg/ml, $p = 0.175$), possibly due to our small sample size (Figure 10). Analysis of variance showed a difference between the NT-proBNP values of the survivors exposed or unexposed to cardiac irradiation ($F_{3.45} = 5.89$, $p = 0.018$), but not between genders ($F_{3.45} = 0.01$, $p = 0.913$).

Among all CCSs, 4/76 (5%) had an abnormal plasma NT-proBNP. Their clinical data are presented in Table 18. All had normal cTns and were cTnAAb-negative. None had a prior diagnosis of anthracycline-induced cardiomyopathy, cardiac symptoms or impaired subjective exercise tolerance. All had a normal FS, two an abnormal LV EF by RT-3DE and all by CMR. An abnormal RV EF by CMR was found in three. All had normal EVD in both LV and RV, but three had an abnormal LV ESV and one an abnormal RV ESV. Furthermore, all CCSs with an abnormal NT-proBNP showed at least one additional risk factor for

anthracycline-induced cardiomyopathy: moderate anthracycline doses, female gender, cardiac irradiation or malignancy treatment under one year of age.

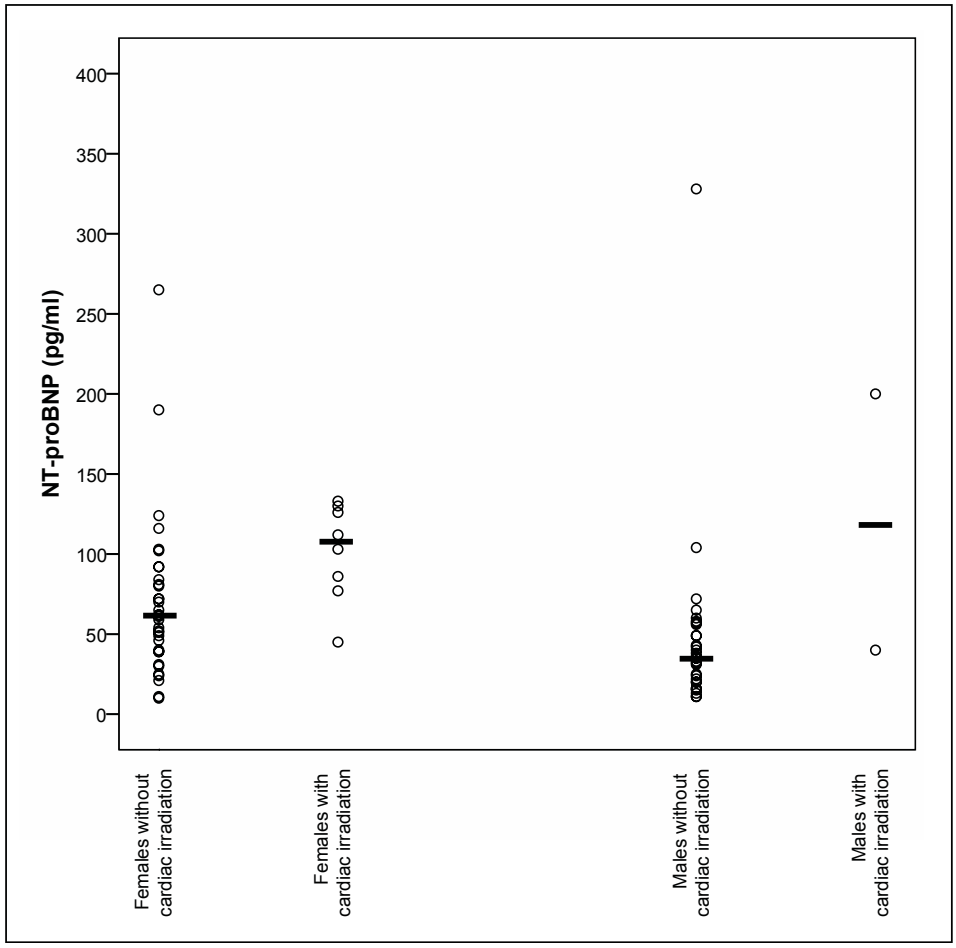

Figure 10. Scatter-plots for NT-proBNP categorized by gender and exposure to cardiac irradiation. The bold horizontal lines represent the medians of each group.

Table 18. Characteristics of the survivors with an abnormal NT-proBNP (Study III).

Variable	Pt 1	Pt 2	Pt 3	Pt 4
Gender	Male	Male	Female	Female
Age (years)	8.1	12.0	17.1	17.2
Age at malignancy diagnosis (years)	0.0	6.1	9.5	11.3
Diagnosis	Neuroblastoma	AML	AML	Osteosarcoma
Cumulative anthracycline dose (mg/m^2)	108	416	265	301
Cardiac irradiation	No	Yes	No	No
Allogeneic stem cell transplantation	No	Yes	No	No
NT-proBNP (pg/ml)	328	200	190	265
FS (%)	30.5	33.1	31.4	29.8
RT-3DE LV EF (%)	43.8	58.3	56.7	48.2
CMR LV EF (%)	44.0	48.8	44.4	51.0
CMR LV EDV > 2SD	No	No	No	No
CMR LV ESV > 2SD	Yes	Yes	Yes	No
CMR RV EF (%)	49.6	61.5	47.9	30.6
CMR RV EDV > 2SD	No	No	No	No
CMR RV ESV > 2SD	No	No	No	Yes

AML, acute myeloid leukemia; CMR, cardiac magnetic resonance; EDV, end-diastolic volume; EF, ejection fraction; ESV, end-systolic volume; FS, fractional shortening; LV, left ventricular; NT-proBNP, N-terminal pro-brain natriuretic peptide; RT-3DE, real-time three-dimensional echocardiography; RV, right ventricular; SD, standard deviation.

5.4.2 Cardiac troponins

All CCSs had their TnT levels below 0.03 μg/l and hs-cTnT levels below 14 ng/l. One survivor yielded an insufficient sample volume for cTnI analysis, but in all 75 with cTnI analysis performed it was unmeasurable (below 0.01 μg/l). Despite normal cTn levels 51/76 (67%) had an abnormal LV EF by either RT-3DE or CMR. An abnormal LV EF by both imaging methods (RT-3DE and CMR) was detected in 8/76 (11%) of these cTn-negative survivors. None had signs of ischemia or infarction in ECG. No previous cTn values were available from the malignancy treatment period.

5.4.3 Autoantibodies to cardiac troponin

The cTnAAbs were analyzed for 75 survivors, one having an insufficient sample volume. cTnAAbs were detected in 4/75 (5%) CCSs. The clinical characteristics of these subjects are presented in Table 19. The cTnAAb-positive survivors were all

cTnT-, hs-cTnT- and cTnI-negative and had normal NT-proBNP levels. All with cTnAAbs experienced normal subjective exercise tolerance.

The cTnAAb-positive survivors had a normal FS and LV EF by RT-3DE. Three of them had CMR performed with an abnormal LV EF and an abnormal RV EF in one. Two had an abnormally large LV EDV and RV EDV. All three had an abnormal LV ESV and RV ESV.

CCSs with cTnAAbs showed no specific risk factors for anthracycline-induced cardiomyopathy.

Table 19. Characteristics of the survivors with autoantibodies to cardiac troponin (Study III).

Variable	Pt 5	Pt 6	Pt 7	Pt 8
Gender	Female	Female	Male	Male
Age (years)	11.0	13.7	14.2	16.2
Age at malignancy diagnosis (years)	3.4	5.1	3.7	5.7
Diagnosis	ALL	ALL	ALL	ALL
Cumulative anthracycline dose (mg/m^2)	180	151	123	120
Cardiac irradiation	No	No	No	No
Allogeneic stem cell transplantation	No	No	No	No
cTnAAb (specific counts)	1996	209	41287	8110
FS (%)	35.5	32.3	30.2	29.0
RT-3DE LV EF (%)	67.2	53.3	54.7	50.4
CMR LV EF (%)	47.5	NA	40.2	42.6
CMR LV EDV > 2SD	Yes	NA	Yes	No
CMR LV ESV > 2SD	Yes	NA	Yes	Yes
CMR RV EF (%)	56.7	NA	56.6	36.9
CMR RV EDV > 2SD	Yes	NA	Yes	No
CMR RV ESV > 2SD	Yes	NA	Yes	Yes

ALL, acute lymphoblastic leukemia; CMR, cardiac magnetic resonance; cTnAAb, autoantibodies to cardiac troponin; EDV, end-diastolic volume; EF, ejection fraction; ESV, end-systolic volume; FS, fractional shortening; LV, left ventricular; NA, not available; RT-3DE, real-time three-dimensional echocardiography; RV, right ventricular; SD, standard deviation.

5.4.4 Survivors with a prior diagnosis of anthracycline-induced cardiomyopathy

The study group included four (5%) survivors with previously diagnosed, late-onset anthracycline-induced cardiomyopathy. Their clinical data are summarized in Table 20. All of them had known risk factors for anthracycline-induced

cardiomyopathy: female gender, high anthracycline dose, cardiac irradiation or malignancy diagnosis before one year of age in one case.

All were cTnAAb-negative and had normal cTns and NT-proBNP at time of study. All had had NT-proBNP measured after the diagnosis of cardiomyopathy, and in three of them it was abnormally high at the time.

An abnormal FS was detected in two and LV EF by RT-3DE in three. Three survivors underwent CMR and all had an abnormal LV EF and RV EF. Only one survivor had an abnormal LV EDV, but all had an LV ESV exceeding +2 SD from reference values. All had RV EDV within normal limits, and only one had an abnormal RV ESV.

Table 20. Characteristics of the survivors with anthracycline-induced cardiomyopathy (Study III).

Variable	Pt 9	Pt 10	Pt 11	Pt 12
Gender	Female	Female	Female	Female
Age (years)	7.9	14.1	15.0	18.3
Age at malignancy diagnosis (years)	0.7	1.8	3.4	3.8
Diagnosis	Neuroblastoma	ALL	ALL	Infantile fibrosarcoma
Cumulative anthracycline dose (mg/m^2)	113	339	360	355
Cardiac irradiation	No	Yes	No	No
Allogeneic stem cell transplantation	No	Yes	No	No
Time from diagnosis to cardiomyopathy (years)	3.9	11.1	8.4	1.2
Lowest FS (%)	26	27	21	21
Peak NT-proBNP (pg/ml)	53	190	253	233
NT-proBNP at study (pg/ml)	49	133	80	65
FS (%)	33.4	28.3	25.5	24.8
RT-3DE LV EF (%)	51.0	40.6	40.2	45.5
CMR LV EF (%)	51.3	NA	46.4	49.4
CMR LV EDV > 2SD	No	NA	No	Yes
CMR LV ESV > 2SD	Yes	NA	Yes	Yes
CMR RV EF (%)	50.6	NA	54.7	46.1
CMR RV EDV > 2SD	No	NA	No	No
CMR RV ESV > 2SD	No	NA	Yes	No

ALL, acute lymphoblastic leukemia; CMR, cardiac magnetic resonance; EDV, end-diastolic volume; EF, ejection fraction; ESV, end-systolic volume; FS, fractional shortening; LV, left ventricular; NA, not available; NT-proBNP, N-terminal pro-brain natriuretic peptide; RT-3DE, real-time three-dimensional echocardiography; RV, right ventricular; SD, standard deviation.

5.5 Cardiac longitudinal function of childhood cancer survivors (Study IV)

5.5.1 Left ventricular longitudinal function

Echocardiographic parameters describing LV longitudinal function in CCSs and their matched controls are summarized in Table 21.

The mitral inflow velocities did not differ between the CCSs and their controls, neither between survivors exposed or unexposed to cardiac irradiation. The CCSs had lower S` in the lateral and septal walls and lower E` in the septal myocardium than the controls. There were no differences in A`. The CCSs had a higher LV E/E` septal than their controls. Lateral S` was the only TDI parameter significantly lower among cardiac irradiation-exposed than unexposed survivors.

The MAD lateral, MAD mid and MAD mid% were all lower among the CCSs than their controls. There was no statistical difference in MAD septal. When comparing the CCSs with or without cardiac irradiation, those exposed to cardiac irradiation had all TMAD parameters for the LV lower than the unexposed survivors.

MAD mid% was lower among the CCSs who had their RT-3DE LV EF <50% compared with those with a LV EF ≥50% (13.8 ± 2.0 vs. 15.6 ± 2.3, p = 0.026, respectively). The survivors with a CMR-derived LV EF <50% also had a lower MAD mid% (15.0 ± 2.4 vs. 16.3 ± 2.2, p = 0.028, respectively). Derived from –2 SD of our healthy controls, the lower normal limit for MAD mid% was 11.8%. Of the CCSs, 3/72 (4%) had an abnormal MAD mid%, and two of them had undergone CMR showing a LV EF <50%.

MAD mid appeared to correlate with the RT-3DE-derived LV volumes (EDV: r = 0.54, ESV: r = 0.42, SV: r = 0.56, p <0.001 for all), and the CMR-derived LV volumes (EDV: r = 0.46, ESV: r = 0.43, SV; r = 0.41, p = 0.001 for all). MAD mid% did not correlate with LV EF (RT-3DE and CMR) (r = 0.26, p = 0.025 and r = 0.10, p = 0.452, respectively).

The mean difference and limits of agreement for intra-observer variability of MAD mid (mm) were -0.2 (-0.9/0.5) and for inter-observer variability 0.1 (-2.1/2.3) (Figure 11).

Table 21. Left ventricular echocardiographic parameters of cardiac longitudinal function (Study IV).

Variable	Survivors (n = 75)	Controls (n = 75)	p value*	Survivors with cardiac irradiation (n = 9)	Survivors without cardiac irradiation (n = 66)	p value**
Doppler						
Mitral E velocity (cm/sec)	91.9 ± 14.6	93.8 ± 15.3	0.419	95.0 ± 17.7	91.5 ± 14.2	0.505
Mitral A velocity (cm/sec)	46.4 ± 10.1	44.2 ± 8.5	0.112	53.6 ± 14.3	45.3 ± 9.0	0.126
Mitral E/A	2.0 ± 0.5	2.2 ± 0.4	0.079	1.9 ± 0.7	2.1 ± 0.4	0.300
M-mode						
LV FS (%)	32.9 ± 3.1	34.9 ± 3.2	<0.001	32.2 ± 2.3	33.0 ± 3.2	0.465
Real-time three-dimensional echocardiography						
LV EF (%)	56.2 ± 6.4	59.4 ± 4.2	<0.001	54.3 ± 8.5	56.5 ± 6.0	0.331
Tissue Doppler imaging						
E` lateral LV (cm/sec)	17.9 ± 3.0	18.7 ± 3.3	0.087	16.4 ± 2.3	18.1 ± 3.0	0.113
A` lateral LV (cm/sec)	5.6 ± 1.3	6.0 ± 1.9	0.091	5.7 ± 1.4	5.5 ± 1.3	0.665
S` lateral LV (cm/sec)	10.2 ± 1.7	10.9 ± 2.0	0.016	8.6 ± 1.3	10.4 ± 1.6	0.002
E` septal LV (cm/sec)	12.2 ± 1.7	13.5 ± 1.6	<0.001	12.0 ± 1.9	12.2 ± 1.7	0.722
A` septal LV (cm/sec)	4.9 ± 1.0	5.2 ± 1.1	0.093	5.1 ± 1.3	4.9 ± 1.0	0.681
S` septal LV (cm/sec)	7.4 ± 1.0	7.8 ± 0.8	0.004	7.1 ± 0.8	7.4 ± 1.1	0.384
LV E/E` septal	7.6 ± 1.4	7.0 ± 1.2	0.003	8.0 ± 0.9	7.6 ± 1.4	0.461
E` middle septal LV (cm/sec)	9.5 ± 1.7	10.5 ± 1.7	0.001	9.1 ± 2.2	9.5 ± 1.6	0.527
A` middle septal LV (cm/sec)	3.8 ± 0.8	4.1 ± 0.9	0.097	4.0 ± 1.0	3.8 ± 0.7	0.473
S` middle septal LV (cm/sec)	5.6 ± 0.7	5.9 ± 0.7	0.022	5.3 ± 0.7	5.7 ± 0.7	0.150
Speckle tracking echocardiography						
MAD lateral (mm)	12.1 ± 2.7	13.0 ± 2.4	0.022	10.1 ± 2.1	12.4 ± 2.6	0.014
MAD septal (mm)	11.9 ± 2.1	12.5 ± 1.9	0.082	10.6 ± 2.1	12.1 ± 2.0	0.039
MAD mid (mm)	12.7 ± 2.3	13.6 ± 2.0	0.006	11.0 ± 1.9	13.0 ± 2.2	0.011
MAD mid (%)	15.4 ± 2.4	16.1 ± 2.2	0.049	13.8 ± 1.8	15.6 ± 2.3	0.031

A, atrial peak flow velocity; A`, late diastolic myocardial velocity associated with atrial contraction; E, early mitral peak flow velocity; E`, early diastolic myocardial relaxation velocity; EF, ejection fraction; FS, fractional shortening; LV, left ventricle; MAD, mitral annular displacement; S`, systolic velocity. *Paired sampled t test was used for comparison between survivors and their matched controls; **Independent samples t test was used for comparison between the survivors with and without cardiac irradiation.

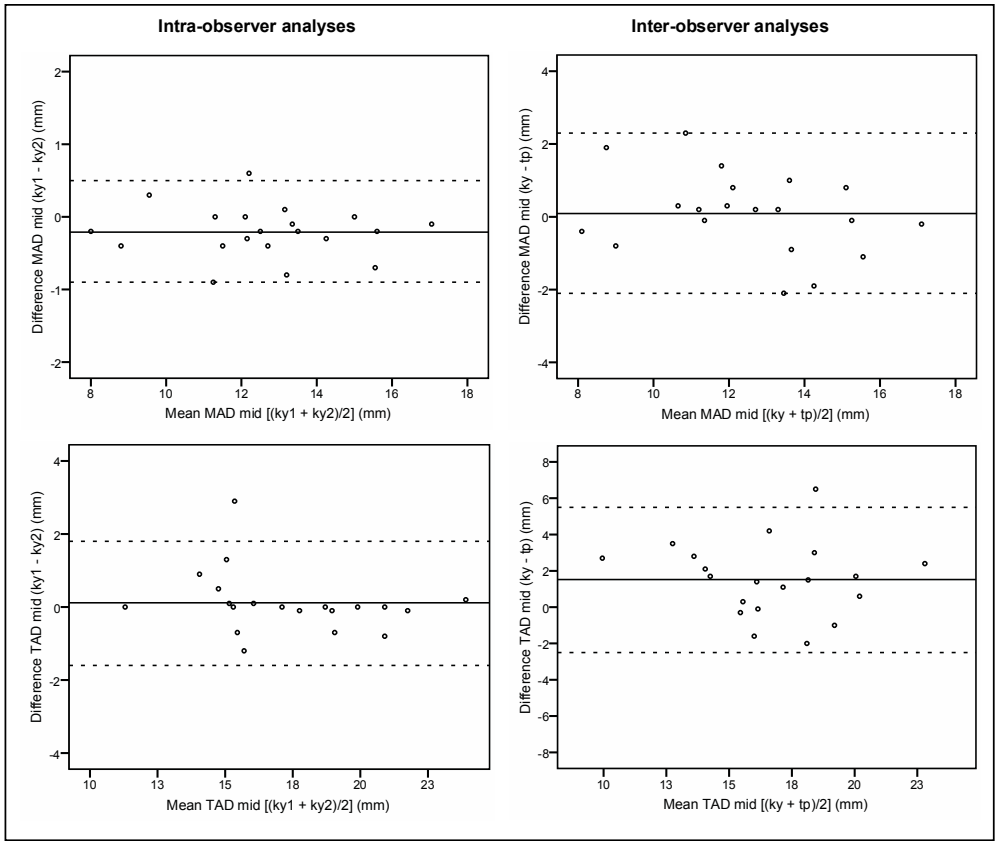

Figure 11. The Bland-Altman plots for the intra- (on the left) and inter-observer (on the right) variability for MAD mid and TAD mid (in millimeters). The horizontal line represents the mean difference, and the dashed horizontal lines represent ± 1.96 SD from the mean between the two measurements.

5.5.2 Right ventricular longitudinal function

Echocardiographic parameters describing RV longitudinal function are summarized in Table 22.

The tricuspid inflow parameters and TAPSE did not differ between the CCSs and their controls, neither between those exposed or unexposed to cardiac irradiation.

The E` of the lateral RV wall and RV E/E` lateral were lower in CCSs than in their controls. A` of the lateral RV wall was the only parameter of RV longitudinal

function which differed significantly between the survivors exposed or unexposed to cardiac irradiation, A` being higher among the former.

TAD septal, mid and mid% were all lower among CCSs than controls.

We derived the lower normal limit for TAD mid% from –2 SD of our healthy controls (17.6%). Of the survivors, 4/75 (5%) had an abnormal TAD mid%. All of these had their CMR-derived RV EF <55% and one also a prior diagnosis of anthracycline-induced cardiomyopathy.

TAD mid correlated with the CMR-derived RV EDV ($r = 0.38$, $p = 0.002$), RV ESV ($r = 0.33$, $p = 0.009$), and RV SV ($r = 0.35$, $p = 0.006$). There was no correlation between TAD mid% and CMR-derived RV EF ($r = 0.19$, $p = 0.145$). However, TAPSE correlated with TAD mid% ($r = 0.302$, $p = 0.008$).

The mean difference and limits of agreement for the intra-observer variability of TAD mid (mm) were 0.1 (-1.6/1.8) and the inter-observer variability 1.5 (-2.5/5.5) (Figure 11).

Table 22. Right ventricular echocardiographic parameters of cardiac longitudinal function (Study IV).

Variable	Survivors (n = 75)	Controls (n = 75)	p value*	Survivors with cardiac irradiation (n = 9)	Survivors without cardiac irradiation (n = 66)	p value**
Doppler						
Tricuspid E velocity (cm/sec)	61.4 ± 10.5	61.3 ± 10.2	0.979	65.0 ± 7.3	60.9 ± 10.8	0.274
Tricuspid A velocity (cm/sec)	33.0 ± 7.2	31.3 ± 6.0	0.117	37.5 ± 8.9	32.5 ± 6.8	0.052
Tricuspid E/A	1.9 ± 0.4	2.0 ± 0.4	0.109	1.8 ± 0.3	1.9 ± 0.4	0.286
M-mode						
TAPSE (mm)	22.7 ± 3.3	23.9 ± 3.6	0.065	22.0 ± 2.9	22.8 ± 3.4	0.486
Tissue Doppler imaging						
E` lateral RV (cm/sec)	14.4 ± 2.4	15.9 ± 3.1	0.005	14.4 ± 2.2	14.5 ± 2.5	0.909
A` lateral RV (cm/sec)	7.8 ± 2.2	7.8 ± 2.5	0.945	9.5 ± 2.9	7.6 ± 2.0	0.015
S` lateral RV (cm/sec)	13.8 ± 1.7	14.3 ± 2.6	0.227	13.9 ± 2.4	13.8 ± 1.6	0.966
RV E/E` lateral	4.4 ± 1.1	4.0 ± 0.8	0.011	4.7 ± 0.7	4.4 ± 1.1	0.458
Speckle tracking echocardiography						
TAD lateral (mm)	19.8 ± 3.5	20.7 ± 3.7	0.104	19.2 ± 3.1	19.9 ± 3.6	0.593
TAD septal (mm)	13.0 ± 2.2	14.0 ± 1.9	0.004	12.4 ± 1.8	13.1 ± 2.3	0.340
TAD mid (mm)	16.9 ± 2.6	18.1 ± 2.6	0.005	16.2 ± 1.7	17.0 ± 2.7	0.357
TAD mid (%)	22.5 ± 3.0	23.5 ± 3.0	0.035	22.0 ± 2.4	22.5 ± 3.1	0.660

A, atrial peak flow velocity; A`, late diastolic myocardial velocity associated with atrial contraction; E, tricuspid peak flow velocity; E`, early diastolic myocardial relaxation velocity; S`, systolic velocity; TAD, tricuspid annular displacement; TAPSE, tricuspid annular systolic excursion; RV, right ventricle.
*Paired sampled t test was used for comparison between survivors and their matched controls; **Independent samples t test was used for comparison between the survivors with and without cardiac irradiation.

6. Discussion

6.1 Cardiac magnetic resonance imaging (Study I)

This present study is the largest published on CMR among anthracycline-exposed CCSs below adult age, and the first to evaluate LGE among non-adult CCSs. We show that a considerable proportion of CCSs have an impaired LV and RV function by CMR, even though their cancer therapies took place in an era (1993-2006) of increased awareness of the cardiac late-effects and their key contributors (total cumulative anthracycline dose and cardiac irradiation). The proportions of sub- or abnormal LV EFs among our CCSs (79%) exceeded figures published e.g. for adult age survivors of Hodgkin´s disease (23%) (Machann et al. 2011), possibly implying that children are more prone to the cardiotoxic late effects. We also demonstrate that CMR finds more impairment in cardiac function than M-mode and RT-3DE, which is in line with the results of a recent study among adult aged of CCSs (Armstrong et al. 2012).

Anthracycline-induced cardiotoxicity may lead to ventricular dilatation and wall thinning resembling dilating cardiomyopathy, or at a later stage, restrictive cardiomyopathy, whereas cardiomyopathy caused by radiation is usually of restrictive nature (Lipshultz et al. 2013a). Our study patients showed dilatation of the ventricles, most prominently in LV and end-systole. However, those exposed to cardiac irradiation showed a trend towards lower ventricular volumes, possibly indicating a restrictive process. In this study, we employed CMR, the most accurate and reproducible imaging method for measuring ventricular volumes (Catalano et al. 2007; Grothues et al. 2002; Jauhiainen et al. 1998; Rehr et al. 1985).

Endomyocardial biopsies have shown the RV also to be affected by anthracyclines. CMR is considered the best method for visualization of the RV (American College of Cardiology Foundation Task Force on Expert Consensus, Documents et al. 2010; Haddad et al. 2008). Due to its complex anatomy and scarcity of optimal imaging methods, RV function after cancer treatment has only gained more attention during the last few years. We found almost a third of our CCSs to house an abnormal RV function and over one half to have a subnormal RV EF. Our results confirm the findings of Oberholzer and colleagues also reporting decreased RV function by CMR associated with anthracyclines (Oberholzer et al. 2004). This RV dysfunction may be due to direct cardiotoxicity

or reflect a restrictive lung disease caused by chest radiation (Armstrong et al. 2013; Patel et al. 2014). Also impaired LV function may impact on the RV function through systolic ventricular interaction (Haddad et al. 2008). The large number of survivors with an impaired RV function in our study emphasizes the need for screening of RV function as part of a structured follow-up program. CMR is indicated as the more sensitive imaging method, in cases of suspicion of abnormal RV function based on symptoms, oxygen saturation, echocardiography or ECG.

Age, gender and size of the individual affect the ventricular parameters, especially among children and adolescents (Sarikouch et al. 2010). Normal CMR data for the LV and RV parameters in the pediatric population have until recently been scarce, and largely remain based on small sample sizes and obtained using older CMR techniques (Helbing et al. 1995; Lorenz 2000). Normative data with the modern SSFP technique and larger samples sizes have been published since 2009 (Buechel et al. 2009; Robbers-Visser et al. 2009), but only one report takes both gender and age simultaneously into account (Sarikouch et al. 2010). In addition, the orientation of imaging slices (axial vs. short axis), the analysis program employed and contouring criteria (inclusion/exclusion of papillary muscles to ventricular cavity, definition of basal decent and outflow tract) may vary, making it challenging to identify appropriate reference values (Schulz-Menger et al. 2013). We used the CMR reference values, which corresponded best to our methods and criterion (Robbers-Visser et al. 2009; Sarikouch et al. 2010). For RV parameters we used axial slices, as they covered the RV volume better than short axis slices.

Our CCSs had LV mass within normal range. Two other studies on CCSs under adult age were in line with our findings, showing normal LV mass by CMR (Tham et al. 2013; Toro-Salazar et al. 2013). In contrast, almost half of adult-aged CCSs had reduced LV mass by CMR (Armstrong et al. 2012). Another study on adults with a prior diagnosis of anthracycline-induced cardiomyopathy demonstrated a lower BSA-indexed LV mass to be a predictor of adverse cardiac effects (Neilan et al. 2012). This discrepancy between children and adults regarding LV mass reduction following anthracyclines probably has multifactorial reasons. Higher anthracycline doses or greater exposure to cardiac irradiation cannot be the only explanations, because reduced LV mass was also detected in adults with low anthracycline doses and without radiation exposure (Armstrong et al. 2012). Ageing, longer follow-up time and the burden of other cardiovascular risk factors might make some contribution to the LV mass reduction seen up to adult age.

Interstitial and replacement fibrosis have been detected in histological specimens of hearts with anthracycline-induced cardiomyopathy (Cascales et al. 2013; Steinherz et al. 1995). Fibrosis has been associated with an unfavorable prognosis in other heart diseases (Assomull et al. 2006; Rubinshtein et al. 2010). Consequently, signs of myocardial fibrosis have also been sought by non-invasive

methods among anthracycline-exposed survivors. LGE has been reported infrequently only among adult cancer survivors exposed to anthracyclines and/or cardiac irradiation (Machann et al. 2011; Neilan et al. 2012; Perel et al. 2006). None of our 62 CCSs had LGE, even though it was assessed by two different methods. Recent studies among CCSs of pediatric age show an absence of LGE and are thus in line with our results (Tham et al. 2013; Toro-Salazar et al. 2013). Higher cumulative anthracycline or radiation doses, presence of additional cardiovascular risk factors and diseases, or extended follow-up may explain the presence of LGE among adult cancer survivors, indicating that the development of replacement fibrosis runs a protracted course.

On the other hand, Toro-Salazar and colleagues propose an elevated cardiac extracellular volume and lower post-contrast T1 time as signs of diffuse fibrosis among pediatric-aged CCSs in the absence of LGE (Toro-Salazar et al. 2013). They also report lower myocardial strain values by CMR, even though the global systolic function remained within normal range among their study subjects (Toro-Salazar et al. 2013). Tham and associates also reported myocardial T1 and extracellular volume to be early tissue markers of ventricular remodeling indicative of diffuse fibrosis among anthracyline-exposed children (Tham et al. 2013). The imaging method we used did not allow for T1 mapping, which renders the assessment of diffuse fibrosis less reliable. Based on the above-mentioned studies it can be hypothesized that diffuse fibrosis may precede replacement fibrosis and overt systolic dysfunction. Lack of methodological consensus and gender- and age-specific reference values make T1 mapping still suboptimal for routine clinical use.

CMR offers many advantages over other diagnostic and imaging modalities. In contrast to endomyocardial biopsy and angiography, CMR is non-invasive and gives information simultaneously on cardiac function and the myocardium (Yoshida et al. 2013). CMR may reduce the need for diagnostic endomyocardial biopsies in the future. Accurate measurement of cardiac parameters enables the detection of early and minute signs of cardiac pathology in stages before CCSs become symptomatic. Independence of the acoustic window is a great benefit of CMR among survivors with postsurgical abnormalities of the thoracic region or obesity. The body mass index of our CCSs was higher than among controls, indicating that obesity is not a rare problem among CCSs. Other assets of CMR include independence of ionizing radiation or radioactive isotopes, important among CCSs exposed to many radiological examinations, some also to radiation therapy. Limited imaging resources, high cost and long imaging time remain challenges with CMR. Most children under school age need sedation for CMR.

6.2 Three-dimensional echocardiography (Study II)

Our study showed anthracycline-exposed CCSs to have a lower LV EF and larger LV ESV by RT-3DE than their matched controls, in accord with previous findings (Cheung et al. 2011; Poutanen et al. 2003b). In contrast to Poutanen and coworkers, we could not demonstrate a difference in ESV between our cardiac irradiation-exposed CCSs and their controls, which may be partly due to small groups of exposed subjects in both of these studies (Poutanen et al. 2003b). However, the irradiation-exposed CCSs had a lower SV than their controls, and showed a trend to lower LV EFs. Lower SV may reflect the restrictive effect of radiation. In the absence of suitable reference values for the CMR-derived LV SV we were unable to confirm this result by CMR.

We confirmed RT-3DE to be superior to M-mode in detecting diminished LV systolic function. In our study group with no prior diagnoses of cardiomyopathy and all having their FS within normal range, RT-3DE revealed an abnormal LV EF in 10% of CCSs. CMR confirmed this result, showing that of those imaged with both RT-3DE and CMR all who had an abnormal LV EF with RT-3DE also had it abnormal with CMR. Three-dimensional imaging methods do not make assumptions on the shape of the ventricles, and thus give accurate measurements of ventricular volumes and EF especially in the case of ventricles of abnormal shape.

Furthermore, we showed the LV volumes measured by CMR to be invariably larger than those measured by RT-3DE, but the two to correlate closely and with minimal variation, in line with published data (Dorosz et al. 2012). According to the literature, LV EF values derived by RT-3DE and CMR usually tally fairly closely (Dorosz et al. 2012; Soliman et al. 2008). In our study, however, LV EF values obtained by CMR were constantly lower than those by RT-3DE. This may be partly due to the CMR criteria for inclusion of basal LV slices, which problem does not exist for the RT-3DE technique using long-axis views for endocardial tracing (Mor-Avi et al. 2008).

RT-3DE and CMR are different methods and both have their own advantages. CMR is the best method for imaging of the RV and in cases of a suboptimal acoustic window. RT-3DE has proved to be more accurate and reproducible among children in the measurement of LV volumes, EF and mass than M-mode, and two-dimensional echocardiography with CMR was used as the reference (Lu et al. 2008). This is in line with our results and previous findings among adult CCSs (Armstrong et al. 2012).

The various cardiac imaging methods have different normal values due to dissimilarities in methodology and algorithms between the modalities (Wood et al. 2014). We took this into account in our study, using either method-specific

reference values or matched controls (Poutanen et al. 2003a; Robbers-Visser et al. 2009; Sarikouch et al. 2010; Ten Harkel et al. 2009).

Non-contrast RT-3DE has been shown to be the most reproducible technique for LV volume and EF measurement when compared to the two-dimensional bi- and triplane methods and contrast-RT-3DE (Thavendiranathan et al. 2013). This is partly due to the semi-automated method for identifying the endocardium by RT-3DE analysis compared with the manual tracing required by 2DE. Automated selection of the frame with minimum volume by RT-3DE tracing technique further improves reproducibility compared with two-dimensional tracing, where the frame selection is based on visual assessment. The moving RT-3DE image is also useful in checking the correctness of the tracing. The American Society of Echocardiography and the European Association of Cardiovascular Imaging state in their consensus that RT-3DE is the preferred technique for monitoring LV function and detecting cardiotoxicity in adult patients with cancer (Plana et al. 2014).

Relatively small sample size, diversity in genetic susceptibility, exposure to other cardiotoxic risk factors, and treatment-related iron load may partly explain why CMR or RT-3DE derived LV EF did not correlate with anthracycline dose, age at diagnosis or with the follow-up time.

The association between LV dyssynchrony and heart failure has been demonstrated among adults (Kapetanakis et al. 2005; Liodakis et al. 2009). In severe cases of dyssynchrony, biventricular pacing has been used as a cardiac resynchronization therapy in adults and recently also in children (Liodakis et al. 2009). RT-3DE enables the assessment of dyssynchrony, and the systolic dyssynchrony index (Tmsv16-SD) has established its role in the assessment of global LV function (Kapetanakis et al. 2005; Ojala et al. 2014; Wang et al. 2012). RT-3DE dyssynchrony indices assess LV regional volumes over time rather than myocardial contraction or motion (Friedberg and Mertens 2013).

A dyssynchronous contraction moves blood around the ventricle from the segments activated early to those activated late, resulting in a reduced SV and impaired systolic function. The negative correlation between dyssynchrony indices and LV EF among our CCSs, in accord with previous studies, supports such a hypothesis (Cheung et al. 2010; Kapetanakis et al. 2005). We also show cardiac irradiation exposed CCSs to have higher dyssyncrony indices in the 12-segment analysis compared with their healthy controls, and in both 12- and 16-segment analyses upon comparison with cardiac irradiation-unexposed survivors. Ours is the first report on LV dyssynchrony assessed by RT-3DE among cardiac irradiation-exposed CCSs. Even though all our CCSs showed a duration of QRS-complexes within normal range, RT-3DE revealed mechanical dyssynchrony of the LV in some of the them. However, the dyssynchrony indices were only slightly

elevated, indicating that the CCSs in this study group had not yet developed a severe LV dysfunction.

The advantages of RT-3DE over CMR include better availability and shorter imaging time. RT-3DE can also be performed on most children without sedation. A movement artifact, on the other hand, may cause a stitch artifact, making dyssynchrony analysis impossible. RT-3DE requires a good acoustic window, which most children have. However, with some obese teenagers optimal RT-3DE images cannot be obtained.

6.3 Cardiac biomarkers (Study III)

In this study, we show elevated plasma NT-proBNP and cTnAAb-positivity to underline a need for more sensitive cardiac imaging with RT-3DE or CMR despite normal findings in conventional echocardiography.

Cardiac biomarkers have gained interest in the screening of cardiotoxicity in being inexpensive, easy to obtain and suitable for wider use. Nonetheless, they have been studied more widely peri- than post-therapy.

Only 5% of our CCSs had an abnormal NT-proBNP. Even though their FSs were normal, all had abnormal RV and/or LV function, and many of them enlarged LV ESV by CMR. A previous study with M-mode has shown that survivors with an abnormal NT-proBNP level have a higher BSA-indexed LV end-diastolic dimension than those with a normal NT-proBNP (Mavinkurve-Groothuis et al. 2009). As CCSs during late follow-up are usually in a stable cardiovascular condition and without fluid therapy, the increase in their NT-proBNP and ventricular dilatation are indicative of a chronic condition.

Previous studies have shown NT-proBNP to be elevated among those with higher cumulative anthracycline doses, and the levels to correlate with the echocardiographic parameters of ventricular dysfunction (Armenian et al. 2014; Lipshultz et al. 2012a; Mavinkurve-Groothuis et al. 2009). However, a cut-off level for NT-proBNP to detect cases of cardiotoxicity remains to be established, though recently proposed for heart failure (Lin et al. 2014). We used +2 SD from normal reference values, aiming to identify survivors with asymptomatic cardiotoxicity. Interestingly, three of our four CCSs with a prior diagnosis of anthracycline-induced cardiomyopathy betrayed an abnormal NT-proBNP level at time of cardiomyopathy diagnosis. Their normal levels at time of study may result from the positive impact of enalapril.

Our data also lent support to the conception of cardiac irradiation increasing NT-proBNP, as suggested by recent studies on adults and children (Brouwer et al. 2011; Lipshultz et al. 2012a).

Based on our data, we suggest NT-proBNP to be a supplementary tool in screening for cardiotoxicity after cancer therapy. Especially subjects with additional risk factors for cardiotoxicity may benefit from NT-proBNP measurements. Abnormal values warrant evaluation with sensitive imaging and a closer follow-up.

In the late 1990s Lipshultz and associates showed troponin release during cancer treatment to predict LV echocardiographic abnormalities at later follow-up (Lipshultz et al. 1997). Cardinale and coworkers confirmed this result with cTnI among adults (Cardinale et al. 2000). They further found that early treatment with enalapril of those with cTnI release during cancer treatment prevented the development of late cardiotoxicity (Cardinale et al. 2006). However, previous studies on CCSs at late follow-up using troponin assays of a previous generation had failed to show any troponin release despite LV dysfunction seen in echocardiography (Mavinkurve-Groothuis et al. 2009; Soker and Kervancioglu 2005).

Exposure to cardiotoxic agents may cause troponin release as a sign of myocardial damage, and echocardiographic findings of abnormal cardiac function may occur later when the compensatory mechanisms of the heart are exceeded. However, adult patients with heart failure may suffer troponin release for reasons other than myocardial infarction (Januzzi et al. 2012). To improve the detection of troponin, a special cTnI assay has been developed which is only minimally impacted by the cTnAAbs, which cause negative interference in many commercial cTnI assays (Eriksson et al. 2005b; Savukoski et al. 2012). Also available are the new high-sensitivity cardiac troponin assays capable of detecting minute amounts of troponin. In this present study, we sought to establish whether long-term CCSs harbor troponin in plasma as a sign of cardiotoxicity. Based on the results obtained using three sensitive troponin methods we were able to document the absence of detectable troponin levels during late pediatric follow-up of our CCSs. Nevertheless, with the majority of the CCSs showing abnormal cardiac function with RT-3DE and/or CMR, we can state that cardiac troponin measured years after malignancy treatment offers no additional information over imaging in the screening of cardiotoxicity in children and adolescents.

This study is the first to evaluate the presence of cTnAAbs among CCSs. Of the present cohort, 5% (n = 4) were cTnAAb-positive, when in the sole published study on healthy children none proved positive (Eerola et al. 2014). This notwithstanding, cTnAAbs have been detected in apparently healthy adults (Adamczyk et al. 2009). Our cTnAAb-positive CCSs had an abnormal LV EF and abnormally large ESVs in both ventricles by CMR, even in the absence of traditional risk factors for anthracycline-induced cardiotoxicity. Interestingly, all four cTnAAb-positive survivors had had a previous ALL diagnosis. Even though the number is small, the question arises whether cTnAAb formation is due to the

pathogenetic mechanisms of ALL, the malignancy therapy used in ALL, or only a coincidence. Data are accruing on autoimmunity mechanisms (Caforio et al. 2013), and cTnAAbs in the pathogenesis of cardiomyopathy and myocarditis (Goser et al. 2006; Okazaki et al. 2003). Oxidative stress is the most plausible mechanism behind anthracycline-induced cardiomyopathy, but other putative mechanisms exist.

6.4 Cardiac longitudinal function (Study IV)

Our study unequivocally demonstrates anthracycline-exposed CCSs to have impaired longitudinal systolic and diastolic function in both ventricles compared with healthy controls. The contribution of the longitudinal function to the global ventricular function was shown here, as the CCSs with abnormal LV EF by RT-3DE or CMR had a lower MAD mid% compared with those with a normal LV EF. In addition, all those with an abnormal TAD mid%, as a sign of decreased RV longitudinal function, also had an abnormal RV EF. Longitudinal function constitutes a key proportion of the LV and RV function. Diastolic function represents the ability of the ventricle to fill, and thus affects the systolic function. Diastolic dysfunction often precedes systolic dysfunction.

We used TDI- and STE-based methods in assessment of the cardiac longitudinal function. Using both we showed decreased LV longitudinal function among the CCSs and especially among those exposed to cardiac irradiation. The location of subendocardial myofibers may influence their susceptibility to toxic impact, including irradiation (Henein and Gibson 1999; Suzuki et al. 2012). Our results are in line with previous TDI data on anthracycline-exposed CCSs, showing diminished LV systolic (Cheung et al. 2010), diastolic (Ganame et al. 2007) or RV diastolic function (Stapleton et al. 2007).

Other STE-based methods have documented decreased longitudinal strain among CCSs (Cheung et al. 2010; Mavinkurve-Groothuis et al. 2010; Moon et al. 2014), but the present study is the first to report on RV function. It is also the first to demonstrate a correlation between the STE-based LV displacement parameter (MAD mid) with RT-3DE and CMR-derived LV volumes.

The echocardiographic parameters measuring the longitudinal systolic function of the lateral wall of the RV (TAPSE, S` lateral RV and TAD lateral) did not differ between CCSs and controls here, but the parameters measuring the septal or combined RV longitudinal function (TAD septal, mid and mid%) were lower among the former. We thus take the decreased RV longitudinal function to result mainly from the decreased displacement of the septal side of the RV. Through

systolic ventricular interaction, impaired LV systolic function may be a key contributor to the deficit in RV longitudinal function on the septal side (Haddad et al. 2008).

The TDI appears to be superior to mitral and tricuspid inflow velocities in the detection of diastolic dysfunction. These inflow velocities failed to show differences between our CCSs and their controls, while TDI demonstrated a decreased diastolic function in both ventricles among the former. A ratio of mitral inflow early diastolic velocity to early diastolic velocity of the mitral annulus by TDI (E/E`) ≥ 15 has reflected an increased mean LV diastolic pressure in invasive analysis (Ommen et al. 2000). None of our CCSs had an E/E`of such magnitude, but their values were higher compared with those of healthy controls, indicating a subtle decline in diastolic function.

The TDI is age-, load- and angle-dependent with a one-dimensional nature. Normal values for TDI parameters among children vary greatly, with additional variability between the velocities measured by different ultrasound systems (Koopman et al. 2010a). Despite this, TDI offers a useful tool for the serial assessment of the same patient to show a trend.

The STE-based TMAD enables a timely assessment of both LV and RV longitudinal function. Angle-independency, two-dimensional nature and good reproducibility make STE superior to TDI (Koopman et al. 2010a). The TAPSE and TDI represent regional function, whereas TMAD measures global longitudinal function. TMAD analysis can also be made on a four-chamber view, thus being a suitable imaging method for children with limited imaging time. Also two-chamber views have been used (Tsang et al. 2010). TMAD analysis is especially useful in RV, because its volumes and EF are difficult to measure. The analysis takes into account size difference of the heart, as MAD and TAD mid% normalize the displacement in relation to the length of the ventricle.

Intra- and inter-observer variability for MAD mid and TAD mid (mm) in our study was low, and in accord with previous reports (Black et al. 2013; Suzuki et al. 2012). For both MAD and TAD mid, intra-observer variability was lower than inter-observer variability, and differences between measurements observed remained within the limits of agreement.

6.5 Strengths and limitations of the study

In our set of studies, we comprehensively evaluated the cardiac function of anthracycline-exposed long-term CCSs with modern imaging and a diversity of cardiac biomarkers. The study population was representative of the patients treated

in a tertiary pediatric center (Tampere University Hospital), with only 12% of patients recruited declining to participate. The study patients were treated in the modern era, without markedly high anthracycline or radiation doses, thus representing the state-of-the-art trend in pediatric oncology.

The present Study I is the first and thus far the largest study on cardiac function and LGE assessed with CMR among CCSs of pediatric age. The LGE was assessed by two different methods and two radiologists. The focus was on the RV function, largely neglected in the cardiac follow-up of CCSs. Since we were not authorized to perform CMR on our healthy controls we used published reference values, allowing us the inclusion of age, gender and size of patient in the analysis.

In the absence of published reference values for many of the echocardiographic parameters, especially it the pediatric population, we used gender, BSA- and age-matched healthy controls (Studies II and IV). We obtained the RT-3DE images for the LV, and in addition to the EF, also reported on the LV volumes and dyssynchrony indices. For the majority of our CCSs we were able to compare the RT-3DE-derived LV EF and volumes with those derived from CMR. We chose to compare the RT-3DE with M-mode-derived FS, the established method in our clinical practice. The dyssynchrony analysis in our study was based solely on RT-3DE. Exercise tolerance assessment was based only on the subjective estimation of the survivors.

In Study IV, we used three different methods for cTn simultaneously, but also carefully appraised the impact of cTnAAbs. With this large study population and the sensitive cTn methods used, we could indisputably demonstrate troponins measured at the late follow-up of pediatric age of CCSs to give no additional information on cardiotoxicity as compared to imaging. The use of sensitive imaging, CMR and RT-3DE, as reference method for measuring cardiac function was also one of the strengths of this study. In the absence of data on the cardiac biomarkers among our control population we used published gender- and age-specific reference values for NT-proBNP, while none was available for cTns or cTnAAbs.

Our analysis of cardiac longitudinal function was comprehensive and covered both ventricles (Study IV). We used well-established echocardiographic methods (i.e. TDI and M-mode), but also the more novel STE-based TMAD method, and were able to relate the results with the global LV and RV function by RT-3DE and/or CMR. A lack of fractional area change in the evaluation of global RV function was one of the limitations of this study.

6.6 Future considerations

CCSs will need screening for cardiotoxicity until a sensitive and specific test to detect individuals at increased risk of treatment-related cardiotoxicity is found. From the clinical point of view, it would be crucial to ascertain the stage of cardiotoxicity when changes are still reversible. A previous study on adults with hypertension showed that treatment with lisinopril may have some anti-fibrotic effects (Brilla et al. 2000). Further research is needed to show whether diffuse fibrosis detected by CMR in anthracycline-exposed CCS could also be detected by echocardiographic methods or biomarkers, and whether medicine therapy could induce regression in diffuse fibrosis. Furthermore, the impact of diffuse fibrosis on dyssynchrony indices warrants further research.

The possible role of cTnAAbs in the pathogenesis of cardiotoxicity should be more thoroughly explored. In addition, more research is needed to establish whether the immunologic mechanisms involved in the pathogenesis of ALL influence cTnAAb formation. Prospective studies with hs-cTnT during cancer treatment may reveal new information on myocardial damage and its contribution to the development of cTnAAb. However, long-term follow-up is also needed to confirm the impact of cTnAAbs on cardiac function.

The TMAD method for the assessment of cardiac function is fast, which is important in children with limited co-operation. However, more studies are required to assess how TMAD parameters correlate with global longitudinal strain in LV and RV in hearts with normal and severely impaired function. Finally, the feasibility of TAD mid% compared with fractional area change in the assessment of RV function after childhood cancer should be evaluated.

7. Summary and conclusions

On the basis of our set of studies the following conclusions can be drawn:

1. A considerable proportion of the long-term survivors of childhood cancer exposed to anthracyclines have an impaired LV and/or RV function by CMR. However, LGE as a sign of focal fibrosis cannot be found nor diffuse fibrosis ruled out. An increase in the end-systolic volumes by CMR is a common finding, especially for the LV.
2. RT-3DE reveals a lower LV EF and a larger LV ESV among anthracycline-exposed long-term CCSs compared with matched healthy controls. It is possible to obtain optimal images for an LV analysis by RT-3DE among children and adolescents. RT-3DE seems to be more sensitive than M-mode in the screening of abnormal LV function.
3. Elevated NT-proBNP levels in the late follow-up after anthracycline exposure indicate a need for sensitive cardiac imaging by RT-3DE or CMR despite normal function in conventional echocardiography, cardiac irradiation also apparently being associated with an increased NT-proBNP. However, while NT-proBNP cannot act as the sole screening method, it is able to complement conventional echocardiography. cTnAAbs appear in survivors in conjunction with enlarged LV volumes.
4. Anthracycline-exposure is associated with impaired systolic and diastolic LV and RV function at the late follow-up. The LV longitudinal function appears particularly susceptible to cardiac irradiation. TMAD is fast and reproducible in the assessment of cardiac longitudinal systolic function among anthracycline-exposed children.
5. Cancer treatment at young age has an adverse long-term impact on LV and RV function despite the fact that anthracycline and cardiac irradiation doses have been reduced during the last few decades. The majority of the CCSs here had signs of cardiotoxicity as seen with sensitive screening methods, even while asymptomatic.

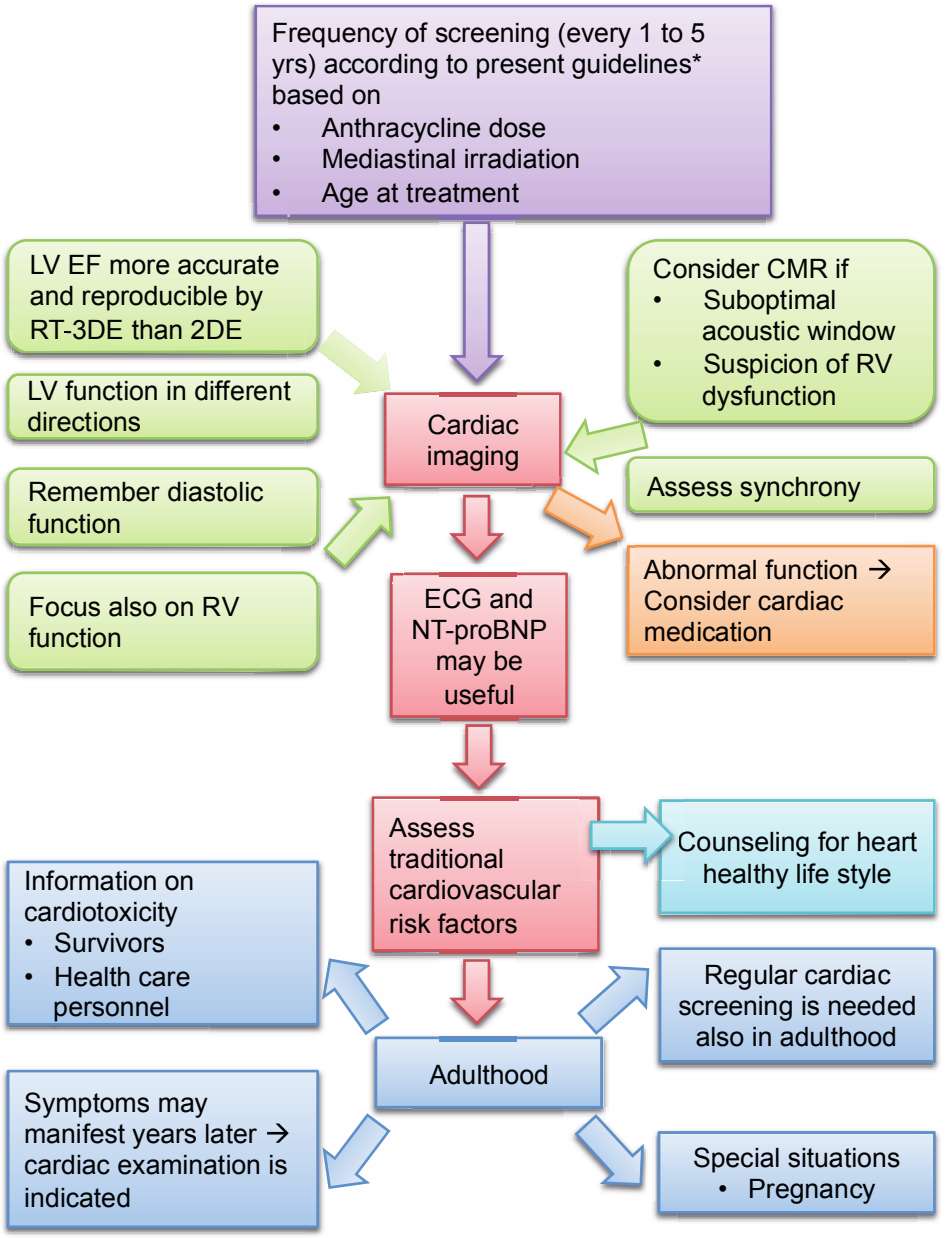

Figure 12. The author`s conception of optimal cardiac screening after childhood cancer.

*http://www.survivorshipguidelines.org

2DE, two-dimensional echocardiography; CMR, cardiac magnetic resonance; ECG, electrocardiogram; EF, ejection fraction; LV, left ventricular; NT-proBNP, N-terminal pro-brain natriuretic peptide; RT-3DE, real-time three-dimensional echocardiography; RV, right ventricular.

8. Acknowledgements

This doctoral work was carried out at the Department of Pediatrics, Tampere University Hospital, at the School of Medicine in the University of Tampere, and at the National Graduate School of Clinical Investigation.

I wish to thank Professor Matti Korppi, M.D., and Professor Markku Mäki, M.D., for creating a positive atmosphere for clinical research at the Pediatric Unit of the Tampere University Hospital. Professor Korppi has always a positive way of looking at things, and finds a solution to every problem. I deeply respect Professor Mäki, who has made a brilliant career in the field of science. I also wish to express my gratitude to the former and present heads of the Department of Pediatrics, Anna-Leena Kuusela, M.D., and Docent Merja Helminen, M.D., for trusting me as a researcher, and providing me with the necessary working facilities.

I wish to express my deepest gratitude to my supervisors, Docent Kim Vettenranta, M.D., and Tuija Poutanen, M.D., for introducing me into the world of scientific work. Kim is an extremely efficient and systematic supervisor, who never loses his nerve. Tuija has been my teacher in pediatric cardiology and echocardiography. She has also taught me other important things in life, such as running to the bus, and how to eat the moon one slice at a time. I am also grateful to my unofficial supervisor, Anneli Eerola, M.D., whose contribution to this research project was crucial. Her knowledge of echocardiography and the systematic approach to scientific writing has often helped me forward during this project.

I express my sincere thanks to my other co-writers Päivi Savikurki-Heikkilä, M.D., Irina Rinta-Kiikka, M.D., and Tanja Savukoski, M.Sc., for their valuable contributions to the articles. I warmly thank Heini Huhtala, M.Sc., for clear answers to my statistical problems.

I owe a debt of gratitude to Docent Tiina Ojala, M.D., and Docent Ulla Wartiovaara-Kautto, M.D., the official referees of this dissertation. Their careful review of this thesis and constructive criticism helped me to improve the quality of the work.

I am grateful to the personnel of the Pediatric Hematology-Oncology Unit of the Tampere University Hospital, for good collaboration in the organization of timetables for the study patients. I wish to express special gratitude to research

nurse Satu Ranta, who has helped me greatly with practical assistance. Every researcher should have a research nurse like Satu.

I am indebted to many people who have helped me during this project: to Docent Marja-Leena Lähdeaho, M.D., for being a very supportive member of the follow-up group, together with Professor Korppi; to Docent Kirsi Lauerma, M.D., for expert advice on CMR techniques; to Tuija Wigren, M.D., for help with the radiation therapy case histories; to research coordinator Mrs. Paula Vihtamäki for helping with permission applications; to secretary Mrs. Anita Severinkangas for saving me from paper work; to Mr. Vesa Laiho from Philips for always finding time and answers to my countless questions about ultrasound machines and analyzing programs, and to Mr. Robert MacGilleon, M.A., for careful revision of the English of this thesis.

I wish to express my profoundest gratitude to the participants and their parents who made this research project possible. My deepest wish is that the results of this study could be of benefit to all children who have survived childhood cancer.

I warmly thank all my colleagues in the Pediatric Unit of Tampere University Hospital for their supportive and positive attitude to my project.

I warmly thank my relatives and friends. I thank with love and respect my parents, Raija and Erkki Hottola, for trusting me and giving me the opportunity to find my own way. To my fantastic friends, Satu, Niina, and the Crazy Ladies from the years in Kuopio, who have regularly pulled me out from the chamber of the researcher.

Finally, I am most grateful to my family. To my dear husband, Antero, who has stood by me all these long years full of work, taking care of our children and me. I could not have managed this project without your help with the computers. My dear children, Aksu, Kalle and Siiri, you are the joy of my life, and you have filled my life with love.

Finally I wish to acknowledge the financial support granted during my work on this thesis by the The Blood Disease Research Foundation, the Competitive Research Funding of Tampere University Hospital [9L114 and 9N084], the EVO funds of Tampere University Hospital, the Emil Aaltonen Foundation, the Finnish Association of Hematology, the Finnish Cancer Foundation, the Finnish Cultural Foundation, the Finnish Cultural Foundation Pirkanmaa Regional Fund, the Finnish Medical Foundation, the Foundation for Pediatric Research, the Päivikki and Sakari Sohlberg Foundation, the Scientific Foundation of the City of Tampere, and the Väre Foundation for Pediatric Cancer.

Tampere, March 2015

Kaisa Ylänen

9. References

Abali G, Tokgozoglu L, Ozcebe OI, Aytemir K, Nazli N. 2005. Which Doppler parameters are load independent? A study in normal volunteers after blood donation. J Am Soc Echocardiogr 18:1260-5.

Adamczyk M, Brashear RJ, Mattingly PG. 2009. Circulating cardiac troponin-I autoantibodies in human plasma and serum. Ann N Y Acad Sci 1173:67-74.

Adams MJ, Lipsitz SR, Colan SD, Tarbell NJ, Treves ST, Diller L, Greenbaum N, Mauch P, Lipshultz SE. 2004. Cardiovascular status in long-term survivors of Hodgkin's disease treated with chest radiotherapy. J Clin Oncol 22:3139-48.

Ahmad H, Mor-Avi V, Lang RM, Nesser HJ, Weinert L, Tsang W, Steringer-Mascherbauer R, Niel J, Salgo IS, Sugeng L. 2012. Assessment of right ventricular function using echocardiographic speckle tracking of the tricuspid annular motion: Comparison with cardiac magnetic resonance. Echocardiography 29:19-24.

Alfakih K, Plein S, Bloomer T, Jones T, Ridgway J, Sivananthan M. 2003a. Comparison of right ventricular volume measurements between axial and short axis orientation using steady-state free precession magnetic resonance imaging. J Magn Reson Imaging 18:25-32.

Alfakih K, Plein S, Thiele H, Jones T, Ridgway JP, Sivananthan MU. 2003b. Normal human left and right ventricular dimensions for MRI as assessed by turbo gradient echo and steady-state free precession imaging sequences. J Magn Reson Imaging 17:323-9.

American College of Cardiology Foundation Task Force on Expert Consensus, Documents, Hundley WG, Bluemke DA, Finn JP, Flamm SD, Fogel MA, Friedrich MG, Ho VB, Jerosch-Herold M, Kramer CM, et al. 2010. ACCF/ACR/AHA/NASCI/SCMR 2010 expert consensus document on cardiovascular magnetic resonance: A report of the American College of Cardiology Foundation task force on expert consensus documents. J Am Coll Cardiol 55:2614-62.

Apple FS. 2009. A new season for cardiac troponin assays: It's time to keep a scorecard. Clin Chem 55:1303-6.

Apple FS, Simpson PA, Murakami MM. 2010. Defining the serum 99th percentile in a normal reference population measured by a high-sensitivity cardiac troponin I assay. Clin Biochem 43:1034-6.

Armenian SH, Gelehrter SK, Vase T, Venkatramani R, Landier W, Wilson KD, Herrera C, Reichman L, Menteer JD, Mascarenhas L, et al. 2014. Screening for cardiac dysfunction in anthracycline-exposed childhood cancer survivors. Clin Cancer Res clincanres.3490.2014.

Armstrong GT, Liu Q, Yasui Y, Neglia JP, Leisenring W, Robison LL, Mertens AC. 2009. Late mortality among 5-year survivors of childhood cancer: A summary from the childhood cancer survivor study. J Clin Oncol 27:2328-38.

Armstrong GT, Plana JC, Zhang N, Srivastava D, Green DM, Ness KK, Daniel Donovan F, Metzger ML, Arevalo A, Durand JB, et al. 2012. Screening adult survivors of childhood cancer for cardiomyopathy: Comparison of echocardiography and cardiac magnetic resonance imaging. J Clin Oncol 30:2876-84.

Armstrong GT, Joshi VM, Zhu L, Srivastava D, Zhang N, Ness KK, Stokes DC, Krasin MT, Fowler JA, Robison LL, et al. 2013. Increased tricuspid regurgitant jet velocity by doppler echocardiography in adult survivors of childhood cancer: A report from the st jude lifetime cohort study. J Clin Oncol 31:774-81.

Assomull RG, Prasad SK, Lyne J, Smith G, Burman ED, Khan M, Sheppard MN, Poole-Wilson PA, Pennell DJ. 2006. Cardiovascular magnetic resonance, fibrosis, and prognosis in dilated cardiomyopathy. J Am Coll Cardiol 48:1977-85.

Assomull RG, Lyne JC, Keenan N, Gulati A, Bunce NH, Davies SW, Pennell DJ, Prasad SK. 2007a. The role of cardiovascular magnetic resonance in patients presenting with chest pain, raised troponin, and unobstructed coronary arteries. Eur Heart J 28:1242-9.

Assomull RG, Pennell DJ, Prasad SK. 2007b. Cardiovascular magnetic resonance in the evaluation of heart failure. Heart 93:985-92.

Bell A, Rawlins D, Bellsham-Revell H, Miller O, Razavi R, Simpson J. 2014. Assessment of right ventricular volumes in hypoplastic left heart syndrome by real-time three-dimensional echocardiography: Comparison with cardiac magnetic resonance imaging. Eur Heart J Cardiovasc Imaging 15:257-66.

Belloni E, De Cobelli F, Esposito A, Mellone R, Perseghin G, Canu T, Del Maschio A. 2008. MRI of cardiomyopathy. AJR Am J Roentgenol 191:1702-10.

Berin R, Zafrir B, Salman N, Amir O. 2014. Single measurement of serum N-terminal pro-brain natriuretic peptide: The best predictor of long-term mortality in patients with chronic systolic heart failure. Eur J Intern Med 25:458-62.

Black D, Bryant J, Peebles C, Godfrey K, Hanson M, Vettukattil J. 2013. Tissue motion annular displacement of the mitral valve using two-dimensional speckle tracking echocardiography predicts the left ventricular ejection fraction in normal children. Cardiol Young 27:1-9.

Blanco JG, Sun CL, Landier W, Chen L, Esparza-Duran D, Leisenring W, Mays A, Friedman DL, Ginsberg JP, Hudson MM, et al. 2012. Anthracycline-related cardiomyopathy after childhood cancer: Role of polymorphisms in carbonyl reductase genes--A report from the children's oncology group. J Clin Oncol 30:1415-21.

Bland JM and Altman DG. 1986. Statistical methods for assessing agreement between two methods of clinical measurement. Lancet 1:307-10.

Bohs LN and Trahey GE. 1991. A novel method for angle independent ultrasonic imaging of blood flow and tissue motion. IEEE Trans Biomed Eng 38:280-6.

Brilla CG, Funck RC, Rupp H. 2000. Lisinopril-mediated regression of myocardial fibrosis in patients with hypertensive heart disease. Circulation 102:1388-93.

Brouwer CA, Postma A, Vonk JM, Zwart N, van den Berg MP, Bink-Boelkens MT, Dolsma WV, Smit AJ, de Vries EG, Tissing WJ, et al. 2011. Systolic and diastolic dysfunction in long-term adult survivors of childhood cancer. Eur J Cancer 47:2453-62.

Bu L, Munns S, Zhang H, Disterhoft M, Dixon M, Stolpen A, Sonka M, Scholz TD, Mahoney LT, Ge S. 2005. Rapid full volume data acquisition by real-time 3-dimensional echocardiography for assessment of left ventricular indexes in children: A validation study compared with magnetic resonance imaging. J Am Soc Echocardiogr 18:299-305.

Buechel EV, Kaiser T, Jackson C, Schmitz A, Kellenberger CJ. 2009. Normal right- and left ventricular volumes and myocardial mass in children measured by steady state free precession cardiovascular magnetic resonance. J Cardiovasc Magn Reson 11:19.

Bukkapatnam RN, Robinson M, Turnipseed S, Tancredi D, Amsterdam E, Srivatsa UN. 2010. Relationship of myocardial ischemia and injury to coronary artery disease in patients with supraventricular tachycardia. Am J Cardiol 106:374-7.

Caforio AL, Pankuweit S, Arbustini E, Basso C, Gimeno-Blanes J, Felix SB, Fu M, Helio T, Heymans S, Jahns R, et al. 2013. Current state of knowledge on aetiology, diagnosis, management, and therapy of myocarditis: A position statement of the European Society of Cardiology working group on myocardial and pericardial diseases. Eur Heart J 34:2636-48.

Cardinale D, Sandri MT, Martinoni A, Tricca A, Civelli M, Lamantia G, Cinieri S, Martinelli G, Cipolla CM, Fiorentini C. 2000. Left ventricular dysfunction predicted by early troponin I release after high-dose chemotherapy. J Am Coll Cardiol 36:517-22.

Cardinale D, Colombo A, Sandri MT, Lamantia G, Colombo N, Civelli M, Martinelli G, Veglia F, Fiorentini C, Cipolla CM. 2006. Prevention of high-dose chemotherapy-induced cardiotoxicity in high-risk patients by angiotensin-converting enzyme inhibition. Circulation 114:2474-81.

Cascales A, Pastor-Quirante F, Sanchez-Vega B, Luengo-Gil G, Corral J, Ortuno-Pacheco G, Vicente V, de la Pena FA. 2013. Association of anthracycline-related cardiac histological lesions with NADPH oxidase functional polymorphisms. Oncologist 18:446-53.

Catalano O, Antonaci S, Opasich C, Moro G, Mussida M, Perotti M, Calsamiglia G, Frascaroli M, Baldi M, Cobelli F. 2007. Intra-observer and interobserver reproducibility of right ventricle volumes, function and mass by cardiac magnetic resonance. J Cardiovasc Med (Hagerstown) 8:807-14.

Cerqueira MD, Weissman NJ, Dilsizian V, Jacobs AK, Kaul S, Laskey WK, Pennell DJ, Rumberger JA, Ryan T, Verani MS, et al. 2002. Standardized myocardial segmentation and nomenclature for tomographic imaging of the heart: A statement for healthcare professionals from the cardiac imaging committee of the Council on Clinical Cardiology of the American Heart Association. Circulation 105:539-42.

Chahal NS, Lim TK, Jain P, Chambers JC, Kooner JS, Senior R. 2012. Population-based reference values for 3D echocardiographic LV volumes and ejection fraction. JACC Cardiovasc Imaging 5:1191-7.

Chen CA, Hsiao CH, Wang JK, Lin MT, Wu ET, Chiu SN, Chiu HH, Wu MH. 2009. Implication of QRS prolongation and its relation to mechanical dyssynchrony in idiopathic dilated cardiomyopathy in childhood. Am J Cardiol 103:103-9.

Chen Y, Daosukho C, Opii WO, Turner DM, Pierce WM, Klein JB, Vore M, Butterfield DA, St Clair DK. 2006. Redox proteomic identification of oxidized cardiac proteins in adriamycin-treated mice. Free Radic Biol Med 41:1470-7.

Cheung YF, Hong WJ, Chan GC, Wong SJ, Ha SY. 2010. Left ventricular myocardial deformation and mechanical dyssynchrony in children with normal ventricular shortening fraction after anthracycline therapy. Heart 96:1137-41.

Cheung YF, Li SN, Chan GC, Wong SJ, Ha SY. 2011. Left ventricular twisting and untwisting motion in childhood cancer survivors. Echocardiography 28:738-45.

Cheung YF, Yu W, Cheuk DK, Cheng FW, Yang JY, Yau JP, Ho KK, Li CK, Li RC, Yuen HL, et al. 2013. Plasma high sensitivity troponin T levels in adult survivors of childhood leukaemias: Determinants and associations with cardiac function. PLoS ONE 8:e77063.

Christiansen JR, Hamre H, Massey R, Dalen H, Beitnes JO, Fossa SD, Kiserud CE, Aakhus S. 2014. Left ventricular function in long-term survivors of childhood lymphoma. Am J Cardiol 114:483-90.

Clark SJ, Pippon M, Hemsworth S, Newland P, Pizer B. 2007. Cardiac troponin T following anthracycline chemotherapy in children and adolescents. J Chemother 19:332-4.

Coats CJ, Gallagher MJ, Foley M, O'Mahony C, Critoph C, Gimeno J, Dawnay A, McKenna WJ, Elliott PM. 2013. Relation between serum N-terminal pro-brain natriuretic peptide and prognosis in patients with hypertrophic cardiomyopathy. Eur Heart J 34:2529-37.

Cranney GB, Lotan CS, Dean L, Baxley W, Bouchard A, Pohost GM. 1990. Left ventricular volume measurement using cardiac axis nuclear magnetic resonance imaging. validation by calibrated ventricular angiography. Circulation 82:154-63.

Creutzig U, Diekamp S, Zimmermann M, Reinhardt D. 2007. Longitudinal evaluation of early and late anthracycline cardiotoxicity in children with AML. Pediatr Blood Cancer 48:651-62.

Cui W, Gambetta K, Zimmerman F, Freter A, Sugeng L, Lang R, Roberson DA. 2010. Real-time three-dimensional echocardiographic assessment of left ventricular systolic dyssynchrony in healthy children. J Am Soc Echocardiogr 23:1153-9.

Danilouchkine MG, Westenberg JJ, de Roos A, Reiber JH, Lelieveldt BP. 2005. Operator induced variability in cardiovascular MR: Left ventricular measurements and their reproducibility. J Cardiovasc Magn Reson 7:447-57.

De Angelis A, Piegari E, Cappetta D, Marino L, Filippelli A, Berrino L, Ferreira-Martins J, Zheng H, Hosoda T, Rota M, et al. 2010. Anthracycline cardiomyopathy is mediated by depletion of the cardiac stem cell pool and is rescued by restoration of progenitor cell function. Circulation 121:276-92.

de Simone G, Daniels SR, Devereux RB, Meyer RA, Roman MJ, de Divitiis O, Alderman MH. 1992. Left ventricular mass and body size in normotensive children and adults: Assessment of allometric relations and impact of overweight. J Am Coll Cardiol 20:1251-60.

DeCara JM, Toledo E, Salgo IS, Lammertin G, Weinert L, Lang RM. 2005. Evaluation of left ventricular systolic function using automated angle-independent motion tracking of mitral annular displacement. J Am Soc Echocardiogr 18:1266-9.

Dekker DL, Piziali RL, Dong E,Jr. 1974. A system for ultrasonically imaging the human heart in three dimensions. Comput Biomed Res 7:544-53.

Devereux RB, Alonso DR, Lutas EM, Gottlieb GJ, Campo E, Sachs I, Reichek N. 1986. Echocardiographic assessment of left ventricular hypertrophy: Comparison to necropsy findings. Am J Cardiol 57:450-8.

Doesch AO, Mueller S, Nelles M, Konstandin M, Celik S, Frankenstein L, Goeser S, Kaya Z, Koch A, Zugck C, et al. 2011. Impact of troponin I-autoantibodies in chronic dilated and ischemic cardiomyopathy. Basic Res Cardiol 106:25-35.

Dorosz JL, Lezotte DC, Weitzenkamp DA, Allen LA, Salcedo EE. 2012. Performance of 3-dimensional echocardiography in measuring left ventricular volumes and ejection fraction: A systematic review and meta-analysis. J Am Coll Cardiol 59:1799-808.

Dungen HD, Platzeck M, Vollert J, Searle J, Muller C, Reiche J, Mehrhof F, Muller R, Mockel M. 2010. Autoantibodies against cardiac troponin I in patients with congestive heart failure. Eur J Heart Fail 12:668-75.

Edvardsen T, Helle-Valle T, Smiseth OA. 2006. Systolic dysfunction in heart failure with normal ejection fraction: Speckle-tracking echocardiography. Prog Cardiovasc Dis 49:207-14.

Eerola A, Jokinen E, Boldt T, Mattila IP, Pihkala JI. 2010. Serum levels of natriuretic peptides in children before and after treatment for an atrial septal defect, a patent ductus arteriosus, and a coarctation of the aorta-A prospective study. Int J Pediatr 2010:674575.

Eerola A, Poutanen T, Savukoski T, Pettersson K, Sairanen H, Jokinen E, Pihkala J. 2014. Cardiac troponin I, cardiac troponin-specific autoantibodies and natriuretic peptides in children with hypoplastic left heart syndrome. Interact Cardiovasc Thorac Surg 18:80-5.

Eidem BW, McMahon CJ, Cohen RR, Wu J, Finkelshteyn I, Kovalchin JP, Ayres NA, Bezold LI, O'Brian Smith E, Pignatelli RH. 2004. Impact of cardiac growth on doppler tissue imaging velocities: A study in healthy children. J Am Soc Echocardiogr 17:212-21.

Eidem BW, McMahon CJ, Ayres NA, Kovalchin JP, Denfield SW, Altman CA, Bezold LI, Pignatelli RH. 2005. Impact of chronic left ventricular preload and afterload on doppler tissue imaging velocities: A study in congenital heart disease. J Am Soc Echocardiogr 18:830-8.

Eindhoven JA, van den Bosch AE, Jansen PR, Boersma E, Roos-Hesselink JW. 2012. The usefulness of brain natriuretic peptide in complex congenital heart disease: A systematic review. J Am Coll Cardiol 60:2140-9.

Ekstein S, Nir A, Rein AJ, Perles Z, Bar-Oz B, Salpeter L, Algur N, Weintraub M. 2007. N-terminal-proB-type natriuretic peptide as a marker for acute anthracycline cardiotoxicity in children. J Pediatr Hematol Oncol 29:440-4.

Erer HB, Guvenc TS, Kemik AS, Yilmaz HY, Kul S, Altay S, Sayar N, Kaya Y, Eren M. 2013. Troponin and anti-troponin autoantibody levels in patients with ventricular noncompaction. PLoS ONE 8:e57648.

Eriksson S, Halenius H, Pulkki K, Hellman J, Pettersson K. 2005a. Negative interference in cardiac troponin I immunoassays by circulating troponin autoantibodies. Clin Chem 51:839-47.

Eriksson S, Ilva T, Becker C, Lund J, Porela P, Pulkki K, Voipio-Pulkki LM, Pettersson K. 2005b. Comparison of cardiac troponin I immunoassays variably affected by circulating autoantibodies. Clin Chem 51:848-55.

Fink FM, Genser N, Fink C, Falk M, Mair J, Maurer-Dengg K, Hammerer I, Puschendorf B. 1995. Cardiac troponin T and creatine kinase MB mass concentrations in children receiving anthracycline chemotherapy. Med Pediatr Oncol 25:185-9.

Flett AS, Hayward MP, Ashworth MT, Hansen MS, Taylor AM, Elliott PM, McGregor C, Moon JC. 2010. Equilibrium contrast cardiovascular magnetic resonance for the measurement of diffuse myocardial fibrosis: Preliminary validation in humans. Circulation 122:138-44.

Franklin RC, Wyse RK, Graham TP, Gooch VM, Deanfield JE. 1990. Normal values for noninvasive estimation of left ventricular contractile state and afterload in children. Am J Cardiol 65:505-10.

Fratz S, Schuhbaeck A, Buchner C, Busch R, Meierhofer C, Martinoff S, Hess J, Stern H. 2009. Comparison of accuracy of axial slices versus short-axis slices for measuring ventricular volumes by cardiac magnetic resonance in patients with corrected tetralogy of Fallot. Am J Cardiol 103:1764-9.

Friedberg MK and Mertens L. 2013. Echocardiographic assessment of ventricular synchrony in congenital and acquired heart disease in children. Echocardiography 30:460-71.

Friedberg MK, Su X, Tworetzky W, Soriano BD, Powell AJ, Marx GR. 2010. Validation of 3D echocardiographic assessment of left ventricular volumes, mass, and ejection fraction in neonates and infants with congenital heart disease: A comparison study with cardiac MRI. Circ Cardiovasc Imaging 3:735-42.

Fukuta H and Little WC. 2008. The cardiac cycle and the physiologic basis of left ventricular contraction, ejection, relaxation, and filling. Heart Fail Clin 4:1-11.

Ganame J, Claus P, Uyttebroeck A, Renard M, D'hooge J, Bijnens B, Sutherland GR, Eyskens B, Mertens L. 2007. Myocardial dysfunction late after low-dose anthracycline treatment in asymptomatic pediatric patients. J Am Soc Echocardiogr 20:1351-8.

Garcia MJ. 2008. Left ventricular filling. Heart Fail Clin 4:47-56.

Gatta G, Zigon G, Capocaccia R, Coebergh JW, Desandes E, Kaatsch P, Pastore G, Peris-Bonet R, Stiller CA, EUROCARE Working G. 2009. Survival of European children and young adults with cancer diagnosed 1995-2002. Eur J Cancer 45:992-1005.

Ghosh A, Nanda NC, Maurer G. 1982. Three-dimensional reconstruction of echo-cardiographic images using the rotation method. Ultrasound Med Biol 8:655-61.

Gorcsan J,3rd, Gulati VK, Mandarino WA, Katz WE. 1996. Color-coded measures of myocardial velocity throughout the cardiac cycle by tissue doppler imaging to quantify regional left ventricular function. Am Heart J 131:1203-13.

Goser S, Andrassy M, Buss SJ, Leuschner F, Volz CH, Ottl R, Zittrich S, Blaudeck N, Hardt SE, Pfitzer G, et al. 2006. Cardiac troponin I but not cardiac troponin T induces severe autoimmune inflammation in the myocardium. Circulation 114:1693-702.

Grothues F, Smith GC, Moon JC, Bellenger NG, Collins P, Klein HU, Pennell DJ. 2002. Comparison of interstudy reproducibility of cardiovascular magnetic resonance with two-dimensional echocardiography in normal subjects and in patients with heart failure or left ventricular hypertrophy. Am J Cardiol 90:29-34.

Haddad F, Hunt SA, Rosenthal DN, Murphy DJ. 2008. Right ventricular function in cardiovascular disease, part I: Anatomy, physiology, aging, and functional assessment of the right ventricle. Circulation 117:1436-48.

Harada M, Saito Y, Kuwahara K, Ogawa E, Ishikawa M, Nakagawa O, Miyamoto Y, Kamitani S, Hamanaka I, Kajiyama N, et al. 1998. Interaction of myocytes and nonmyocytes is necessary for mechanical stretch to induce ANP/BNP production in cardiocyte culture. J Cardiovasc Pharmacol 31:S357-9.

Helbing WA, Rebergen SA, Maliepaard C, Hansen B, Ottenkamp J, Reiber JH, de Roos A. 1995. Quantification of right ventricular function with magnetic resonance imaging in children with normal hearts and with congenital heart disease. Am Heart J 130:828-37.

Henein MY and Gibson DG. 1999. Long axis function in disease. Heart 81:229-31.

Higgins CB. 1992. Which standard has the gold?. J Am Coll Cardiol 19:1608-9.
Ho CY and Solomon SD. 2006. A clinician's guide to tissue Doppler imaging. Circulation 113:e396-8.

Ho PK, Lai CT, Wong SJ, Cheung YF. 2012. Three-dimensional mechanical dyssynchrony and myocardial deformation of the left ventricle in patients with tricuspid atresia after Fontan procedure. J Am Soc Echocardiogr 25:393-400.

Hollander Z. Lazarova M. Lam KK. Ignaszewski A. Oudit GY. Dyck JR. Schreiner G. Pauwels J. Chen V. Cohen Freue GV. Ng RT. Wilson-McManus JE. Balshaw R. Tebbutt SJ. McMaster RW. Keown PA. McManus BM. NCE CECR PROOF Prevention of Organ Failure (PROOF) Centre of Excellence. 2014. Proteomic biomarkers of recovered heart function. Eur J Heart Fail 16:551-9.

Holmberg SR and Williams AJ. 1990. Patterns of interaction between anthraquinone drugs and the calcium-release channel from cardiac sarcoplasmic reticulum. Circ Res 67:272-83.

Hopkins WE, Chen Z, Fukagawa NK, Hall C, Knot HJ, LeWinter MM. 2004. Increased atrial and brain natriuretic peptides in adults with cyanotic congenital heart disease: Enhanced understanding of the relationship between hypoxia and natriuretic peptide secretion. Circulation 109:2872-7.

Hovi L, Kurimo M, Taskinen M, Vettenranta J, Vettenranta K, Saarinen-Pihkala UM. 2010. Suboptimal long-term physical performance in children and young adults after pediatric allo-SCT. Bone Marrow Transplant 45:738-45.

Iles L, Pfluger H, Phrommintikul A, Cherayath J, Aksit P, Gupta SN, Kaye DM, Taylor AJ. 2008. Evaluation of diffuse myocardial fibrosis in heart failure with cardiac magnetic resonance contrast-enhanced T1 mapping. J Am Coll Cardiol 52:1574-80.

Isaaz K, Thompson A, Ethevenot G, Cloez JL, Brembilla B, Pernot C. 1989. Doppler echocardiographic measurement of low velocity motion of the left ventricular posterior wall. Am J Cardiol 64:66-75.

Januzzi JL,Jr, Filippatos G, Nieminen M, Gheorghiade M. 2012. Troponin elevation in patients with heart failure: On behalf of the third universal definition of myocardial infarction global task force: Heart failure section. Eur Heart J 33:2265-71.

Jauhiainen T, Jarvinen VM, Hekali PE, Poutanen VP, Penttila A, Kupari M. 1998. MR gradient echo volumetric analysis of human cardiac casts: Focus on the right ventricle. J Comput Assist Tomogr 22:899-903.

Jenei Z, Bardi E, Magyar MT, Horvath A, Paragh G, Kiss C. 2013. Anthracycline causes impaired vascular endothelial function and aortic stiffness in long term survivors of childhood cancer. Pathol Oncol Res 19:375-83.

Jeyaseelan R, Poizat C, Wu HY, Kedes L. 1997. Molecular mechanisms of doxorubicin-induced cardiomyopathy. Selective suppression of reiske iron-sulfur protein, ADP/ATP translocase, and phosphofructokinase genes is associated with ATP depletion in rat cardiomyocytes. J Biol Chem 272:5828-32.

Kampmann C, Wiethoff CM, Wenzel A, Stolz G, Betancor M, Wippermann CF, Huth RG, Habermehl P, Knuf M, Emschermann T, et al. 2000. Normal values of M mode echocardiographic measurements of more than 2000 healthy infants and children in Central Europe. Heart 83:667-72.

Kapetanakis S, Kearney MT, Siva A, Gall N, Cooklin M, Monaghan MJ. 2005. Real-time three-dimensional echocardiography: A novel technique to quantify global left ventricular mechanical dyssynchrony. Circulation 112:992-1000.

Katus HA, Remppis A, Looser S, Hallermeier K, Scheffold T, Kubler W. 1989. Enzyme linked immuno assay of cardiac troponin T for the detection of acute myocardial infarction in patients. J Mol Cell Cardiol 21:1349-53.

Katus HA, Remppis A, Neumann FJ, Scheffold T, Diederich KW, Vinar G, Noe A, Matern G, Kuebler W. 1991. Diagnostic efficiency of troponin T measurements in acute myocardial infarction. Circulation 83:902-12.

Katz J, Milliken MC, Stray-Gundersen J, Buja LM, Parkey RW, Mitchell JH, Peshock RM. 1988. Estimation of human myocardial mass with MR imaging. Radiology 169:495-8.

Kaul S, Tei C, Hopkins JM, Shah PM. 1984. Assessment of right ventricular function using two-dimensional echocardiography. Am Heart J 107:526-31.

Keenan NG and Pennell DJ. 2007. CMR of ventricular function. Echocardiography 24:185-93.

Kim G, Lee OJ, Kang IS, Song J, Huh J. 2013. Clinical implications of serial serum N-terminal prohormone brain natriuretic peptide levels in the prediction of outcome in children with dilated cardiomyopathy. Am J Cardiol 112:1455-60.

Kim RJ, Fieno DS, Parrish TB, Harris K, Chen EL, Simonetti O, Bundy J, Finn JP, Klocke FJ, Judd RM. 1999. Relationship of MRI delayed contrast enhancement to irreversible injury, infarct age, and contractile function. Circulation 100:1992-2002.

Kismet E, Varan A, Ayabakan C, Alehan D, Portakal O, Buyukpamukcu M. 2004. Serum troponin T levels and echocardiographic evaluation in children treated with doxorubicin. Pediatr Blood Cancer 42:220-4.

Kobayashi D, Patel SR, Mattoo TK, Valentini RP, Aggarwal S. 2012. The impact of change in volume and left-ventricular hypertrophy on left-ventricular mechanical dyssynchrony in children with end-stage renal disease. Pediatr Cardiol 33:1124-30.

Koerbin G, Abhayaratna WP, Potter JM, Apostoloska S, Telford RD, Hickman PE. 2012. NTproBNP concentrations in healthy children. Clin Biochem 45:1158-60.

Koestenberger M, Ravekes W, Everett AD, Stueger HP, Heinzl B, Gamillscheg A, Cvirn G, Boysen A, Fandl A, Nagel B. 2009. Right ventricular function in infants, children and adolescents: Reference values of the tricuspid annular plane systolic excursion (TAPSE) in 640 healthy patients and calculation of z score values. J Am Soc Echocardiogr 22:715-9.

Koopman LP, Slorach C, Hui W, Manlhiot C, McCrindle BW, Friedberg MK, Jaeggi ET, Mertens L. 2010a. Comparison between different speckle tracking and color tissue Doppler techniques to measure global and regional myocardial deformation in children. J Am Soc Echocardiogr 23:919-28.

Koopman LP, Slorach C, Manlhiot C, McCrindle BW, Friedberg MK, Mertens L, Jaeggi ET. 2010b. Myocardial tissue Doppler velocity imaging in children: Comparative study between two ultrasound systems. J Am Soc Echocardiogr 23:929-37.

Kramer CM, Barkhausen J, Flamm SD, Kim RJ, Nagel E, Society for Cardiovascular Magnetic Resonance Board of Trustees Task Force on Standardized,Protocols. 2008. Standardized cardiovascular magnetic resonance imaging (CMR) protocols, Society for Cardiovascular Magnetic Resonance: Board of trustees task force on standardized protocols. J Cardiovasc Magn Reson 10:35.

Kremer LC, Bastiaansen BA, Offringa M, Lam J, van Straalen JP, de Winter RJ, Voute PA. 2002a. Troponin T in the first 24 hours after the administration of chemotherapy and the detection of myocardial damage in children. Eur J Cancer 38:686-9.

Kremer LC, van Dalen EC, Offringa M, Voute PA. 2002b. Frequency and risk factors of anthracycline-induced clinical heart failure in children: A systematic review. Ann Oncol 13:503-12.

Kremer LC, van der Pal HJ, Offringa M, van Dalen EC, Voute PA. 2002c. Frequency and risk factors of subclinical cardiotoxicity after anthracycline therapy in children: A systematic review. Ann Oncol 13:819-29.

Krischer JP, Epstein S, Cuthbertson DD, Goorin AM, Epstein ML, Lipshultz SE. 1997. Clinical cardiotoxicity following anthracycline treatment for childhood cancer: The pediatric oncology group experience. J Clin Oncol 15:1544-52.

Landier W, Bhatia S, Eshelman DA, Forte KJ, Sweeney T, Hester AL, Darling J, Armstrong FD, Blatt J, Constine LS, et al. 2004. Development of risk-based guidelines for pediatric cancer survivors: The children's oncology group long-term follow-up guidelines from the children's oncology group late effects committee and nursing discipline. J Clin Oncol 22:4979-90.

Landy DC, Miller TL, Lipsitz SR, Lopez-Mitnik G, Hinkle AS, Constine LS, Adams MJ, Lipshultz SE. 2013. Cranial irradiation as an additional risk factor for anthracycline cardiotoxicity in childhood cancer survivors: An analysis from the cardiac risk factors in childhood cancer survivors study. Pediatr Cardiol 34:826-34.

Lang RM, Bierig M, Devereux RB, Flachskampf FA, Foster E, Pellikka PA, Picard MH, Roman MJ, Seward J, Shanewise JS, et al. 2005. Recommendations for chamber quantification: A report from the American Society of Echocardiography's guidelines and standards committee and the chamber quantification writing group, developed in conjunction with the European Association of Echocardiography, a branch of the European Society of Cardiology. J Am Soc Echocardiogr 18:1440-63.

Lang RM, Badano LP, Tsang W, Adams DH, Agricola E, Buck T, Faletra FF, Franke A, Hung J, de Isla LP, et al. 2012. EAE/ASE recommendations for image acquisition and display using three-dimensional echocardiography. J Am Soc Echocardiogr 25:3-46.

Latini R, Masson S, Anand IS, Missov E, Carlson M, Vago T, Angelici L, Barlera S, Parrinello G, Maggioni AP, et al. 2007. Prognostic value of very low plasma concentrations of troponin T in patients with stable chronic heart failure. Circulation 116:1242-9.

Lauer B, Niederau C, Kuhl U, Schannwell M, Pauschinger M, Strauer BE, Schultheiss HP. 1997. Cardiac troponin T in patients with clinically suspected myocarditis. J Am Coll Cardiol 30:1354-9.

Leuschner F, Li J, Goser S, Reinhardt L, Ottl R, Bride P, Zehelein J, Pfitzer G, Remppis A, Giannitsis E, et al. 2008. Absence of auto-antibodies against cardiac troponin I predicts improvement of left ventricular function after acute myocardial infarction. Eur Heart J 29:1949-55.

Levitt G, Anazodo A, Burch M, Bunch K. 2009. Cardiac or cardiopulmonary transplantation in childhood cancer survivors: An increasing need?. Eur J Cancer 45:3027-34.

Lim CC, Zuppinger C, Guo X, Kuster GM, Helmes M, Eppenberger HM, Suter TM, Liao R, Sawyer DB. 2004. Anthracyclines induce calpain-dependent titin proteolysis and necrosis in cardiomyocytes. J Biol Chem 279:8290-9.

Lin CW, Zeng XL, Zhang JF, Meng XH. 2014. Determining the optimal cutoff values of plasma N-terminal pro-B-type natriuretic peptide levels for the diagnosis of heart failure in children of age up to 14 years. J Card Fail 20:168-73.

Lindahl B, Venge P, Eggers K, Gedeborg R, Ristiniemi N, Wittfooth S, Pettersson K. 2010. Autoantibodies to cardiac troponin in acute coronary syndromes. Clin Chim Acta 411:1793-8.

Liodakis E, Sharef OA, Dawson D, Nihoyannopoulos P. 2009. The use of real-time three-dimensional echocardiography for assessing mechanical synchronicity. Heart 95:1865-71.

Lipshultz SE, Colan SD, Gelber RD, Perez-Atayde AR, Sallan SE, Sanders SP. 1991. Late cardiac effects of doxorubicin therapy for acute lymphoblastic leukemia in childhood. N Engl J Med 324:808-15.

Lipshultz SE, Rifai N, Sallan SE, Lipsitz SR, Dalton V, Sacks DB, Ottlinger ME. 1997. Predictive value of cardiac troponin T in pediatric patients at risk for myocardial injury. Circulation 96:2641-8.

Lipshultz SE, Rifai N, Dalton VM, Levy DE, Silverman LB, Lipsitz SR, Colan SD, Asselin BL, Barr RD, Clavell LA, et al. 2004. The effect of dexrazoxane on myocardial injury in doxorubicin-treated children with acute lymphoblastic leukemia. N Engl J Med 351:145-53.

Lipshultz SE, Lipsitz SR, Sallan SE, Dalton VM, Mone SM, Gelber RD, Colan SD. 2005. Chronic progressive cardiac dysfunction years after doxorubicin therapy for childhood acute lymphoblastic leukemia. J Clin Oncol 23:2629-36.

Lipshultz SE, Landy DC, Lopez-Mitnik G, Lipsitz SR, Hinkle AS, Constine LS, French CA, Rovitelli AM, Proukou C, Adams MJ, et al. 2012a. Cardiovascular status of childhood cancer survivors exposed and unexposed to cardiotoxic therapy. J Clin Oncol 30:1050-7.

Lipshultz SE, Miller TL, Scully RE, Lipsitz SR, Rifai N, Silverman LB, Colan SD, Neuberg DS, Dahlberg SE, Henkel JM, et al. 2012b. Changes in cardiac biomarkers during doxorubicin treatment of pediatric patients with high-risk acute lymphoblastic leukemia: Associations with long-term echocardiographic outcomes. J Clin Oncol 30:1042-9.

Lipshultz SE. Adams MJ. Colan SD. Constine LS. Herman EH. Hsu DT. Hudson MM. Kremer LC. Landy DC. Miller TL. Oeffinger KC. Rosenthal DN. Sable CA. Sallan SE. Singh GK. Steinberger J. Cochran TR. Wilkinson JD. American Heart Association Congenital Heart Defects Committee of the Council on Cardiovascular Disease in the Young, Council on Basic Cardiovascular Sciences, Council on Cardiovascular and Stroke Nursing, Council on Cardiovascular Radiolo. 2013a. Long-term cardiovascular toxicity in children, adolescents, and young adults who receive cancer therapy: Pathophysiology, course, monitoring, management, prevention, and research directions: A scientific statement from the American Heart Association. Circulation 128:1927-95.

Lipshultz SE, Cochran TR, Franco VI, Miller TL. 2013b. Treatment-related cardiotoxicity in survivors of childhood cancer. Nat Rev Clin Oncol 10:697-710.

Lipshultz SE, Lipsitz SR, Kutok JL, Miller TL, Colan SD, Neuberg DS, Stevenson KE, Fleming MD, Sallan SE, Franco VI, et al. 2013c. Impact of hemochromatosis gene mutations on cardiac status in doxorubicin-treated survivors of childhood high-risk leukemia. Cancer 119:3555-62.

Lopez L, Colan SD, Frommelt PC, Ensing GJ, Kendall K, Younoszai AK, Lai WW, Geva T. 2010. Recommendations for quantification methods during the performance of a pediatric echocardiogram: A report from the pediatric measurements writing group of the american society of echocardiography pediatric and congenital heart disease council. J Am Soc Echocardiogr 23:465-95.

Lorenz CH. 2000. The range of normal values of cardiovascular structures in infants, children, and adolescents measured by magnetic resonance imaging. Pediatr Cardiol 21:37-46.

Lu X, Xie M, Tomberlin D, Klas B, Nadvoretskiy V, Ayres N, Towbin J, Ge S. 2008. How accurately, reproducibly, and efficiently can we measure left ventricular indices using M-mode, 2-dimensional, and 3-dimensional echocardiography in children?. Am Heart J 155:946-53.

Lytrivi ID, Bhatla P, Ko HH, Yau J, Geiger MK, Walsh R, Parness IA, Srivastava S, Nielsen JC. 2011. Normal values for left ventricular volume in infants and young children by the echocardiographic subxiphoid five-sixth area by length (bullet) method. J Am Soc Echocardiogr 24:214-8.

Machann W, Beer M, Breunig M, Stork S, Angermann C, Seufert I, Schwab F, Kolbl O, Flentje M, Vordermark D. 2011. Cardiac magnetic resonance imaging findings in 20-year survivors of mediastinal radiotherapy for Hodgkin's disease. Int J Radiat Oncol Biol Phys 79:1117-23.

Magga J, Marttila M, Mantymaa P, Vuolteenaho O, Ruskoaho H. 1994. Brain natriuretic peptide in plasma, atria, and ventricles of vasopressin- and phenylephrine-infused conscious rats. Endocrinology 134:2505-15.

Marcus KA, Mavinkurve-Groothuis AM, Barends M, van Dijk A, Feuth T, de Korte C, Kapusta L. 2011. Reference values for myocardial two-dimensional strain echocardiography in a healthy pediatric and young adult cohort. J Am Soc Echocardiogr 24:625-36.

Mason JW, Bristow MR, Billingham ME, Daniels JR. 1978. Invasive and noninvasive methods of assessing adriamycin cardiotoxic effects in man: Superiority of histopathologic assessment using endomyocardial biopsy. Cancer Treat Rep 62:857-64.

Mathew P, Suarez W, Kip K, Bayar E, Jasty R, Matloub Y, Raisch D. 2001. Is there a potential role for serum cardiac troponin I as a marker for myocardial dysfunction in pediatric patients receiving anthracycline-based therapy? A pilot study. Cancer Invest 19:352-9.

Mavinkurve-Groothuis AM, Groot-Loonen J, Bellersen L, Pourier MS, Feuth T, Bokkerink JP, Hoogerbrugge PM, Kapusta L. 2009. Abnormal NT-pro-BNP levels in asymptomatic long-term survivors of childhood cancer treated with anthracyclines. Pediatr Blood Cancer 52:631-6.

Mavinkurve-Groothuis AM, Groot-Loonen J, Marcus KA, Bellersen L, Feuth T, Bokkerink JP, Hoogerbrugge PM, de Korte C, Kapusta L. 2010. Myocardial strain and strain rate in monitoring subclinical heart failure in asymptomatic long-term survivors of childhood cancer. Ultrasound Med Biol 36:1783-91.

McDonald KM, Parrish T, Wennberg P, Stillman AE, Francis GS, Cohn JN, Hunter D. 1992. Rapid, accurate and simultaneous noninvasive assessment of right and left ventricular mass with nuclear magnetic resonance imaging using the snapshot gradient method. J Am Coll Cardiol 19:1601-7.

Messroghli DR, Niendorf T, Schulz-Menger J, Dietz R, Friedrich MG. 2003. T1 mapping in patients with acute myocardial infarction. J Cardiovasc Magn Reson 5:353-9.

Mewton N, Liu CY, Croisille P, Bluemke D, Lima JA. 2011. Assessment of myocardial fibrosis with cardiovascular magnetic resonance. J Am Coll Cardiol 57:891-903.

Moon JC, McKenna WJ, McCrohon JA, Elliott PM, Smith GC, Pennell DJ. 2003. Toward clinical risk assessment in hypertrophic cardiomyopathy with gadolinium cardiovascular magnetic resonance. J Am Coll Cardiol 41:1561-7.

Moon TJ, Miyamoto SD, Younoszai AK, Landeck BF. 2014. Left ventricular strain and strain rates are decreased in children with normal fractional shortening after exposure to anthracycline chemotherapy. Cardiol Young 24:854-65.

Mor-Avi V, Jenkins C, Kuhl HP, Nesser HJ, Marwick T, Franke A, Ebner C, Freed BH, Steringer-Mascherbauer R, Pollard H, et al. 2008. Real-time 3-dimensional echocardiographic quantification of left ventricular volumes: Multicenter study for validation with magnetic resonance imaging and investigation of sources of error. JACC Cardiovasc Imaging 1:413-23.

Mor-Avi V and Lang RM. 2009. The use of real-time three-dimensional echocardiography for the quantification of left ventricular volumes and function. Curr Opin Cardiol 24:402-9.

Mor-Avi V, Lang RM, Badano LP, Belohlavek M, Cardim NM, Derumeaux G, Galderisi M, Marwick T, Nagueh SF, Sengupta PP, et al. 2011. Current and evolving echocardiographic techniques for the quantitative evaluation of cardiac mechanics: ASE/EAE consensus statement on methodology and indications endorsed by the Japanese Society of Echocardiography. J Am Soc Echocardiogr 24:277-313.

Mulrooney DA, Yeazel MW, Kawashima T, Mertens AC, Mitby P, Stovall M, Donaldson SS, Green DM, Sklar CA, Robison LL, et al. 2009. Cardiac outcomes in a cohort of adult survivors of childhood and adolescent cancer: Retrospective analysis of the childhood cancer survivor study cohort. BMJ 339:b4606.

Nakamae H, Tsumura K, Terada Y, Nakane T, Nakamae M, Ohta K, Yamane T, Hino M. 2005. Notable effects of angiotensin II receptor blocker, valsartan, on acute cardiotoxic changes after standard chemotherapy with cyclophosphamide, doxorubicin, vincristine, and prednisolone. Cancer 104:2492-8.

Neilan TG, Coelho-Filho OR, Pena-Herrera D, Shah RV, Jerosch-Herold M, Francis SA, Moslehi J, Kwong RY. 2012. Left ventricular mass in patients with a cardiomyopathy after treatment with anthracyclines. Am J Cardiol 110:1679-86.

Nir A, Lindinger A, Rauh M, Bar-Oz B, Laer S, Schwachtgen L, Koch A, Falkenberg J, Mir TS. 2009. NT-pro-B-type natriuretic peptide in infants and children: Reference values based on combined data from four studies. Pediatr Cardiol 30:3-8.

Nussinovitch U and Shoenfeld Y. 2010. Anti-troponin autoantibodies and the cardiovascular system. Heart 96:1518-24.

Oberholzer K, Kunz RP, Dittrich M, Thelen M. 2004. [Anthracycline-induced cardiotoxicity: Cardiac MRI after treatment for childhood cancer]. ROFO Fortschr Geb Rontgenstr Nuklearmed 176:1245-50.

Octavia Y, Tocchetti CG, Gabrielson KL, Janssens S, Crijns HJ, Moens AL. 2012. Doxorubicin-induced cardiomyopathy: From molecular mechanisms to therapeutic strategies. J Mol Cell Cardiol 52:1213-25.

Ojala T, Mathur S, Vatanen A, Sinha MD, Jahnukainen K, Simpson J. 2014. Repeatability and agreement of real time three-dimensional echocardiography measurements of left ventricular mass and synchrony in young patients. Echocardiography Jun 28. doi: 10.1111/echo.12672.

Okazaki T, Tanaka Y, Nishio R, Mitsuiye T, Mizoguchi A, Wang J, Ishida M, Hiai H, Matsumori A, Minato N, et al. 2003. Autoantibodies against cardiac troponin I are responsible for dilated cardiomyopathy in PD-1-deficient mice. Nat Med 9:1477-83.

Omland T. de Lemos JA. Sabatine MS. Christophi CA. Rice MM. Jablonski KA. Tjora S. Domanski MJ. Gersh BJ. Rouleau JL. Pfeffer MA. Braunwald E. Prevention of Events with Angiotensin Converting Enzyme Inhibition (PEACE) Trial Investigators. 2009. A sensitive cardiac troponin T assay in stable coronary artery disease. N Engl J Med 361:2538-47.

Omland T and Hagve TA. 2009. Natriuretic peptides: Physiologic and analytic considerations. Heart Fail Clin 5:471-87.

Ommen SR, Nishimura RA, Appleton CP, Miller FA, Oh JK, Redfield MM, Tajik AJ. 2000. Clinical utility of doppler echocardiography and tissue doppler imaging in the estimation of left ventricular filling pressures: A comparative simultaneous doppler-catheterization study. Circulation 102:1788-94.

Ordovas KG and Higgins CB. 2011. Delayed contrast enhancement on MR images of myocardium: Past, present, future. Radiology 261:358-74.

Patel A, Weismann C, Weiss P, Russell K, Bazzy-Asaad A, Kadan-Lottick NS. 2014. Association between right ventricular dysfunction and restrictive lung disease in childhood cancer survivors as measured by quantitative echocardiography. Pediatr Blood Cancer 61:2059-64.

Pein F, Sakiroglu O, Dahan M, Lebidois J, Merlet P, Shamsaldin A, Villain E, de Vathaire F, Sidi D, Hartmann O. 2004. Cardiac abnormalities 15 years and more after adriamycin therapy in 229 childhood survivors of a solid tumour at the Institut Gustave Roussy. Br J Cancer 91:37-44.

Pemberton CJ, Johnson ML, Yandle TG, Espiner EA. 2000. Deconvolution analysis of cardiac natriuretic peptides during acute volume overload. Hypertension 36:355-9.

Perel RD, Slaughter RE, Strugnell WE. 2006. Subendocardial late gadolinium enhancement in two patients with anthracycline cardiotoxicity following treatment for Ewing's sarcoma. J Cardiovasc Magn Reson 8:789-91.

Pettersson K, Eriksson S, Wittfooth S, Engstrom E, Nieminen M, Sinisalo J. 2009. Autoantibodies to cardiac troponin associate with higher initial concentrations and longer release of troponin I in acute coronary syndrome patients. Clin Chem 55:938-45.

Plana JC, Galderisi M, Barac A, Ewer MS, Ky B, Scherrer-Crosbie M, Ganame J, Sebag IA, Agler DA, Badano LP, et al. 2014. Expert consensus for multimodality imaging evaluation of adult patients during and after cancer therapy: A report from the American Society of Echocardiography and the European Association of Cardiovascular Imaging. J Am Soc Echocardiogr 27:911-39.

Plein S, Bloomer TN, Ridgway JP, Jones TR, Bainbridge GJ, Sivananthan MU. 2001. Steady-state free precession magnetic resonance imaging of the heart: Comparison with segmented k-space gradient-echo imaging. J Magn Reson Imaging 14:230-6.

Pouleur AC, le Polain de Waroux JB, Pasquet A, Gerber BL, Gerard O, Allain P, Vanoverschelde JL. 2008. Assessment of left ventricular mass and volumes by three-dimensional echocardiography in patients with or without wall motion abnormalities: Comparison against cine magnetic resonance imaging. Heart 94:1050-7.

Poutanen T, Ikonen A, Jokinen E, Vainio P, Tikanoja T. 2001. Transthoracic three-dimensional echocardiography is as good as magnetic resonance imaging in measuring dynamic changes in left ventricular volume during the heart cycle in children. Eur J Echocardiogr 2:31-9.

Poutanen T, Jokinen E, Sairanen H, Tikanoja T. 2003a. Left atrial and left ventricular function in healthy children and young adults assessed by three dimensional echocardiography. Heart 89:544-9.

Poutanen T, Tikanoja T, Riikonen P, Silvast A, Perkkio M. 2003b. Long-term prospective follow-up study of cardiac function after cardiotoxic therapy for malignancy in children. J Clin Oncol 21:2349-56.

Quinones MA, Otto CM, Stoddard M, Waggoner A, Zoghbi WA, Doppler Quantification Task Force of the Nomenclature and Standards Committee of the American Society of,Echocardiography. 2002. Recommendations for quantification of Doppler echocardiography: A report from the doppler quantification task force of the nomenclature and standards committee of the American Society of Echocardiography. J Am Soc Echocardiogr 15:167-84.

Rathe M, Carlsen NL, Oxhoj H. 2007. Late cardiac effects of anthracycline containing therapy for childhood acute lymphoblastic leukemia. Pediatr Blood Cancer 48:663-7.

Rehr RB, Malloy CR, Filipchuk NG, Peshock RM. 1985. Left ventricular volumes measured by MR imaging. Radiology 156:717-9.

Robbers-Visser D, Boersma E, Helbing WA. 2009. Normal biventricular function, volumes, and mass in children aged 8 to 17 years. J Magn Reson Imaging 29:552-9.

Romano S, Fratini S, Ricevuto E, Procaccini V, Stifano G, Mancini M, Di Mauro M, Ficorella C, Penco M. 2011. Serial measurements of NT-proBNP are predictive of not-high-dose anthracycline cardiotoxicity in breast cancer patients. Br J Cancer 105:1663-8.

Rubinshtein R, Glockner JF, Ommen SR, Araoz PA, Ackerman MJ, Sorajja P, Bos JM, Tajik AJ, Valeti US, Nishimura RA, et al. 2010. Characteristics and clinical significance of late gadolinium enhancement by contrast-enhanced magnetic resonance imaging in patients with hypertrophic cardiomyopathy. Circ Heart Fail 3:51-8.

Ruggiero A, De Rosa G, Rizzo D, Leo A, Maurizi P, De Nisco A, Vendittelli F, Zuppi C, Mordente A, Riccardi R. 2013. Myocardial performance index and biochemical markers for early detection of doxorubicin-induced cardiotoxicity in children with acute lymphoblastic leukaemia. Int J Clin Oncol 18:927-33.

Sado DM, Flett AS, Moon JC. 2011. Novel imaging techniques for diffuse myocardial fibrosis. Future Cardiol 7:643-50.

Sandri MT, Salvatici M, Cardinale D, Zorzino L, Passerini R, Lentati P, Leon M, Civelli M, Martinelli G, Cipolla CM. 2005. N-terminal pro-B-type natriuretic peptide after high-dose chemotherapy: A marker predictive of cardiac dysfunction?. Clin Chem 51:1405-10.

Santamore WP and Dell'Italia LJ. 1998. Ventricular interdependence: Significant left ventricular contributions to right ventricular systolic function. Prog Cardiovasc Dis 40:289-308.

Sarikouch S, Peters B, Gutberlet M, Leismann B, Kelter-Kloepping A, Koerperich H, Kuehne T, Beerbaum P. 2010. Sex-specific pediatric percentiles for ventricular size and mass as reference values for cardiac MRI: Assessment by steady-state free-precession and phase-contrast MRI flow. Circ Cardiovasc Imaging 3:65-76.

Sarvazyan N. 1996. Visualization of doxorubicin-induced oxidative stress in isolated cardiac myocytes. Am J Physiol 271:H2079-85.

Sato Y, Yamada T, Taniguchi R, Nagai K, Makiyama T, Okada H, Kataoka K, Ito H, Matsumori A, Sasayama S, et al. 2001. Persistently increased serum concentrations of cardiac troponin t in patients with idiopathic dilated cardiomyopathy are predictive of adverse outcomes. Circulation 103:369-74.

Savukoski T, Engstrom E, Engblom J, Ristiniemi N, Wittfooth S, Lindahl B, Eggers KM, Venge P, Pettersson K. 2012. Troponin-specific autoantibody interference in different cardiac troponin I assay configurations. Clin Chem 58:1040-8.

Schellong G, Riepenhausen M, Bruch C, Kotthoff S, Vogt J, Bolling T, Dieckmann K, Potter R, Heinecke A, Bramswig J, et al. 2010. Late valvular and other cardiac diseases after different doses of mediastinal radiotherapy for Hodgkin disease in children and adolescents: Report from the longitudinal GPOH follow-up project of the German-Austrian DAL-HD studies. Pediatr Blood Cancer 55:1145-52.

Schiller NB, Skioldebrand CG, Schiller EJ, Mavroudis CC, Silverman NH, Rahimtoola SH, Lipton MJ. 1983. Canine left ventricular mass estimation by two-dimensional echocardiography. Circulation 68:210-6.

Schiller NB, Shah PM, Crawford M, DeMaria A, Devereux R, Feigenbaum H, Gutgesell H, Reichek N, Sahn D, Schnittger I. 1989. Recommendations for quantitation of the left ventricle by two-dimensional echocardiography. American Society of Echocardiography committee on standards, subcommittee on quantitation of two-dimensional echocardiograms. J Am Soc Echocardiogr 2:358-67.

Schulz-Menger J, Bluemke DA, Bremerich J, Flamm SD, Fogel MA, Friedrich MG, Kim RJ, von Knobelsdorff-Brenkenhoff F, Kramer CM, Pennell DJ, et al. 2013. Standardized image interpretation and post processing in cardiovascular magnetic resonance: Society for cardiovascular magnetic resonance (SCMR) board of trustees task force on standardized post processing. J Cardiovasc Magn Reson 15:35.

Sengupta PP, Korinek J, Belohlavek M, Narula J, Vannan MA, Jahangir A, Khandheria BK. 2006. Left ventricular structure and function: Basic science for cardiac imaging. J Am Coll Cardiol 48:1988-2001.

Sherief LM, Kamal AG, Khalek EA, Kamal NM, Soliman AA, Esh AM. 2012. Biomarkers and early detection of late onset anthracycline-induced cardiotoxicity in children. Hematol 17:151-6.

Shmilovich H, Danon A, Binah O, Roth A, Chen G, Wexler D, Keren G, George J. 2007. Autoantibodies to cardiac troponin I in patients with idiopathic dilated and ischemic cardiomyopathy. Int J Cardiol 117:198-203.

Sieswerda E. Postma A. van Dalen EC. van der Pal HJ. Tissing WJ. Rammeloo LA. Kok WE. van Leeuwen FE. Caron HN. Kremer LC. Late Effects of Childhood Cancer task force of the Dutch Childhood Oncology Group (DCOG LATER). 2012. The Dutch childhood oncology group guideline for follow-up of asymptomatic cardiac dysfunction in childhood cancer survivors. Ann Oncol 23:2191-8.

Simpson JM, Savis A, Rawlins D, Qureshi S, Sinha MD. 2010. Incidence of left ventricular hypertrophy in children with kidney disease: Impact of method of indexation of left ventricular mass. Eur J Echocardiogr 11:271-7.

Soker M and Kervancioglu M. 2005. Plasma concentrations of NT-pro-BNP and cardiac troponin-I in relation to doxorubicin-induced cardiomyopathy and cardiac function in childhood malignancy. Saudi Med J 26:1197-202.

Soliman OI, Kirschbaum SW, van Dalen BM, van der Zwaan HB, Mahdavian Delavary B, Vletter WB, van Geuns RJ, Ten Cate FJ, Geleijnse ML. 2008. Accuracy and reproducibility of quantitation of left ventricular function by real-time three-dimensional echocardiography versus cardiac magnetic resonance. Am J Cardiol 102:778-83.

Soriano BD, Hoch M, Ithuralde A, Geva T, Powell AJ, Kussman BD, Graham DA, Tworetzky W, Marx GR. 2008. Matrix-array 3-dimensional echocardiographic assessment of volumes, mass, and ejection fraction in young pediatric patients with a functional single ventricle: A comparison study with cardiac magnetic resonance. Circulation 117:1842-8.

Stapleton GE, Stapleton SL, Martinez A, Ayres NA, Kovalchin JP, Bezold LI, Pignatelli R, Eidem BW. 2007. Evaluation of longitudinal ventricular function with tissue doppler echocardiography in children treated with anthracyclines. J Am Soc Echocardiogr 20:492-7.

Steinherz LJ, Graham T, Hurwitz R, Sondheimer HM, Schwartz RG, Shaffer EM, Sandor G, Benson L, Williams R. 1992. Guidelines for cardiac monitoring of children during and after anthracycline therapy: Report of the cardiology committee of the childrens cancer study group. Pediatrics 89:942-9.

Steinherz LJ, Steinherz PG, Tan C. 1995. Cardiac failure and dysrhythmias 6-19 years after anthracycline therapy: A series of 15 patients. Med Pediatr Oncol 24:352-61.

Stewart JR and Fajardo LF. 1971. Radiation-induced heart disease. clinical and experimental aspects. Radiol Clin North Am 9:511-31.

Stewart JR, Fajardo LF, Gillette SM, Constine LS. 1995. Radiation injury to the heart. Int J Radiat Oncol Biol Phys 31:1205-11.

Suzuki K, Akashi YJ, Mizukoshi K, Kou S, Takai M, Izumo M, Hayashi A, Ohtaki E, Nobuoka S, Miyake F. 2012. Relationship between left ventricular ejection fraction and mitral annular displacement derived by speckle tracking echocardiography in patients with different heart diseases. J Cardiol 60:55-60.

Swain SM, Whaley FS, Ewer MS. 2003. Congestive heart failure in patients treated with doxorubicin: A retrospective analysis of three trials. Cancer 97:2869-79.

Takahashi K, Mackie AS, Rebeyka IM, Ross DB, Robertson M, Dyck JD, Inage A, Smallhorn JF. 2010. Two-dimensional versus transthoracic real-time three-dimensional echocardiography in the evaluation of the mechanisms and sites of atrioventricular valve regurgitation in a congenital heart disease population. J Am Soc Echocardiogr 23:726-34.

Tang G, Wu Y, Zhao W, Shen Q. 2012. Multiple immunoassay systems are negatively interfered by circulating cardiac troponin I autoantibodies. Clin Exp Med 12:47-53.

Teichholz LE, Kreulen T, Herman MV, Gorlin R. 1976. Problems in echocardiographic volume determinations: Echocardiographic-angiographic correlations in the presence or absence of asynergy. Am J Cardiol 37:7-11.

Ten Harkel AD, Van Osch-Gevers M, Helbing WA. 2009. Real-time transthoracic three dimensional echocardiography: Normal reference data for left ventricular dyssynchrony in adolescents. J Am Soc Echocardiogr 22:933-8.

Tham EB, Haykowsky MJ, Chow K, Spavor M, Kaneko S, Khoo NS, Pagano JJ, Mackie AS, Thompson RB. 2013. Diffuse myocardial fibrosis by T1-mapping in children with subclinical anthracycline cardiotoxicity: Relationship to exercise capacity, cumulative dose and remodeling. J Cardiovasc Magn Reson 15:48.

Thavendiranathan P, Grant AD, Negishi T, Plana JC, Popovic ZB, Marwick TH. 2013. Reproducibility of echocardiographic techniques for sequential assessment of left ventricular ejection fraction and volumes: Application to patients undergoing cancer chemotherapy. J Am Coll Cardiol 61:77-84.

Thygesen K, Alpert JS, Jaffe AS, Simoons ML, Chaitman BR, White HD. 2012. Third universal definition of myocardial infarction. Circulation 126:2020-35.

Tokarska-Schlattner M, Zaugg M, Zuppinger C, Wallimann T, Schlattner U. 2006. New insights into doxorubicin-induced cardiotoxicity: The critical role of cellular energetics. J Mol Cell Cardiol 41:389-405.

Toro-Salazar OH, Gillan E, O'Loughlin MT, Burke GS, Ferranti J, Stainsby J, Liang B, Mazur W, Raman SV, Hor KN. 2013. Occult cardiotoxicity in childhood cancer survivors exposed to anthracycline therapy. Circ Cardiovasc Imaging 6:873-80.

Torti FM, Bristow MM, Lum BL, Carter SK, Howes AE, Aston DA, Brown BW,Jr, Hannigan JF,Jr, Meyers FJ, Mitchell EP. 1986. Cardiotoxicity of epirubicin and doxorubicin: Assessment by endomyocardial biopsy. Cancer Res 46:3722-7.

Tsang W, Ahmad H, Patel AR, Sugeng L, Salgo IS, Weinert L, Mor-Avi V, Lang RM. 2010. Rapid estimation of left ventricular function using echocardiographic speckle-tracking of mitral annular displacement. J Am Soc Echocardiogr 23:511-5.

Tsuruda T, Boerrigter G, Huntley BK, Noser JA, Cataliotti A, Costello-Boerrigter LC, Chen HH, Burnett JC, Jr. 2002. Brain natriuretic peptide is produced in cardiac fibroblasts and induces matrix metalloproteinases. Circ Res 91:1127-34.

van Dalen EC, van der Pal HJ, Kok WE, Caron HN, Kremer LC. 2006. Clinical heart failure in a cohort of children treated with anthracyclines: A long-term follow-up study. Eur J Cancer 42:3191-8.

van der Pal HJ, van Dalen EC, van Delden E, van Dijk IW, Kok WE, Geskus RB, Sieswerda E, Oldenburger F, Koning CC, van Leeuwen FE, et al. 2012. High risk of symptomatic cardiac events in childhood cancer survivors. J Clin Oncol 30:1429-37.

ver Elst KM, Spapen HD, Nguyen DN, Garbar C, Huyghens LP, Gorus FK. 2000. Cardiac troponins I and T are biological markers of left ventricular dysfunction in septic shock. Clin Chem 46:650-7.

Vettukattil JJ. 2012. Three dimensional echocardiography in congenital heart disease. Heart 98:79-88.

Visscher H, Ross CJ, Rassekh SR, Barhdadi A, Dube MP, Al-Saloos H, Sandor GS, Caron HN, van Dalen EC, Kremer LC, et al. 2012. Pharmacogenomic prediction of anthracycline-induced cardiotoxicity in children. J Clin Oncol 30:1422-8.

Vogel M, Staller W, Buhlmeyer K. 1991. Left ventricular myocardial mass determined by cross-sectional echocardiography in normal newborns, infants, and children. Pediatr Cardiol 12:143-9.

Vogel M, Stern H, Bauer R, Buhlmeyer K. 1992. Comparison of magnetic resonance imaging with cross-sectional echocardiography in the assessment of left ventricular mass in children without heart disease and in aortic isthmic coarctation. Am J Cardiol 69:941-4.

von Ramm OT and Smith SW. 1990. Real time volumetric ultrasound imaging system. J Digit Imaging 3:261-6.

Walker LA and Buttrick PM. 2013. The right ventricle: Biologic insights and response to disease: Updated. Curr Cardiol Rev 9:73-81.

Walsh R, Salem Y, Shah A, Lai WW, Nielsen JC. 2011. Repeatability of cardiac-MRI-measured right ventricular size and function in congenital heart disease. Pediatr Radiol 41:1000-7.

Wang H, Shuraih M, Ahmad M. 2012. Real time three-dimensional echocardiography in assessment of left ventricular dyssynchrony and cardiac resynchronization therapy. Echocardiography 29:192-9.

Wood PW, Choy JB, Nanda NC, Becher H. 2014. Left ventricular ejection fraction and volumes: It depends on the imaging method. Echocardiography 31:87-100.

Wu E, Judd RM, Vargas JD, Klocke FJ, Bonow RO, Kim RJ. 2001. Visualisation of presence, location, and transmural extent of healed Q-wave and non-Q-wave myocardial infarction. Lancet 357:21-8.

Wyatt HL, Heng MK, Meerbaum S, Hestenes JD, Cobo JM, Davidson RM, Corday E. 1979. Cross-sectional echocardiography. I. analysis of mathematic models for quantifying mass of the left ventricle in dogs. Circulation 60:1104-13.

Yang HS, Bansal RC, Mookadam F, Khandheria BK, Tajik AJ, Chandrasekaran K, American Society of E. 2008. Practical guide for three-dimensional transthoracic echocardiography using a fully sampled matrix array transducer. J Am Soc Echocardiogr 21:979-89.

Yoshida A, Ishibashi-Ueda H, Yamada N, Kanzaki H, Hasegawa T, Takahama H, Amaki M, Asakura M, Kitakaze M. 2013. Direct comparison of the diagnostic capability of cardiac magnetic resonance and endomyocardial biopsy in patients with heart failure. Eur J Heart Fail 15:166-75.

Zhang S, Liu X, Bawa-Khalfe T, Lu LS, Lyu YL, Liu LF, Yeh ET. 2012. Identification of the molecular basis of doxorubicin-induced cardiotoxicity. Nat Med 18:1639-42.

Zver S, Zadnik V, Bunc M, Rogel P, Cernelc P, Kozelj M. 2007. Cardiac toxicity of high-dose cyclophosphamide in patients with multiple myeloma undergoing autologous hematopoietic stem cell transplantation. Int J Hematol 85:408-14.

Journal of the American College of Cardiology
© 2013 by the American College of Cardiology Foundation
Published by Elsevier Inc.

Vol. 61, No. 14, 2013
ISSN 0735-1097/$36.00
http://dx.doi.org/10.1016/j.jacc.2013.01.019

Cardiac Magnetic Resonance Imaging in the Evaluation of the Late Effects of Anthracyclines Among Long-Term Survivors of Childhood Cancer

Kaisa Ylänen, MD,* Tuija Poutanen, MD, PhD,* Päivi Savikurki-Heikkilä, MD,†
Irina Rinta-Kiikka, MD, PhD,† Anneli Eerola, MD, PhD,* Kim Vettenranta, MD, PhD*
Tampere, Finland

Objectives This study sought to examine the left ventricular (LV) and right ventricular (RV) function and signs of focal fibrosis among long-term survivors of childhood cancer with the use of cardiac magnetic resonance (CMR) imaging.

Background Increased myocardial fibrosis has been detected in the endomyocardial biopsies of survivors. CMR has established its role in the assessment of both cardiac function and structure, and focal fibrosis of the myocardium is detectable with late gadolinium enhancement (LGE).

Methods Sixty-two anthracycline-exposed long-term survivors of childhood cancer were studied at a mean age of 14.6 years. The LV and RV ejection fractions (EFs) and volumes were measured, and LGE was assessed using CMR.

Results An abnormal LV function (EF <45%) was detected in 18% (11 of 62) of the survivors, and an abnormal RV function was detected in 27% (17 of 62) of the survivors. Subnormal (45% ≤ EF <55%) LV function were demonstrated in 61% (38 of 62) and subnormal RV function in 53% (33 of 62) of the survivors, respectively. Both the LV and RV end-systolic and LV end-diastolic volumes were increased compared with reference values. None of the study patients showed LGE.

Conclusions A considerable proportion of the long-term survivors of childhood cancer with anthracycline exposure demonstrate signs of cardiac dysfunction detectable by CMR, with the RV also being involved. Yet, myocardial fibrosis does not seem to be detectable at a median of 7.8 years after anthracycline therapy. (J Am Coll Cardiol 2013; 61:1539–47) © 2013 by the American College of Cardiology Foundation

Anthracyclines are widely used in the treatment of many childhood malignancies, but a dose-dependent cardiotoxicity is limiting their use. Late toxicity is defined as cardiac abnormalities developing no earlier than 1 year after anthracycline treatment, but in some cases it is not discernible until years or decades later. Late cardiotoxicity can manifest as subclinical abnormalities in the cardiac function, dilated cardiomyopathy, and/or heart failure and is usually irreversible. The cumulative drug dose, mediastinal irradiation, young age at exposure, female sex, and time post-exposure are known risk factors for anthracycline cardiomyopathy also modified by genetic factors (1–3). The prevalence of subclinical cardiotoxicity is between 0% and 57% (4), and the prevalence of anthracycline-induced clinical heart failure is between 0% and 16% (5). Mulrooney et al. (2) reported a cumulative incidence of congestive heart failure exceeding 7.5% at 30 years among those with a cumulative anthracycline dose ≥250 mg/m^2 and 2.5% among those with a lower dose. Published data also indicate that a left ventricular (LV) dysfunction, frank heart failure (6), and terminal cardiomyopathy (7) may occur even at lower doses. Childhood cancer survivors thus seem at an increased risk for anthracycline cardiotoxicity with their young age at exposure and longer life expectancy.

Among the cancer survivors, echocardiography has been widely used in the follow-up of cardiac function, but it has limitations in sensitivity and problems caused by a suboptimal acoustic window (8,9). Cardiac magnetic resonance (CMR) imaging is considered a standard of reference in the assessment of cardiac function and structure against which

From the *Department of Pediatrics, Tampere University and the University Hospital, Tampere, Finland; and the †Department of Radiology, Tampere University and the University Hospital, Tampere, Finland. This study was financially supported by the Competitive Research Funding of the Tampere University Hospital (Grant 9L114), the EVO funds of the Tampere University Hospital, the Emil Aaltonen Foundation, the Finnish Cultural Foundation, the Finnish Cultural Foundation Pirkanmaa Regional Fund, the Finnish Association of Hematology, the National Graduate School of Clinical Investigations, the Päivikki and Sakari Sohlberg Foundation, the Foundation for Pediatric Research, the Scientific Foundation of the City of Tampere, the Finnish Cancer Foundation, and the Blood Disease Research Foundation. All authors have reported they have no relationships relevant to the contents of this paper to disclose.

Manuscript received November 23, 2012; revised manuscript received December 21, 2012, accepted January 8, 2013.

JACC Vol. 61, No. 14, 2013
April 9, 2013:1539–47

Abbreviations and Acronyms

BSA = body surface area
CMR = cardiac magnetic resonance
EDV = end-diastolic volume
EF = ejection fraction
ESV = end-systolic volume
Gd-CA = gadolinium-chelated contrast agent
LGE = late gadolinium enhancement
LV = left ventricle/ventricular
PSIR = phase-sensitive inversion recovery
RV = right ventricle/ventricular
TI = inversion time

other modalities are validated (10,11). With anthracycline cardiomyopathy having been thought to involve mainly the LV, the follow-up protocols of cancer survivors have, until recently, largely neglected the right ventricle (RV) with its complex anatomy and scarcity of optimal imaging methods. CMR is considered the best method for visualizing the RV (12) and thus used in the follow-up of heart diseases affecting the RV (13).

Many cardiac diseases lead to fibrosis of the myocardium classifiable for clinical purposes as local or diffuse (14). Late gadolinium enhancement (LGE) in CMR after the administration of a gadolinium-chelated contrast agent (Gd-CA) is a well-established method for assessing focal fibrosis (15). LGE for fibrosis or deposition of abnormal substrates in the myocardium can be used in patients with myocardial infarction, hypertrophic and dilated cardiomyopathies, infiltrative diseases, and myocarditis (16).

The pathogenesis of late-onset cardiac toxicity remains incompletely understood, but evidence exists on myocyte apoptosis after anthracycline exposure (17), resulting in myocardial fibrosis detectable on LGE. Steinherz et al. (18) have reported on increased fibrosis in the endomyocardial biopsies taken from the RV and at autopsy among the long-term cancer survivors with anthracycline cardiomyopathy.

The aim of our study was to evaluate the prevalence of LV and RV dysfunction and signs of focal fibrosis with CMR among anthracycline-exposed long-term childhood cancer survivors in a single-center setting.

Methods

Characteristics of the study population. The study population consisted of 62 long-term survivors of childhood cancer (34 female and 28 male) attending the population-based pediatric hematology-oncology service of the Tampere University Hospital (Tampere, Finland) between February 2010 and June 2011. The survivors enrolled had received anthracyclines (doxorubicin, daunorubicin, idarubicin, or mitoxantrone) as a part of their therapy, had a minimum follow-up of 5 years, had no congenital heart disease, and were in remission. Of the 86 survivors initially recruited, 62 agreed to participate in the study. The body surface area (BSA) at diagnosis was used to calculate the cumulative anthracycline dose. Dose conversion to doxorubicin isotoxic equivalents was performed according to the Children's Oncology Group recommendations. CMR was performed only for study purposes with only 1 child requiring anesthesia to achieve optimal images. The institutional review board of the Tampere University Hospital approved the study protocol. All survivors and their legal guardian(s) gave their written informed consent.

The key characteristics of the study patients are presented in Tables 1 and 2. The age of the survivors was 14.6 ± 3.2 years. The median (range) age at the time of the malignancy diagnosis was 3.8 years (0.0 to 13.8 years), and the follow-up time was 7.8 years (4.9 to 18.0 years). Their median cumulative anthracycline dose was 222 mg/m^2 (80 to 419 mg/m^2). Seven survivors (11%) had received radiotherapy involving the heart with a median average cumulative cardiac dose of 10.0 Gy (3.6 to 12.0 Gy). The average cardiac dose of those without total body irradiation was derived from the radiotherapy planning charts. The dose among those with total body irradiation was estimated to equal the total radiation dose.

Three survivors (5%) had experienced a relapse but at the time of inclusion were in remission. Three survivors were taking enalaprile for their cardiomyopathy, and 1 survivor was taking bisoprolol for a long QT-syndrome. One survivor had an asymptomatic patent ductus arteriosus. One survivor had had a thrombus resected from the right atrium during primary therapy but remained asymptomatic.

Table 1 Clinical Characteristics of Study Patients

Sex	
Female	34 (55)
Male	28 (45)
Diagnosis	
ALL	28 (45)
AML	7 (11)
Hodgkin disease	6 (10)
Non–Hodgkin lymphoma	7 (11)
Neuroblastoma	7 (11)
Wilms' tumor	1 (2)
Osteosarcoma	1 (2)
Rhabdomyosarcoma	1 (2)
Other	4 (6)
Anthracycline therapy	
Doxorubicin	59 (95)
Daunorubicin	17 (27)
Mitoxantrone	7 (11)
Idarubicin	4 (6)
Radiotherapy involving heart	
No	55 (89)
Yes	7 (11)
History of relapse	
No	59 (95)
Yes	3 (5)
History of stem cell transplantation	
No	54 (87)
Autologous	4 (6)
Allogeneic	4 (6)

Values are n (%).
ALL = acute lymphoblastic leukemia; AML = acute myelogenous leukemia.

Table 2 Clinical Characteristics of Study Patients by Sex

Characteristic	Female (n = 34)	Male (n = 28)	p Value
Age at study time (yrs)	14.4 ± 3.4	14.9 ± 2.9	0.565
Age at diagnosis (yrs)	3.8 (0.5–12.6)	4.7 (0.0–13.8)	0.760
Follow-up (yrs)	7.7 (4.9–13.6)	7.8 (5.0–18.0)	0.809
Cumulative anthracycline (mg/m^2)	224 (108–419)	184 (80–416)	0.372
Height (cm)	156.4 ± 14.1	164.2 ± 16.7	0.051
Weight (kg)	51.9 ± 15.2	58.5 ± 18.7	0.133
BSA (m^2)	1.49 ± 0.28	1.63 ± 0.34	0.094
Heart rate (beats/min)	81 ± 16	75 ± 13	0.106

Values are mean ± SD or median (range).
BSA = body surface area.

Magnetic resonance imaging technique and analysis. CMR was performed on a 1.5-T scanner (Siemens Magnetom Avanto; Siemens Healthcare, Erlangen, Germany) using a 6-channel body array coil with a spine coil and electrocardiogram gating. Cine TrueFISP slices of 8 mm without any gap from the heart apex to valves were obtained in the short-axis plane to analyze the LV and in the axial plane to analyze the RV function. After injection of gadoterate meglumine (0.1 mmol/kg, Dotarem [Guerbet, Roissy, France]), a 5-min delay was used before obtaining a segmented inversion recovery cine TrueFISP pulse sequence at the midventricular short-axis level for the determination of the inversion time (TI) value for the nullification of the impact of the normal myocardium. Within the next 5 min, the LGE images were obtained using a TrueFISP gradient echo sequence with a determined TI (range: 280 to 330 ms) with a slice thickness of 8 mm in the short axis, 2-chamber view (vertical long axis through the left atrium and ventricle), 4-chamber view (horizontal long axis), and axial stacks covering the heart from apex to valves. Thereafter, the corresponding views were recovered using a phase-sensitive inversion recovery (PSIR) technique with a constant TI value of 300 ms. The late-enhancement imaging was performed within 15 min from the beginning of the gadoterate injection.

In the analysis, ARGUS software (Siemens AG, Munich, Germany) was used. All measurements were done manually. The end-systolic and diastolic frames were identified by determining the ventricular blood-pool areas. The LV volumes were calculated from the short axis, and the RV volumes were calculated from the axial cine views. The aortic outflow tract below the valve and the LV portion of the slice in the basal region near the left atrium were included in the LV volume measurements. The same principles were used for the RV. The free papillary muscles were included for both the ventricular volumes (Fig. 1). The LGE in the TrueFISP and PSIR sequences was independently analyzed by 2 radiologists (P.S.H, I.R.K.), who also independently analyzed 15 randomly selected data sets to evaluate the interobserver variability. One investigator (PSH) measured 15 data sets twice to assess the intraobserver variability.

Statistical analysis. Descriptive statistics and analyses were performed using PASW Statistics 18.0 software (SPSS Inc., Chicago, Illinois). Descriptive statistics are presented as the frequencies and percentages for categoric data and the mean ± SD or median and (range) for continuous data. The CMR parameters were compared with published data (19,20) using the 1-sample Student *t* test. The categoric variables were compared using the chi-square test (the Fisher exact test when appropriate). For continuous data, the independent samples *t* test and the Mann-Whitney *U* test were used. All tests were 2-sided, and p values <0.05 were considered statistically significant. The intraobserver and interobserver variations were assessed using the Bland-Altman analysis (21).

The reference values for the CMR were deduced from published data. The LV parameters were compared with the data of Robbers-Visser et al. (19) describing the short-axis slices from 60 healthy children age 8 to 17 years. For the RV analysis, the data of Sarikouch et al. (20) on 99 healthy children age 8 to 20 years obtained by the axial slices were used. Abnormally large ventricular volumes were defined as those exceeding the published mean volumes by at least 2 SD.

Results

Left ventricle. We classified the ejection fraction (EF) as normal (EF ≥55%), subnormal (EF 45% ≤ EF <55%), or abnormal (EF <45%). Of the survivors, 21% (13 of 62) had a normal LV EF, 61% (38 of 62) had a subnormal LVEF, and 18% (11 of 62) had an abnormal LVEF. There was a trend toward a male predominance among those with an abnormal LVEF (n = 11); 29% (8 of 28) were male and 9% (3 of 34) were female (p = 0.053). Survivors with an LVEF <45% were older than those with an LVEF ≥45% (16.3 vs. 14.2 years, p = 0.047). Eight percent of the survivors (5 of 62) thought their exercise tolerance was compromised when compared with peers and had an LVEF <55% (range: 44.3% to 54.7%). The cumulative anthracycline dose, age at diagnosis, and follow-up time seemed not to be associated with the LV EF (data not shown).

The LV parameters were compared in 3 age groups (8 to 11, 12 to 14, and 15 to 17 years) with the data of Robbers-Visser et al. (19) (Table 3). No reference data are available for the short-axis LV parameters taking both age group and sex simultaneously into account. The LV end-diastolic volume (EDV) and end-systolic volume (ESV) were significantly larger in the study group. A total of 82% (28 of 34) of the female subjects and 100% (28 of 28) of the male subjects had their LV ESV above the +2 SD of the reference values. The upper normal limits of the LV EDV were exceeded by 18% (6 of 34) of the female subjects and 43% (12 of 28) of the male subjects. The LVEF was significantly lower in all age groups compared with the reference values. The LV mass did not differ significantly from the normal values.

JACC Vol. 61, No. 14, 2013
April 9, 2013:1539–47

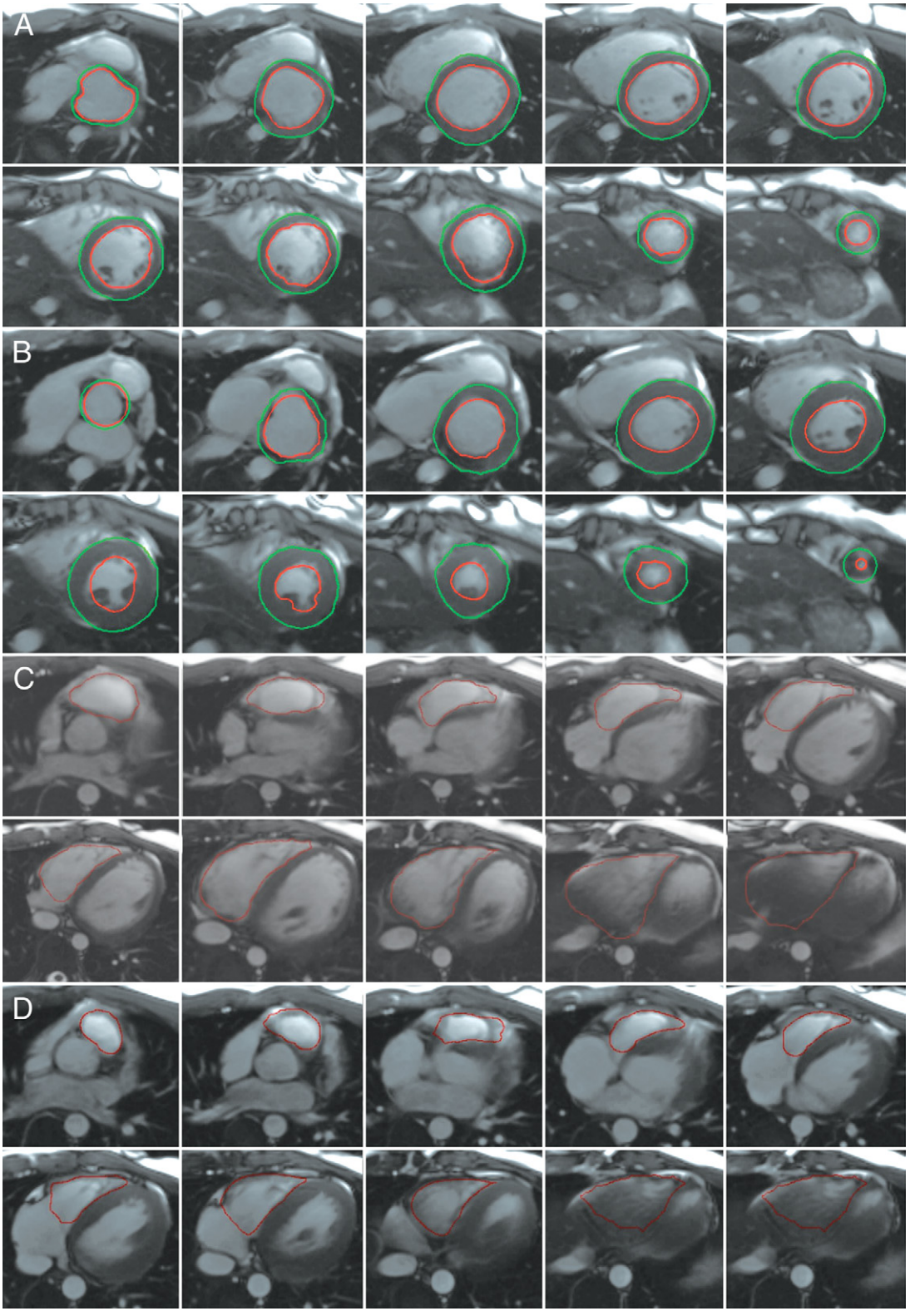

Figure 1 **Volumetric Analyses**

Endocardial and epicardial contours for short-axis images of left ventricular (LV) end-diastole volume (EDV) **(A)** and end-systole volume (ESV) **(B)**. Axial images of right ventricular (RV) EDV **(C)** and ESV **(D)**.

Table 3 BSA-Indexed LV Parameters per Age Group Compared With Reference Values by 1-Sample *t* Test

	Age Group 8–11 yrs (n = 14), 12–14 yrs (n = 15), 15–17 yrs (n = 33)	Mean ± SD	Range	Mean ± SD From Reference Values*	Range From Reference Values*	p Value	95% CI of the Difference	
							Lower	Upper
LVEF (%)	8–11 yrs	52.1 ± 5.2	44.0–61.8	69 ± 5	NA	<0.001	−19.9	−13.9
	12–14 yrs	51.1 ± 4.3	43.5–58.6	69 ± 5	NA	<0.001	−20.3	−15.5
	15–17 yrs	49.0 ± 6.0	33.7–61.7	69 ± 5	NA	<0.001	−22.1	−17.8
LV EDV (ml/m^2)	8–11 yrs	84.1 ± 13.4	69.4–118.8	71 ± 8	58–87	0.003	5.3	20.8
	12–14 yrs	89.5 ± 11.0	71.4–117.8	78 ± 9	66–97	0.001	5.4	17.6
	15–17 yrs	91.1 ± 15.8	58.7–131.3	77 ± 12	62–102	<0.001	8.5	19.7
LV ESV (ml/m^2)	8–11 yrs	40.3 ± 8.0	29.6–60.5	22 ± 5	15–33	<0.001	13.7	22.9
	12–14 yrs	43.8 ± 6.2	36.0–52.8	24 ± 5	16–34	<0.001	16.3	23.2
	15–17 yrs	46.3 ± 9.5	28.9–71.9	25 ± 6	18–39	<0.001	18.0	24.7
LV SV (ml/m^2)	8–11 yrs	43.8 ± 7.9	31.6–58.2	NA	NA	ND	ND	ND
	12–14 yrs	45.8 ± 7.2	34.8–65.1	NA	NA	ND	ND	ND
	15–17 yrs	44.7 ± 10.2	27.3–71.0	NA	NA	ND	ND	ND
LV mass (g/m^2)	8–11 yrs	64.4 ± 13.3	44.0–92.5	59 ± 8	44–84	0.153	−2.3	13.1
	12–14 yrs	68.7 ± 10.1	53.6–91.2	66 ± 11	54–87	0.310	−2.8	8.3
	15–17 yrs	68.2 ± 12.8	50.4–90.9	70 ± 17	42–98	0.417	−6.4	2.7

*Robbers-Visser D, Boersma E, Helbing WA. Normal biventricular function, volumes, and mass in children aged 8 to 17 years. J Magn Reson Imaging 2009;29:552–9.

BSA = body surface area; CI = confidence interval; EDV = end-diastolic volume; EF = ejection fraction; ESV = end-systolic volume; LV = ventricular; NA = not available; ND = not determined; SV = stroke volume.

Right ventricle. A normal RVEF was found in 19% (12 of 62) of the survivors, a subnormal RVEF was found in 53% (33 of 62) of the survivors, and an abnormal RVEF was found in 27% (17 of 62) of the survivors. More male subjects (39% [11 of 28]) than female subjects (18% [6 of 34]) had an abnormal RVEF (p = 0.057). The RVEF was not associated with the cumulative anthracycline dose, age at diagnosis, or follow-up time (data not shown).

For the RV parameters, a comparison with the reference values was done in 2 age groups (8 to 15 years and 16 to 20 years) and separately for female and male subjects (20) (Table 4). The RV ESV and stroke volume were signifi-

Table 4 BSA-Indexed RV Parameters per Sex and Age Group Compared With Reference Values by 1-Sample *t* Test

	Age Group	Mean ± SD	Range	Mean ± SD From Reference Values*	p Value	95% CI of the Difference	
						Lower	Upper
Female (n = 34)	8–15 yrs (n = 23), 16–20 yrs (n = 11)						
RVEF (%)	8–15 yrs	51.2 ± 8.4	26.5–65.4	62.6 ± 3.6	<0.001	−15.0	−7.8
	16–20 yrs	47.8 ± 8.9	30.6–64.5	62.1 ± 6.0	<0.001	−20.3	−8.3
RV EDV (ml/m^2)	8–15 yrs	84.6 ± 16.3	56.6–113.0	78.3 ± 9.7	0.076	−0.7	13.4
	16–20 yrs	77.8 ± 12.3	56.3–100.2	79.7 ± 10.3	0.629	−10.1	6.4
RV ESV (ml/m^2)	8–15 yrs	41.5 ± 11.8	26.0–67.1	29.2 ± 4.6	<0.001	7.2	17.4
	16–20 yrs	41.2 ± 11.7	20.0–64.0	30.4 ± 6.9	0.012	3.0	18.7
RV SV (ml/m^2)	8–15 yrs	43.1 ± 10.2	24.3–55.4	49.1 ± 6.8	0.01	−10.4	−1.6
	16–20 yrs	36.6 ± 5.6	23.3–43.6	49.3 ± 6.3	<0.001	−16.4	−8.9
Male (n = 28)	8–15 yrs (n = 17), 16–20 yrs (n = 11)						
RVEF (%)	8–15 yrs	48.8 ± 6.7	38.0–61.5	62.3 ± 4.3	<0.001	−16.9	−10.0
	16–20 yrs	40.6 ± 8.3	28.8–54.7	60.0 ± 4.4	<0.001	−24.9	−13.8
RV EDV (ml/m^2)	8–15 yrs	89.6 ± 23.5	60.5–142.3	82.9 ± 12.6	0.256	−5.4	18.8
	16–20 yrs	102.0 ± 14.2	81.8–128.7	90.2 ± 10.9	0.02	2.3	21.3
RV ESV (ml/m^2)	8–15 yrs	45.7 ± 12.4	26.9–66.0	31.3 ± 6.1	<0.001	8.1	20.8
	16–20 yrs	60.7 ± 12.8	41.8–85.3	36.1 ± 6.3	<0.001	16.0	33.2
RV SV (ml/m^2)	8–15 yrs	43.9 ± 14.3	28.0–80.6	51.6 ± 8.4	0.042	−15.1	−0.3
	16–20 yrs	41.3 ± 9.4	27.0–59.8	54.1 ± 7.3	0.001	−19.1	−6.5

*Sarikouch S, Peters B, Gutberlet M, et al. Sex-specific pediatric percentiles for ventricular size and mass as reference values for cardiac MRI: assessment by steady-state free-precession and phase-contrast MRI flow. Circ Cardiovasc Imaging 2010;3:65–76.

BSA = body surface area; CI = confidence interval; EDV = end-diastolic volume; EF = ejection fraction; ESV = end-systolic volume; RV = right ventricular; SV = stroke volume.

JACC Vol. 61, No. 14, 2013
April 9, 2013:1539–47

Table 5 Comparison of Ventricular Volumes and Mass Between Survivors Exposed or Unexposed to Cardiac Irradiation

	Survivors With Cardiac Irradiation (n = 7)	Survivors Without Cardiac Irradiation (n = 55)	p Value
LV EDV (ml/m^2)	83.6 ± 19.0	89.8 ± 13.6	0.278
LV ESV (ml/m^2)	41.1 ± 9.9	44.8 ± 8.6	0.300
RV EDV (ml/m^2)	77.6 ± 15.4	89.2 ± 19.0	0.128
RV ESV (ml/m^2)	35.2 ± 13.9	47.4 ± 13.3	0.027
LV mass (g/m^2)	61.7 ± 14.4	68.2 ± 11.9	0.190

Values are mean ± SD.
EDV = end-diastolic volume; ESV = end-systolic volume; LV = left ventricular; RV = right ventricular.

cantly larger in the study group. some 41% (14 of 34) of the female and 64% (18 of 28) of the male subjects had their RV ESV above the +2 SD of the reference values. An abnormally large RV EDV was found in 15% (5 of 34) of the female subjects and 21% (6 of 28) of the male subjects. Only the male subjects aged 16 to 20 years had a significantly larger RV EDV compared with the reference values. The RVEF was significantly lower in all age groups compared with reference values. The RV mass was not measured in our study.

Cardiac irradiation. Those with a history of cardiac irradiation did not have larger ventricular volumes or an altered LV mass compared with the other survivors (Table 5). Among the irradiation-exposed subjects, 29% (2 of 7) had their LV EDV, 86% (6 of 7) had their LV ESV, and 14% (1 of 7) had their RV ESV above the +2 SD of the reference values.

None of the study patients showed LGE. The intraobserver and interobserver data are presented in Figure 2 and Table 6. The limits of agreement were defined as ±1.96 SD from the mean between 2 measurements. Intraobserver variability was lower than interobserver variability. Interobserver variability was lower for the LV than for the RV.

Discussion

The current study is the first to report on the LGE and LV and RV function with CMR in a pediatric population after anthracycline treatment. The data unequivocally document a marked LV and RV dysfunction without signs of focal myocardial fibrosis among the anthracycline-exposed long-term survivors of childhood cancer. However, the myocardial dysfunction remains mostly asymptomatic at approximately 1 decade post-therapy. Only 6% (4 of 62) were taking medication, and 92% of the total considered their exercise tolerance normal. Armstrong et al. (9) found an abnormal LVEF with CMR in 32% of their adult survivors of childhood cancer previously undiagnosed with cardiotoxicity. Yet, although asymptomatic, the survivors may be at risk of a symptomatic heart failure on exposure to a stress such as pregnancy (22) or hypertension (23), warranting a regular cardiologic follow-up and lifestyle counseling.

CMR volumetry and function. CMR imaging is a well-established, accurate, reproducible, and noninvasive method for assessing both the LV and RV function (10,24). Advantages over echocardiography include independence of the acoustic window and geometric assumptions, as well as freely selectable imaging planes. Among the survivors of childhood cancer, the impact of factors such as obesity, postoperative abnormalities of the thorax, or a marked dilatation of the ventricles emphasizes the benefits of CMR. Furthermore, CMR remains optimal for the imaging of cardiomyopathies with an ability to visualize the myocardium (25).

Until recently, the CMR reference values in children have been based on the gradient-echo sequences from a limited number of small studies (26–28). Recent papers (19,20) report pediatric data using steady-state, free-precession, gradient-echo sequences, currently the standard method in a functional and volumetric CMR. The availability of age group–specific data (19,20) made it possible for us to compare the ventricular volumes with the pediatric reference values.

The screening for an anthracycline-induced cardiotoxicity has previously focused on the LV. The normal values for the fractional shortening and EF are age-independent, facilitating their use in a pediatric population. However, the BSA-indexed ventricular volumes offer a valuable tool for an earlier detection of overload changes in the heart chambers. A sizeable proportion of our study patients had abnormally large LV and RV ESVs, with the EDVs being less affected. This may represent an early stage in the progression of dysfunction. The fractional shortening and EF may remain within the normal limits despite LV dilatation. In many heart diseases, the BSA-indexed ventricular volumes are used at the clinic (13). Therefore, abnormally large ventricular volumes with a normal EF emphasize the need for a regular cardiac follow-up among pediatric cancer survivors.

Our results are in agreement with the data of Oberholzer et al. (29) on the biventricular cardiac function of anthracycline-exposed pediatric patients. One-half of their patients had an LVEF <55% but remained asymptomatic, and the RVEF after chemotherapy was 48.2 ± 7.1%, reflecting an additional impairment in the RV function (29).

The cardiotoxic effects of irradiation are more diverse than those of anthracyclines and are reported to be predominantly restrictive (30). Adams et al. (31) reported reduced LV dimensions by echocardiography among mediastinal irradiation–exposed long-term survivors of Hodgkin dis-

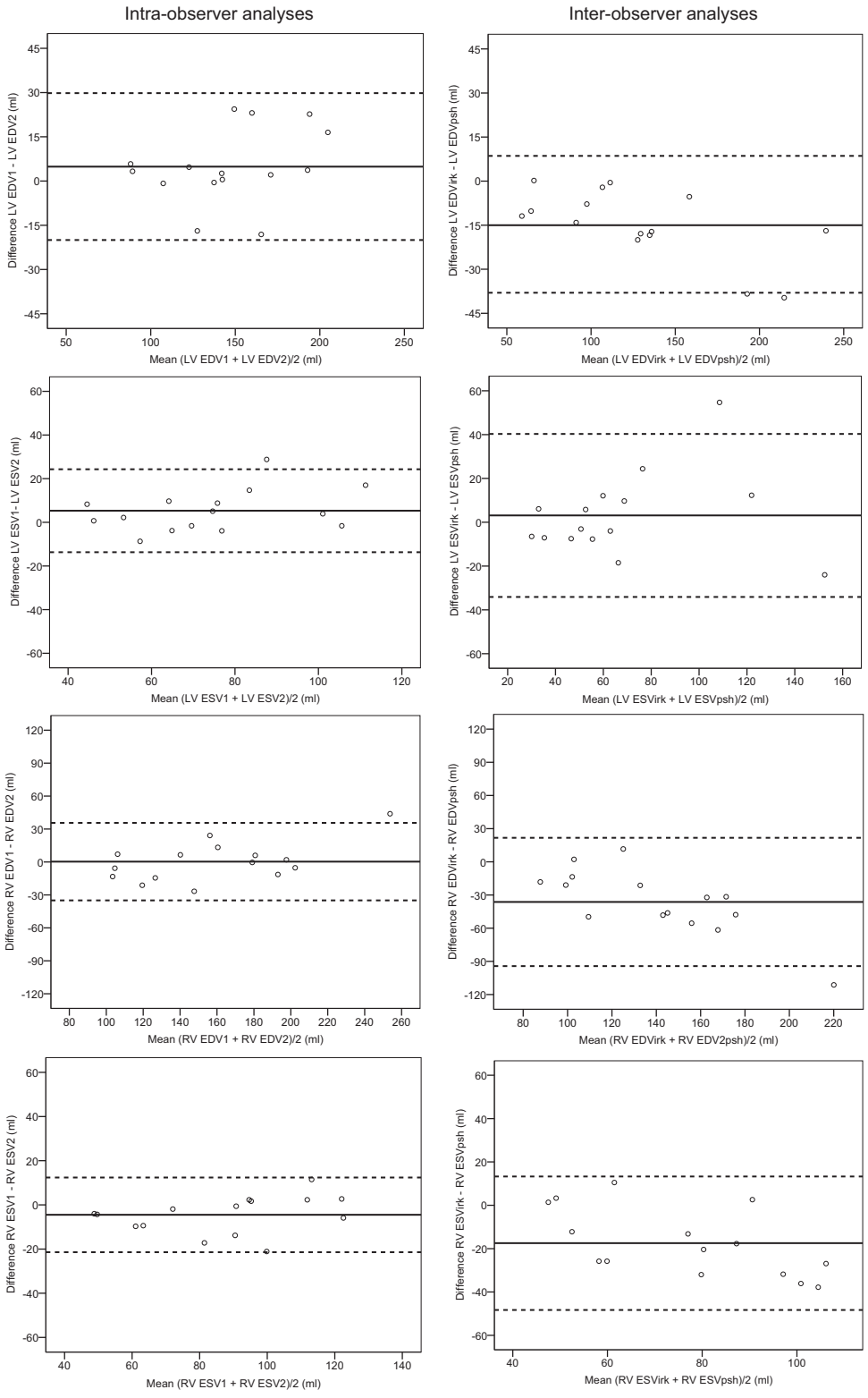

Figure 2 **Bland-Altman Plots for CMR Intraobserver and Interobserver Analyses**

Intraobserver plots are shown on the **left**, and interobserver plots are shown on the **right**. Interobserver analyses were independently reviewed by 2 of the investigators (IRK and PSH). The **bold horizontal line** represents the mean difference, and the **dashed horizontal lines** represent ±1.96 SD from the mean between the 2 measurements. CMR = cardiac magnetic resonance; EDV = end-diastolic volume; ESV = end-systolic volume; LV = left ventricular; RV = right ventricular.

JACC Vol. 61, No. 14, 2013
April 9, 2013:1539–47

Table 6 Intraobserver and Interobserver Variability (Bland-Altman)

	LV EDV	LV ESV	RV EDV	RV ESV
Intraobserver variability				
Mean difference	4.9	5.3	0.3	−4.5
Limits of agreement	−20.0 to 29.8	−13.7 to 24.3	−35.0 to 35.6	−21.4 to 12.4
Interobserver variability				
Mean difference	−14.7	3.1	−36.3	−17.5
Limits of agreement	−38.0 to 8.6	−34.1 to 40.3	−94.3 to 21.7	−48.3 to 13.3

Values are given in milliliters.
EDV = end-diastolic volume; ESV = end-systolic volume; LV = ventricular; RV = right ventricular.

ease. In our study, there was a trend toward smaller ventricular volumes among the cardiac irradiation–exposed survivors. Yet, because of the small sample size and heterogeneity of the cohort, reliable conclusions could not be drawn.

Late gadolinium enhancement. A delayed enhancement could not be detected even though 2 different methods were used: one using the changing TI time and one using a sensitive PSIR method with a constant TI time. Gd-CA doses in the LGE imaging of various heart diseases have varied between 0.1 and 0.2 mmol/kg (32–34). It remains unsettled whether a larger Gd-CA dose could have produced more LGE among our study patients, but for safety reasons the lower recommended dose was used (35).

Data on the myocardial LGE among anthracycline-exposed long-term survivors of childhood cancer have not been reported. Wassmuth et al. (36) studied 22 adult patients and reported on a transient increase in the myocardial enhancement early after the administration of anthracycline. Perel et al. (37) described 2 adults with an anthracycline cardiomyopathy, LV dysfunction, and subendocardial LGE years after chemotherapy, with one having LGE in the RV. Furthermore, LGE also was detected in 29% of 36 adult patients with mediastinal radiotherapy for Hodgkin disease more than 2 decades earlier (38).

Data on fibrosis in anthracycline-induced cardiomyopathy remain limited but indicate a prolonged process (18,37). The incidence of frank cardiac pathology increases with time since exposure. The estimated risk of developing cardiomyopathy after anthracycline therapy has been reported to be 4.5% at 10 years and increases to 9.8% at 20 years after therapy among patients with cumulative doses of ≥300 mg/m^2 (39). The median follow-up of 7.8 years in our study may not have been long enough for myocardial fibrosis to develop. This may be partly due to age-related cardiovascular events promoting cardiac damage and myocardial fibrosis, emphasizing the importance of lifestyle counseling among the long-term survivors. Furthermore, endomyocardial biopsies remain infrequently performed during pediatric follow-up. This may negatively affect the possibility of documenting myocardial fibrosis among children.

A diffuse myocardial fibrosis cannot be visualized on LGE with diffuse fibrosis being nulled out to highlight focal fibrosis and information on a possible background diffuse fibrosis thus being obliterated (14). Flett et al. (40) recently reported on a novel, noninvasive equilibrium-contrast CMR approach to detect the diffuse fibrosis validated using surgical myocardial biopsies in patients with aortic stenosis and hypertrophic cardiomyopathy. Bernaba et al. (41) found both interstitial and diffuse fibrosis in the myocardial tissue of 10 adult patients with an anthracycline-induced cardiomyopathy. It is conceivable that some of our study patients may have diffuse fibrosis not detectable with the technique used.

Published data (18,37,41) clearly indicate that some patients with anthracycline exposure will have focal or diffuse fibrosis detectable on LGE or through an equilibrium-contrast CMR. The limited number of reports on an established myocardial fibrosis with anthracycline cardiomyopathy invariably document a concomitant symptomatic heart failure, and many of these patients have undergone heart transplantation (18,37,41).

Study limitations. Because of ethical reasons and resource limitations, we had no own healthy controls analyzed with CMR.

Conclusions

A markedly high proportion of the long-term survivors of childhood cancer with anthracycline exposure appear to have a cardiac dysfunction detectable by CMR with the RV also being involved, but without focal myocardial fibrosis. In the follow-up of these patients, the CMR is highly usable, particularly among those with poor acoustic windows or the RV function at focus. Whether a longer follow-up will render putative anthracycline-induced myocardial fibrosis detectable (e.g., LGE) among the long-term survivors of childhood cancer remains to be established.

Acknowledgments

The authors thank Tuija Wigren, MD, for help with the radiation therapy case histories; Kirsi-Maria Lauerma, MD, for expert advice with CMR techniques; and Satu Ranta, RN, for practical assistance during the project.

Reprint requests and correspondence: Dr. Kaisa Ylänen, Tampere University Hospital, Department of Pediatrics, P.O. Box 2000, FI-33521 Tampere, Finland. E-mail: kaisa@ylanen.fi.

REFERENCES

1. Lipshultz SE, Colan SD, Gelber RD, Perez-Atayde AR, Sallan SE, Sanders SP. Late cardiac effects of doxorubicin therapy for acute lymphoblastic leukemia in childhood. N Engl J Med 1991;324:808–15.
2. Mulrooney DA, Yeazel MW, Kawashima T, et al. Cardiac outcomes in a cohort of adult survivors of childhood and adolescent cancer: retrospective analysis of the childhood cancer survivor study cohort. BMJ 2009;339:b4606.
3. Blanco JG, Sun CL, Landier W, et al. Anthracycline-related cardiomyopathy after childhood cancer: role of polymorphisms in carbonyl reductase genes—a report from the Children's Oncology Group. J Clin Oncol 2012;30:1415–21.
4. Kremer LC, van der Pal HJ, Offringa M, van Dalen EC, Voute PA. Frequency and risk factors of subclinical cardiotoxicity after anthracycline therapy in children: a systematic review. Ann Oncol 2002;13:819–29.
5. Kremer LC, van Dalen EC, Offringa M, Voute PA. Frequency and risk factors of anthracycline-induced clinical heart failure in children: a systematic review. Ann Oncol 2002;13:503–12.
6. Swain SM, Whaley FS, Ewer MS. Congestive heart failure in patients treated with doxorubicin: a retrospective analysis of three trials. Cancer 2003;97:2869–79.
7. Levitt G, Anazodo A, Burch M, Bunch K. Cardiac or cardiopulmonary transplantation in childhood cancer survivors: an increasing need? Eur J Cancer 2009;45:3027–34.
8. Ganame J, Claus P, Uyttebroeck A, et al. Myocardial dysfunction late after low-dose anthracycline treatment in asymptomatic pediatric patients. J Am Soc Echocardiogr 2007;20:1351–8.
9. Armstrong GT, Plana JC, Zhang N, et al. Screening adult survivors of childhood cancer for cardiomyopathy: comparison of echocardiography and cardiac magnetic resonance imaging. J Clin Oncol 2012;30:2876–84.
10. Keenan NG, Pennell DJ. CMR of ventricular function. Echocardiography 2007;24:185–93.
11. American College of Cardiology Foundation Task Force on Expert Consensus, Documents, Hundley WG, Bluemke DA, et al. ACCF/ACR/AHA/NASCI/SCMR 2010 expert consensus document on cardiovascular magnetic resonance: a report of the American College of Cardiology Foundation Task Force on Expert Consensus Documents. J Am Coll Cardiol 2010;55:2614–62.
12. Haddad F, Hunt SA, Rosenthal DN, Murphy DJ. Right ventricular function in cardiovascular disease, part I: anatomy, physiology, aging, and functional assessment of the right ventricle. Circulation 2008;117:1436–48.
13. Fratz S, Schuhbaeck A, Buchner C, et al. Comparison of accuracy of axial slices versus short-axis slices for measuring ventricular volumes by cardiac magnetic resonance in patients with corrected tetralogy of Fallot. Am J Cardiol 2009;103:1764–9.
14. Sado DM, Flett AS, Moon JC. Novel imaging techniques for diffuse myocardial fibrosis. Future Cardiol 2011;7:643–50.
15. Wu E, Judd RM, Vargas JD, Klocke FJ, Bonow RO, Kim RJ. Visualisation of presence, location, and transmural extent of healed Q-wave and non-Q-wave myocardial infarction. Lancet 2001;357:21–8.
16. Ordovas KG, Higgins CB. Delayed contrast enhancement on MR images of myocardium: past, present, future. Radiology 2011;261:358–74.
17. Sawyer DB, Peng X, Chen B, Pentassuglia L, Lim CC. Mechanisms of anthracycline cardiac injury: can we identify strategies for cardioprotection? Prog Cardiovasc Dis 2010;53:105–13.
18. Steinherz LJ, Steinherz PG, Tan C. Cardiac failure and dysrhythmias 6-19 years after anthracycline therapy: a series of 15 patients. Med Pediatr Oncol 1995;24:352–61.
19. Robbers-Visser D, Boersma E, Helbing WA. Normal biventricular function, volumes, and mass in children aged 8 to 17 years. J Magn Reson Imaging 2009;29:552–9.
20. Sarikouch S, Peters B, Gutberlet M, et al. Sex-specific pediatric percentiles for ventricular size and mass as reference values for cardiac MRI: assessment by steady-state free-precession and phase-contrast MRI flow. Circ Cardiovasc Imaging 2010;3:65–76.
21. Bland JM, Altman DG. Statistical methods for assessing agreement between two methods of clinical measurement. Lancet 1986;1:307–10.
22. Hadar A, Sheiner E, Press F, Katz A, Katz M. Dilated cardiomyopathy in a pregnant woman after doxorubicin and radiotherapy for Hodgkin's disease: a case report. J Reprod Med 2004;49:401–3.
23. Ryberg M, Nielsen D, Cortese G, Nielsen G, Skovsgaard T, Andersen PK. New insight into epirubicin cardiac toxicity: competing risks analysis of 1097 breast cancer patients. J Natl Cancer Inst 2008;100:1058–67.
24. Higgins CB. Which standard has the gold? J Am Coll Cardiol 1992;19:1608–9.
25. Belloni E, De Cobelli F, Esposito A, et al. MRI of cardiomyopathy. AJR Am J Roentgenol 2008;191:1702–10.
26. Helbing WA, Rebergen SA, Maliepaard C, et al. Quantification of right ventricular function with magnetic resonance imaging in children with normal hearts and with congenital heart disease. Am Heart J 1995;130:828–37.
27. Lorenz CH. The range of normal values of cardiovascular structures in infants, children, and adolescents measured by magnetic resonance imaging. Pediatr Cardiol 2000;21:37–46.
28. Cain PA, Ahl R, Hedstrom E, et al. Age and gender specific normal values of left ventricular mass, volume and function for gradient echo magnetic resonance imaging: a cross sectional study. BMC Med Imaging 2009;9:2.
29. Oberholzer K, Kunz RP, Dittrich M, Thelen M. [Anthracycline-induced cardiotoxicity: cardiac MRI after treatment for childhood cancer]. ROFO Fortschr Geb Rontgenstr Nuklearmed 2004;176:1245–50.
30. Chen MH, Colan SD, Diller L. Cardiovascular disease: cause of morbidity and mortality in adult survivors of childhood cancers. Circ Res 2011;108:619–28.
31. Adams MJ, Lipsitz SR, Colan SD, et al. Cardiovascular status in long-term survivors of Hodgkin's disease treated with chest radiotherapy. J Clin Oncol 2004;22:3139–48.
32. Moon JC, McKenna WJ, McCrohon JA, Elliott PM, Smith GC, Pennell DJ. Toward clinical risk assessment in hypertrophic cardiomyopathy with gadolinium cardiovascular magnetic resonance. J Am Coll Cardiol 2003;41:1561–7.
33. Assomull RG, Prasad SK, Lyne J, et al. Cardiovascular magnetic resonance, fibrosis, and prognosis in dilated cardiomyopathy. J Am Coll Cardiol 2006;48:1977–85.
34. Wadhwa D, Fallah-Rad N, Grenier D, et al. Trastuzumab mediated cardiotoxicity in the setting of adjuvant chemotherapy for breast cancer: a retrospective study. Breast Cancer Res Treat 2009;117:357–64.
35. Assomull RG, Pennell DJ, Prasad SK. Cardiovascular magnetic resonance in the evaluation of heart failure. Heart 2007;93:985–92.
36. Wassmuth R, Lentzsch S, Erdbruegger U, et al. Subclinical cardiotoxic effects of anthracyclines as assessed by magnetic resonance imaging-a pilot study. Am Heart J 2001;141:1007–13.
37. Perel RD, Slaughter RE, Strugnell WE. Subendocardial late gadolinium enhancement in two patients with anthracycline cardiotoxicity following treatment for Ewing's sarcoma. J Cardiovasc Magn Reson 2006;8:789–91.
38. Machann W, Beer M, Breunig M, et al. Cardiac magnetic resonance imaging findings in 20-year survivors of mediastinal radiotherapy for Hodgkin's disease. Int J Radiat Oncol Biol Phys 2011;79:1117–23.
39. van Dalen EC, van der Pal HJ, Kok WE, Caron HN, Kremer LC. Clinical heart failure in a cohort of children treated with anthracyclines: a long-term follow-up study. Eur J Cancer 2006;42:3191–8.
40. Flett AS, Hayward MP, Ashworth MT, et al. Equilibrium contrast cardiovascular magnetic resonance for the measurement of diffuse myocardial fibrosis: Preliminary validation in humans. Circulation 2010;122:138–44.
41. Bernaba BN, Chan JB, Lai CK, Fishbein MC. Pathology of late-onset anthracycline cardiomyopathy. Cardiovasc Pathol 2010;19:308–11.

Key Words: anthracycline ■ dysfunction ■ fibrosis ■ late gadolinium enhancement ■ magnetic resonance imaging.

Three-Dimensional Echocardiography and Cardiac Magnetic Resonance Imaging in the Screening of Long-Term Survivors of Childhood Cancer After Cardiotoxic Therapy

Kaisa Ylänen, MD[a,b,*], Anneli Eerola, MD, PhD[a], Kim Vettenranta, MD, PhD[c,d], and Tuija Poutanen, MD, PhD[a,b]

The left ventricular (LV) volumes, ejection fraction (EF), and dyssynchrony indexes for the 16 and 12 cardiac segments (Tmsv16-SD and Tmsv12-SD, respectively) were analyzed among nonadult, anthracycline-exposed long-term survivors of childhood cancer and compared with those of healthy controls using conventional and real-time 3-dimensional echocardiography (RT-3DE) with cardiac magnetic resonance (CMR) imaging in a prospective, cross-sectional, single tertiary center setting. Seventy-one survivors and gender-, body surface area-, and age-matched healthy controls were studied by conventional echocardiography and RT-3DE. Fifty-eight of the 71 survivors underwent also CMR. The survivors were evaluated in 2 groups. Group I consisted of 63 exposed to anthracyclines and group II consisted of 8 also exposed to cardiac irradiation. By RT-3DE, the group I survivors had a lower LVEF (57% vs 60%, respectively, $p = 0.003$) and larger body surface area−indexed LV end-systolic volume (31 vs 28 ml/m^2, respectively, $p = 0.001$) than controls. The Tmsv16-SD was higher in group II than in I (1.93% vs 1.39%, respectively, $p = 0.003$). None of the survivors had an abnormal fractional shortening (<28%), but 10% had an LVEF <50% by RT-3DE. An LVEF <55% was detected in 45 of 58 (78%) of those imaged with CMR. In conclusion, RT-3DE seems to detect more abnormalities in cardiac function than conventional echocardiography following childhood cancer therapy. The LV dyssynchrony indexes derived from RT-3DE appear potentially useful in assessing the early signs of cardiotoxicity between anthracycline and cardiac irradiation exposed long-term survivors of childhood cancer. **(Am J Cardiol 2014;113:1886−1892)**

Anthracyclines and radiotherapy, both with cardiotoxic side effects, are used in the treatment of many childhood malignancies.[1] The Children's Oncology Group recommends transthoracic 2-dimensional echocardiography for the assessment of the left ventricular (LV) function among the survivors due to its broad availability and noninvasiveness.[2] However, the M-mode−derived fractional shortening remains insensitive in detecting subtle changes in cardiac function.[3−5] The real-time, 3-dimensional echocardiography (RT-3DE) is a well-validated method for the assessment of the LV dimensions and ejection fraction (EF)[6,7] not relying on geometrical assumptions. Many factors, including the synchronicity of the LV contraction, impact the function. Indexes for assessing the LV mechanical dyssynchrony can be derived from the time-volume data provided by the RT-3DE.[8] There is an obvious need for more sensitive methods for cardiotoxicity screening especially in the pediatric population with a long life expectancy. Our aim was to evaluate the prevalence of LV dysfunction among asymptomatic childhood cancer survivors by means of conventional echocardiography, RT-3DE, and cardiac magnetic resonance (CMR) imaging and to test whether the RT-3DE is a method employable in the screening.

Methods

All consecutive, long-term survivors of childhood cancer in remission attending the population-based, pediatric hematology-oncology service of the Tampere University Hospital (Tampere, Finland) from February 2010 to June 2011, and having received anthracyclines as part of their chemotherapy no <5 years earlier, were prospectively enrolled. Survivors with a congenital heart disease were excluded. Of the 86 initially recruited 76 (42 women and 34 men) agreed to participate. We studied survivors

[a]Department of Pediatrics, Tampere University Hospital, Tampere, Finland; [b]University of Tampere, Tampere, Finland; [c]Hospital for Children and Adolescents, Helsinki, Finland; and [d]University of Helsinki, Helsinki, Finland. Manuscript received December 18, 2013; revised manuscript received and accepted March 6, 2014.

This work was supported by the following Finnish foundations: the Blood Disease Research Foundation, Helsinki; the Competitive Research Funding of the Tampere University Hospital, 9L114 and 9N084, Tampere; the EVO funds of the Tampere University Hospital, Tampere; the Emil Aaltonen Foundation, Tampere; the Finnish Association of Hematology, Helsinki; the Finnish Cancer Foundation, Helsinki; the Finnish Cultural Foundation, Helsinki; the Finnish Cultural Foundation Pirkanmaa Regional Fund, Ylöjärvi; the Foundation for Pediatric Research, Helsinki; the National Graduate School of Clinical Investigations, Helsinki; the Päivikki and Sakari Sohlberg Foundation, Helsinki; the Scientific Foundation of the City of Tampere, Tampere; and the Väre Foundation for Pediatric Cancer, Helsinki.

See page 1891 for disclosure information.

*Corresponding author: Tel: (+358)-3-31164058; fax: (+358)-3-31165511.

E-mail address: kaisa@ylanen.fi (K. Ylänen).

0002-9149/14/$ - see front matter
http://dx.doi.org/10.1016/j.amjcard.2014.03.019

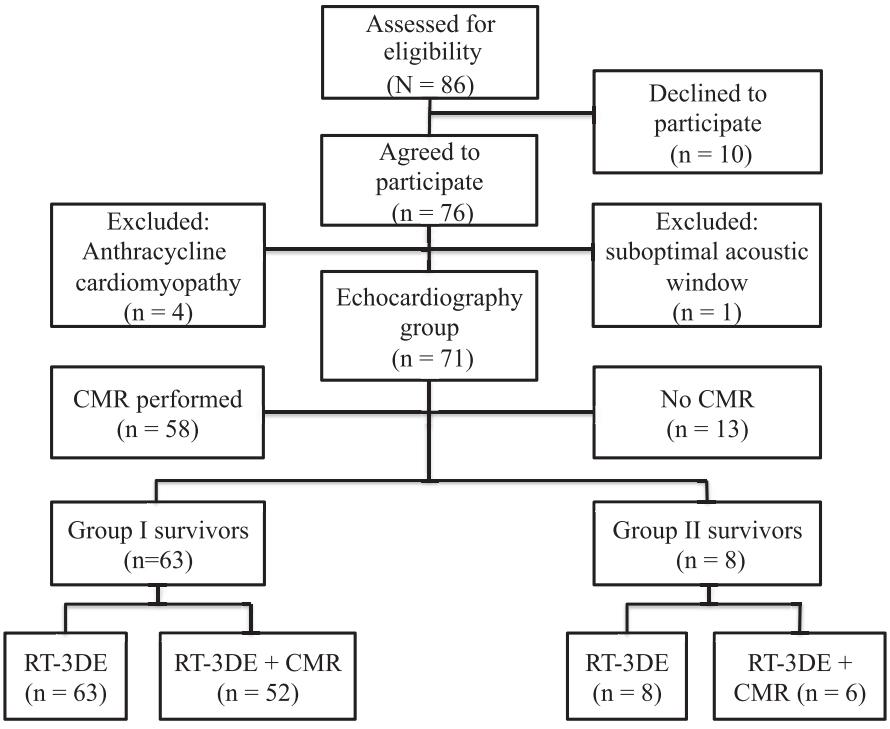

Figure 1. Study recruitment flow chart with the numbers indicating study patients with different imaging methods performed.

Table 1
The clinical characteristic of the survivors and controls

Variable	Group I (n = 63)	Control I (n = 63)	p Value	Group II (n = 8)	Control II (n = 8)	p Value
Women	31 (49)	31 (49)		6 (75)	6 (75)	
Men	32 (51)	32 (51)		2 (25)	2 (25)	
Age (yrs)	14 ± 3	14 ± 3	0.099	13 ± 3	14 ± 3	0.020
Height (cm)	161 ± 16	162 ± 17	0.012	152 ± 15	154 ± 13	0.585
Weight (kg)	55 ± 17	54 ± 17	0.147	46 ± 13	47 ± 11	0.376
Body surface area (m^2)	1.6 ± 0.3	1.6 ± 0.3	0.573	1.4 ± 0.3	1.4 ± 0.2	0.435
Acute lymphoblastic leukemia	31 (49)			0		
Acute myeloid leukemia	3 (5)			6 (75)		
Solid tumor	29 (46)			2 (25)		
Age at diagnosis (yrs)	4 (0−14)			5 (0−13)		
Follow-up (yrs)	7 (5−18)			6 (5−12)		
Cumulative anthracycline dose (mg/m^2)	218 (80−386)			382 (163−454)		
Cardiac irradiation	0			8 (100)		
Relapse	1 (2)			3 (38)		
Allogeneic stem cell transplantation	0			6 (75)		

Values are presented as n (%), mean ± SD, or median (range).
Group I = no cardiac irradiation; Group II = cardiac irradiation.

without previously diagnosed cardiotoxicity, and thus 4 women with a previous diagnosis of late-onset anthracycline-associated cardiomyopathy were excluded. One woman with a suboptimal acoustic window was also excluded, resulting in a total of 71 survivors in the study cohort (Figure 1). The total cumulative anthracycline dose was calculated per the recommendations of the Children's Oncology Group (*www.survivorshipguidelines.org*). A total of 71 healthy volunteers without cardiac pathology were recruited as gender-, body surface area-, and age-matched controls. This study complies with the Declaration of Helsinki. The Institutional Review Board of the Tampere University Hospital approved the study protocol. All patients/controls and their legal guardian(s) gave their written informed consent.

The key clinical data on the survivors and controls are listed in Table 1. The former were divided into 2 groups by therapy. Group I consisted of 63 anthracycline-exposed survivors, group II consisted of 8 exposed to both anthracyclines and cardiac irradiation, and controls I and II of their respective controls. The average cumulative cardiac radiation dose was deduced from the radiotherapy records (median 10.0 Gy [range 3.6 to 12.0]). Electrocardiogram was obtained from all survivors.

Table 2
The cardiac imaging parameters

Variable	Group I (n = 63)	Control I (n = 63)	p Value	Group II (n = 8)	Control II (n = 8)	p Value
M-mode						
LV end-diastolic dimension	0.8 ± 0.8	0.7 ± 0.9	0.282	0.3 ± 0.8	0.4 ± 1.1	0.831
LV end-systolic dimension	1.1 ± 0.7	0.7 ± 0.8	0.003	0.8 ± 0.6	0.4 ± 0.8	0.289
Interventricular septum diastolic diameter	0.4 ± 0.8	0.5 ± 1.0	0.535	0.4 ± 1.0	1.0 ± 0.8	0.220
LV posterior wall diastolic diameter	−0.2 ± 0.7	−0.2 ± 0.6	0.950	−0.5 ± 0.4	0.1 ± 0.6	0.089
LV mass (g/m^2)	75 ± 13	75 ± 16	0.975	63 ± 9	74 ± 13	0.119
LV mass/volume ratio (g/ml)	1.1 ± 0.2	1.1 ± 0.2	0.558	1.0 ± 0.1	1.2 ± 0.1	0.039
Fractional shortening (%)	33 ± 3	35 ± 3	0.003	33 ± 2	35 ± 3	0.045
RT-3DE						
LV end-diastolic volume (ml/m^2)	73 ± 10	70 ± 9	0.060	67 ± 7	72 ± 8	0.218
LV end-systolic volume (ml/m^2)	31 ± 6	28 ± 5	0.001	30 ± 5	30 ± 6	0.963
LV stroke volume (ml/m^2)	41 ± 7	42 ± 6	0.890	38 ± 6	43 ± 3	0.039
LVEF (%)	57 ± 6	60 ± 4	0.003	56 ± 7	59 ± 5	0.131
Tmsv16-SD (%)	1.39 ± 0.43	1.49 ± 0.40	0.164	1.93 ± 0.72	1.37 ± 0.24	0.098
Tmsv16-Dif (%)	5.13 ± 1.60	5.48 ± 1.57	0.208	6.92 ± 2.01	5.56 ± 1.19	0.192
Tmsv12-SD (%)	1.19 ± 0.44	1.30 ± 0.43	0.207	1.76 ± 0.48	1.11 ± 0.35	0.008
Tmsv12-Dif (%)	3.95 ± 1.51	4.33 ± 1.50	0.178	5.92 ± 1.64	3.85 ± 1.43	0.007
Frame rate (frames/s)	23 ± 3	25 ± 4	<0.001	25 ± 3	24 ± 3	0.554
CMR imaging	(n = 52)			(n = 6)		
LV end-diastolic volume (ml/m^2)	90 ± 14	—	—	82 ± 20	—	—
LV end-systolic volume (ml/m^2)	45 ± 9	—	—	41 ± 11	—	—
LV mass (g/m^2)	69 ± 12	—	—	63 ± 16	—	—
LV mass/volume ratio (g/ml)	0.8 ± 0.1	—	—	0.8 ± 0.1	—	—
LVEF (%)	50 ± 6	—	—	50 ± 6	—	—

Values are presented as mean ± SD.

Group I = no cardiac irradiation; Group II = cardiac irradiation; Tmsv12-Dif/Tmsv16-Dif = the maximum time difference to reach the minimum systolic volume between the earliest and latest contracting segments for the 12/16 segments as a percentage of the RR interval; Tmsv12-SD/Tmsv16-SD = standard deviation of the time to minimum systolic volume for the 12/16 segments as a percentage of the RR interval.

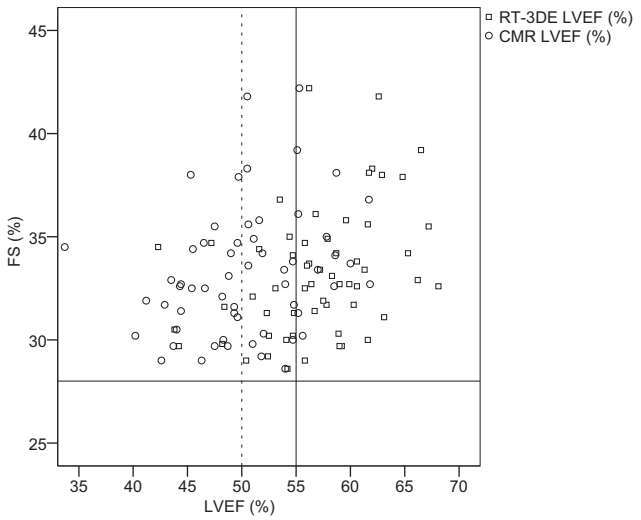

Figure 2. Scatter plot of LVEF with RT-3DE and CMR and fractional shortening by M-mode among the 58 survivors with all imaging methods used. LVEF 50% represents the lowest normal EF value measured by RT-3DE, LVEF 55% measured by CMR, and FS 28% represents the lowest normal value measured by M-mode.

Echocardiographic examination was performed using the iE33 ultrasound machine (Royal Philips Electronics, Philips Healthcare, Bothell, Washington). A 2-dimensional, Doppler, and M-mode examination was performed from the standard subcostal, apical, and parasternal views using the S8-3, S5-1, or X5-1 transducers. All measurements in the M-mode were made according to the recommendations of the American Society of Echocardiography,[9] and the average of 3 cardiac cycles used in the analysis. M-mode–derived LV mass was calculated according to the American Society of Echocardiography recommendation[9,10] and mass/volume ratio using the LV volume derived from the formula of Teichholz.[11] RT-3DE was performed in the left lateral semi-recumbent position using either the X3-1 or the X5-1 matrix-array transducers. The RT-3DE full-volume data sets were acquired from the apical 4-chamber view during 4 consecutive cardiac cycles and normal breathing. At least 3 data sets were acquired for each individual, stored off-line, and the highest quality data set selected for analysis.

A single investigator (KY) performed the off-line analysis on a Q-lab workstation (Philips Q-lab, version 8.1; 3DQA; Philips Healthcare, Bothell, Washington). The frame immediately before the full closure of the mitral valve was selected as end-diastole and that immediately before the full closure of the aortic valve as end-systole. The septal and lateral mitral annuli in the 4-chamber, the anterior and inferior mitral annuli in the 2-chamber view, and the LV apex in either of the 2 were set in both the end-diastolic and end-systolic frames. A semiautomated endocardial border detection was used to track the LV endocardium throughout the entire cardiac cycle. The software created a 3-dimensional dynamic model representing the cardiac cycle in the whole LV cavity and divided it into 16 segments excluding the apex as defined by the American Society of Echocardiography.[12] The software displayed the LV end-diastolic

and end-systolic volumes, EF, and time-volume data for each segment. The time to reach the minimum systolic volume for each of the segments was calculated. The dyssynchrony index for the 16 segments (Tmsv16-SD) was defined as the SD of this time as a percentage of the RR interval to correct for differences in heart rate between subjects. The maximum time difference to reach the minimum regional volume between the segments reaching the volume earliest and latest was calculated as a percentage of the RR interval (Tmsv16-Dif). The corresponding measurements (Tmsv12-SD and Tmsv12-Dif) were also performed for the 12 segments (6 basal and 6 middle) with the more synchronous the ventricular contraction, the lower the dyssynchrony index obtained. Two investigators (KY and AE) measured independently 20 randomly selected data sets for interobserver and the former independently 20 data sets twice for intraobserver variability.

Fifty-eight of the 71 survivors also agreed to undergo CMR imaging as previously described.[13] LV end-diastolic and end-systolic volumes and LVEF were measured. The CMR data of Robber-Visser et al[14] on 60 healthy children of the same age range with comparable size and imaged with comparable CMR method were employed as reference. Due to ethical reasons, CMR on the healthy controls was not performed.

The statistical analysis was performed using the IBM SPSS Statistics version 21 (IBM Corp., Armonk, New York) software. The data are presented as frequencies and percentages for categorical data, mean ± SD for normally distributed data, or median and range in case of non-normality. The group means were compared between the survivors and controls with the paired-samples *t* test. The Mann-Whitney *U* test was employed for the medians and the independent samples *t* test for the means among the survivors. The correlations were assessed with the Pearson correlation coefficients with data normally distributed and the Spearman's rho test in case of non-normality. The linear regression analysis was used to establish the predictors for Tmsv16-SD. All tests were 2-sided and $p < 0.05$ considered significant. Intraclass correlation coefficients were calculated for the intra and interobserver variabilities for RT-3DE measurements. An agreement between CMR and RT-3DE assessment of LV volumes and EF was evaluated using the Bland-Altman analysis.[15] With none of the controls having an RT-3DE LVEF <50% and their −2 SD for LVEF lying at 51%, we concluded 50% to be the appropriate lower normal limit by RT-3DE, in accordance with published reference values on children.[6,16] The lower normal limit for CMR-derived LVEF was set at 55% as deduced from literature.[14,17] The upper normal limits for dyssynchrony indexes were derived from +2 SD of our 71 healthy controls: Tmsv16-SD 2.26% and Tmsv12-SD 2.11%, in line with published.[16]

Results

None of the controls had a fractional shortening <28% or an RT-3DE LVEF <50%. The echocardiographic data of the 71 survivors and controls and the CMR data of 58 survivors are listed in Table 2. The M-mode classified 7 of the survivors with an abnormal LVEF by RT-3DE to have a normal LV function (fractional shortening). One case-control pair was left out of the dyssynchrony analysis due to a stitch artifact. Three of the 70 survivors (4%) had an

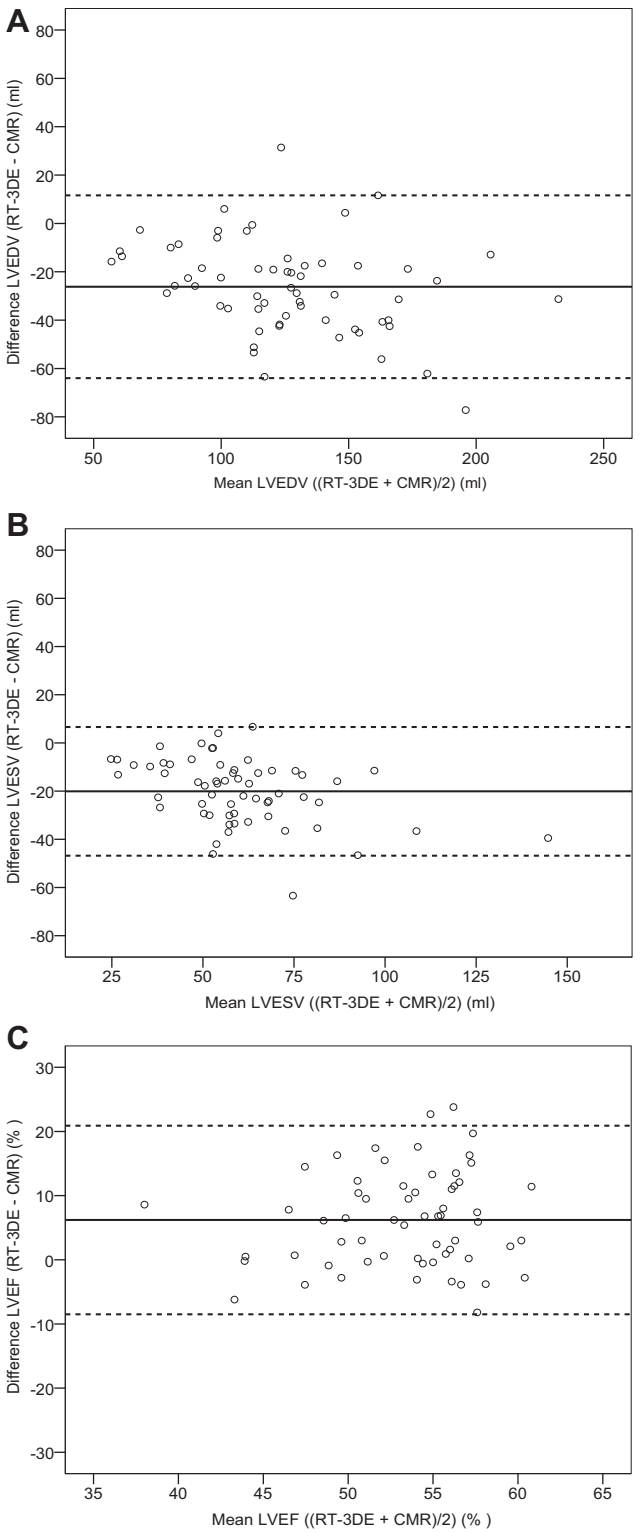

Figure 3. Comparisons between RT-3DE and CMR measurements of LV volumes and EF by Bland-Altman analyses: *(A)* LVEDV, *(B)* LVESV, and *(C)* LVEF. The *bold horizontal line* represents the mean difference. The *dashed horizontal lines* represent ±1.96 SD from the mean between the 2 techniques. LVEDV = LV end-diastolic volume; LVESV = LV end-systolic volume.

Table 3
The intraobserver and interobserver variabilities for the RT-3DE measurements

	Left Ventricular End-Diastolic Volume (ml)	Left Ventricular End-Systolic Volume (ml)	Tmsv16-SD (%)
Intraobserver variability			
Intraclass correlation coefficient	0.98	0.92	0.52
95% CI	0.94−0.99	0.81−0.97	0.12−0.78
Interobserver variability			
Intraclass correlation coefficient	0.88	0.78	0.25
95% CI	0.72−0.95	0.52−0.91	−0.21 to 0.61

CI = confidence interval.

abnormally high Tmsv16-SD, and 4 of 70 (6%) had a high Tmsv12-SD, but all had QRS-duration within normal limits in electrocardiograms.

Among the survivors, the RT-3DE LVEF correlated negatively with the Tmsv16-SD ($r = -0.44$, $p < 0.001$), Tmsv12-SD ($r = -0.34$, $p = 0.005$), Tmsv16-Dif ($r = -0.43$, $p < 0.001$), and Tmsv12-Dif ($r = -0.27$, $p = 0.024$). The body surface area−indexed LV end-systolic volume correlated positively with Tmsv16-SD ($r = 0.32$, $p < 0.007$). No significant correlation was found between the RT-3DE LVEF or Tmsv16-SD and the age at study, at diagnosis, at follow-up time, or cumulative anthracycline dose (data not shown). In the linear regression analysis, the Tmsv16-SD was predictable with the RT-3DE LVEF ($p < 0.001$) and cardiac irradiation ($p = 0.002$) with an adjusted R^2 of 0.28.

Figure 2 shows the data on the fractional shortening derived by M-mode and LVEF derived by RT-3DE and CMR among 58 survivors with all imaging performed. None of them had an abnormal fractional shortening. LVEF <50% was detected by RT-3DE in 6 of 58 (10%) and an abnormal LVEF (<55%) by CMR in 45 of 58 (78%). Even with the CMR-derived cutoff being was set <50%, 29 of 58 (50%) had an abnormal LVEF. Of those who underwent both RT-3DE and CMR, all 6 with an abnormal LVEF by RT-3DE also had an abnormal LVEF by CMR. The LV end-diastolic and end-systolic volumes were larger as measured by CMR than RT-3DE (89 ± 14 vs 73 ± 11 ml/m^2 and 44 ± 9 vs 31 ± 7 ml/m^2, $p < 0.001$, for both, respectively).

The survivors in group I had larger LV end-systolic dimensions and a lower fractional shortening in the M-mode than their controls (Table 2). In group I, the RT-3DE-derived LV end-systolic volumes were larger and LVEFs lower among the survivors. An RT-3DE LVEF <50% was detected in 5 of 63 (8%) and the CMR-derived <55% in 40 of 52 (77%) in group I.

The survivors in group II had a lower fractional shortening and M-mode−derived LV mass/volume ratio than their controls. Again, the RT-3DE-derived stroke volume was lower among the former, and the dyssynchrony indexes for the 12 segments were higher among the survivors in group II than controls. In group II, 2 of 8 (25%) had an RT-3DE LVEF <50%, and 5 of 6 (83%) had the CMR-derived <55%.

Age at study, at diagnosis, or at follow-up time did not differ significantly between groups I and II (Table 2), but the latter had a higher anthracycline dose ($p = 0.001$). The fractional shortening, EF (RT-3DE- and CMR-derived), and RT-3DE-derived, body surface area−indexed LV volumes did not differ between the groups (data not shown). All dyssynchrony indexes were higher in group II than group I survivors: Tmsv16-SD ($p = 0.003$), Tmsv16-Dif ($p = 0.005$), Tmsv12-SD ($p = 0.001$), and Tmsv12-Dif ($p = 0.001$), respectively (Table 2).

The Bland-Altman plots for the LV volumes and EF by RT-3DE compared with CMR are shown in Figure 3. Correlations between the RT-3DE and the CMR were for the LV end-diastolic ($r = 0.880$, $p < 0.001$) and end-systolic volumes ($r = 0.831$, $p < 0.001$) and LVEF ($r = 0.189$, $p = 0.155$). Intraobserver and interobserver variabilities of the LV volumes and Tmsv16-SD derived from RT-3DE are listed in Table 3.

Discussion

We document a lower LVEF with RT-3DE among anthracycline-exposed long-term survivors of childhood cancer without signs of cardiomyopathy, compared with that of gender-, body surface area-, and age-matched healthy controls. An enlarged LV end-systolic volume seems to be an early indicator of cardiotoxicity. In addition, we demonstrate a more dyssynchronous LV contraction among those exposed to irradiation.

Two-dimensional echocardiography and especially M-mode have limitations because of the geometrical assumptions posed on the LV and the ventricular dimensions measured only in 1 or 2 planes possibly leading to a lack of identification of the dyssynchrony. We demonstrate the RT-3DE-derived LVEF to detect more abnormalities in the systolic LV function than M-mode. The better sensitivity of the RT-3DE over that of the 2-dimensional echocardiography has recently been demonstrated in a CMR-validated study among adult survivors of childhood cancer.[5] Speckle tracking imaging has also proved to be useful in detecting an impaired LV function.[18]

The RT-3DE has been validated against CMR in assessing the LV volumes, EF, and mass in both children and adults.[7,19−21] It offers a better accuracy and reproducibility for the LV volume measurements over 2-dimensional echocardiography.[21,22] In most pediatric cases, the acoustic window for RT-3DE is excellent with only 1 of our patients having a suboptimal window. Its advantage over CMR is noninvasiveness and good accessibility. Children <8 to 10 years of age usually need sedation for CMR but not for RT-3DE. The myocardial damage caused by cardiotoxicity impairs contraction resulting in a gradual enlargement of the

LV in systole, and volume measurements serve as a tool in the follow-up. Our findings with the RT-3DE, the larger end-systolic volumes, and lower LVEFs among survivors agree with studies previously published.[3,4,18] The CMR confirms our results by also showing larger LV end-systolic volumes and lower LVEFs among the survivors.[13] Recent advances in the RT-3DE and analysis software have resulted in a better image quality and endocardial detection as well as somewhat larger ventricular volumes.[23] Despite that, among our cases, the RT-3DE-derived LV volumes were constantly smaller than those measured by CMR, in accordance with previous studies comparing the 2.[21]

The published lower normal limit for the CMR-derived LVEF among children varies from 51% to 59%.[14,17,24] We used 55% as the lower limit with its wide use and the reference data of Robber-Visser et al[14] being comparable with ours. Our main result remained same even with the CMR-derived LVEF cutoff set at 50%, the same as RT-3DE: CMR recognized most cases with an abnormal LV systolic function followed by RT-3DE and tailed by M-mode. Although RT-3DE has been validated against CMR, they remain dissimilar with varying normal values. The latter has an excellent spatial resolution, but the temporal resolution may cause challenges especially with higher heart rates, whereas the former has a good temporal resolution.

An association between LV dyssynchrony and heart failure has been demonstrated among adults.[8,25] A dyssynchronous contraction leads to a reduced stroke volume with blood moving around the ventricle from segments activated early to those activated late resulting in an impaired systolic function. The RT-3DE−derived dyssynchrony indexes are a novel method to assess the synchronicity of the contraction. The systolic dyssynchrony index (Tmsv16-SD) has established its role in the assessment of the global LV function.[8,26] Yet, stich artifacts caused by body movement or an irregular heart rhythm may result in unanalyzable RT-3DE data, 1 case in our cohort. The mechanical dyssynchrony may act as an indicator of LV dysfunction[4] useful in identifying the risk patients at an early stage. To our knowledge, ours is the first study to report on an association between the combined impacts of anthracycline treatment, cardiac irradiation, and LV dyssynchrony assessed by the RT-3DE. We found higher dyssynchrony indexes in the 12-segment analysis among the irradiation-exposed survivors compared with the controls. When comparing the echocardiographic parameters of those unexposed or exposed to irradiation, the dyssynchrony indexes were the only ones to differentiate the 2 although among asymptomatic survivors, the differences were small. Larger sample sizes and a longer follow-up are needed to confirm the putative association between the high dyssynchrony indexes and cardiac irradiation or to establish suitable cut-off values for those at an increased risk for LV dysfunction. We found a negative correlation between the LVEF and dyssynchrony indexes among our patients, in accordance with studies previously published.[4,8,25] The assessment of synchrony should be considered when evaluating the global LV systolic function of the cancer survivors.

The late complications of cardiac irradiation include premature coronary artery disease, valvular damage, pericarditis, arrhythmias, conduction disturbances, heart failure, and restrictive cardiomyopathy.[1,27] The guidelines of the Children's Oncology Group define the group with a highest risk to include those with a radiation dose $\geq$40 Gy without or $\geq$30 Gy with exposure to anthracyclines. Yet, even an average irradiation dose exceeding 5 Gy has shown to pose an increased risk.[28] The combined effects of irradiation and anthracycline therapy have presented as key risk factors for late morbidity, even mortality, among childhood cancer survivors with 1 in 8 developing a severe heart disease by 30 years after treatment.[29] Myocardial fibrosis has been detected among those with a radiation-induced heart disease,[30] possibly contributing to the mechanical dyssynchrony detectable by the RT-3DE. In the CMR, none of our 58 survivors had late gadolinium enhancement as a sign of focal fibrosis[13] and only mildly increased dyssynchrony by the RT-3DE. Yet, the presence of diffuse fibrosis could not be ruled out with the CMR method employed.[31] The reduced LV end-diastolic dimensions and mass with a reduced wall thickness can be found among survivors with mediastinal irradiation.[27] Even among our 8 cases exposed to irradiation and anthracyclines, we could demonstrate a lower LV mass/volume ratio in M-mode and a lower stroke volume with the RT-3DE.

In our study, a correlation between the echocardiographic parameters and established risk factors for anthracycline cardiomyopathy could not be documented. This may be due to a small sample size, genetic heterogeneity, or young age. Yet, with their cardiovascular morbidity and mortality increasing with age, the minor echocardiographic abnormalities among asymptomatic children and adolescents with a history of cancer therapy deserve attention and follow-up as well as health counseling. RT-3DE seems to find more cardiotoxicity than M-mode and is more widely employable with a shorter imaging time and higher temporal resolution than CMR, the reference method.

Acknowledgment: The contributions of Tuija Wigren, MD, in the calculation of the cardiac radiation doses and that of Satu Ranta, RN, for practical assistance during the project are gratefully acknowledged.

Disclosures

The authors have no conflicts of interest to disclose.

1. Chen MH, Colan SD, Diller L. Cardiovascular disease: cause of morbidity and mortality in adult survivors of childhood cancers. *Circ Res* 2011;108:619−628.
2. Shankar SM, Marina N, Hudson MM, Hodgson DC, Adams MJ, Landier W, Bhatia S, Meeske K, Chen MH, Kinahan KE, Steinberger J, Rosenthal D, Cardiovascular Disease Task Force of the Children's Oncology, Group. Monitoring for cardiovascular disease in survivors of childhood cancer: report from the Cardiovascular Disease Task Force of the Children's Oncology Group. *Pediatrics* 2008;121:e387−e396.
3. Poutanen T, Tikanoja T, Riikonen P, Silvast A, Perkkio M. Long-term prospective follow-up study of cardiac function after cardiotoxic therapy for malignancy in children. *J Clin Oncol* 2003;21:2349−2356.
4. Cheung YF, Hong WJ, Chan GC, Wong SJ, Ha SY. Left ventricular myocardial deformation and mechanical dyssynchrony in children with normal ventricular shortening fraction after anthracycline therapy. *Heart* 2010;96:1137−1141.
5. Armstrong GT, Plana JC, Zhang N, Srivastava D, Green DM, Ness KK, Daniel Donovan F, Metzger ML, Arevalo A, Durand JB, Joshi V, Hudson MM, Robison LL, Flamm SD. Screening adult survivors of childhood cancer for cardiomyopathy: comparison of echocardiography

and cardiac magnetic resonance imaging. *J Clin Oncol* 2012;30:2876−2884.
6. Poutanen T, Jokinen E, Sairanen H, Tikanoja T. Left atrial and left ventricular function in healthy children and young adults assessed by three dimensional echocardiography. *Heart* 2003;89:544−549.
7. Pouleur AC, le Polain de Waroux JB, Pasquet A, Gerber BL, Gerard O, Allain P, Vanoverschelde JL. Assessment of left ventricular mass and volumes by three-dimensional echocardiography in patients with or without wall motion abnormalities: comparison against cine magnetic resonance imaging. *Heart* 2008;94:1050−1057.
8. Kapetanakis S, Kearney MT, Siva A, Gall N, Cooklin M, Monaghan MJ. Real-time three-dimensional echocardiography: a novel technique to quantify global left ventricular mechanical dyssynchrony. *Circulation* 2005;112:992−1000.
9. Lang RM, Bierig M, Devereux RB, Flachskampf FA, Foster E, Pellikka PA, Picard MH, Roman MJ, Seward J, Shanewise JS, Solomon SD, Spencer KT, Sutton MS, Stewart WJ, Chamber Quantification Writing G, American Society of Echocardiography's Guidelines and Standards, Committee, European Association of E. Recommendations for chamber quantification: a report from the American Society of Echocardiography's Guidelines and Standards Committee and the Chamber Quantification Writing Group, developed in conjunction with the European Association of Echocardiography, a branch of the European Society of Cardiology. *J Am Soc Echocardiogr* 2005;18:1440−1463.
10. Devereux RB, Alonso DR, Lutas EM, Gottlieb GJ, Campo E, Sachs I, Reichek N. Echocardiographic assessment of left ventricular hypertrophy: comparison to necropsy findings. *Am J Cardiol* 1986;57:450−458.
11. Teichholz LE, Kreulen T, Herman MV, Gorlin R. Problems in echocardiographic volume determinations: echocardiographic-angiographic correlations in the presence of absence of asynergy. *Am J Cardiol* 1976;37:7−11.
12. Cerqueira MD, Weissman NJ, Dilsizian V, Jacobs AK, Kaul S, Laskey WK, Pennell DJ, Rumberger JA, Ryan T, Verani MS, American Heart Association Writing Group on Myocardial Segmentation and Registration for Cardiac, Imaging. Standardized myocardial segmentation and nomenclature for tomographic imaging of the heart: a statement for healthcare professionals from the Cardiac Imaging Committee of the Council on Clinical Cardiology of the American Heart Association. *Circulation* 2002;105:539−542.
13. Ylänen K, Poutanen T, Savikurki-Heikkilä P, Rinta-Kiikka I, Eerola A, Vettenranta K. Cardiac magnetic resonance imaging in the evaluation of the late effects of anthracyclines among long-term survivors of childhood cancer. *J Am Coll Cardiol* 2013;61:1539−1547.
14. Robbers-Visser D, Boersma E, Helbing WA. Normal biventricular function, volumes, and mass in children aged 8 to 17 years. *J Magn Reson Imaging* 2009;29:552−559.
15. Bland JM, Altman DG. Statistical methods for assessing agreement between two methods of clinical measurement. *Lancet* 1986;1:307−310.
16. Ten Harkel AD, Van Osch-Gevers M, Helbing WA. Real-time transthoracic three dimensional echocardiography: normal reference data for left ventricular dyssynchrony in adolescents. *J Am Soc Echocardiogr* 2009;22:933−938.
17. Buechel EV, Kaiser T, Jackson C, Schmitz A, Kellenberger CJ. Normal right- and left ventricular volumes and myocardial mass in children measured by steady state free precession cardiovascular magnetic resonance. *J Cardiovasc Magn Reson* 2009;11:19.
18. Cheung YF, Li SN, Chan GC, Wong SJ, Ha SY. Left ventricular twisting and untwisting motion in childhood cancer survivors. *Echocardiography* 2011;28:738−745.
19. Poutanen T, Ikonen A, Jokinen E, Vainio P, Tikanoja T. Transthoracic three-dimensional echocardiography is as good as magnetic resonance imaging in measuring dynamic changes in left ventricular volume during the heart cycle in children. *Eur J Echocardiogr* 2001;2:31−39.
20. Friedberg MK, Su X, Tworetzky W, Soriano BD, Powell AJ, Marx GR. Validation of 3D echocardiographic assessment of left ventricular volumes, mass, and ejection fraction in neonates and infants with congenital heart disease: a comparison study with cardiac MRI. *Circ Cardiovasc Imaging* 2010;3:735−742.
21. Dorosz JL, Lezotte DC, Weitzenkamp DA, Allen LA, Salcedo EE. Performance of 3-dimensional echocardiography in measuring left ventricular volumes and ejection fraction: a systematic review and meta-analysis. *J Am Coll Cardiol* 2012;59:1799−1808.
22. Thavendiranathan P, Grant AD, Negishi T, Plana JC, Popovic ZB, Marwick TH. Reproducibility of echocardiographic techniques for sequential assessment of left ventricular ejection fraction and volumes: application to patients undergoing cancer chemotherapy. *J Am Coll Cardiol* 2013;61:77−84.
23. Mor-Avi V, Jenkins C, Kuhl HP, Nesser HJ, Marwick T, Franke A, Ebner C, Freed BH, Steringer-Mascherbauer R, Pollard H, Weinert L, Niel J, Sugeng L, Lang RM. Real-time 3-dimensional echocardiographic quantification of left ventricular volumes: multicenter study for validation with magnetic resonance imaging and investigation of sources of error. *JACC Cardiovasc Imaging* 2008;1:413−423.
24. Sarikouch S, Peters B, Gutberlet M, Leismann B, Kelter-Kloepping A, Koerperich H, Kuehne T, Beerbaum P. Sex-specific pediatric percentiles for ventricular size and mass as reference values for cardiac MRI: assessment by steady-state free-precession and phase-contrast MRI flow. *Circ Cardiovasc Imaging* 2010;3:65−76.
25. Liodakis E, Sharef OA, Dawson D, Nihoyannopoulos P. The use of real-time three-dimensional echocardiography for assessing mechanical synchronicity. *Heart* 2009;95:1865−1871.
26. Wang H, Shuraih M, Ahmad M. Real time three-dimensional echocardiography in assessment of left ventricular dyssynchrony and cardiac resynchronization therapy. *Echocardiography* 2012;29:192−199.
27. Adams MJ, Lipsitz SR, Colan SD, Tarbell NJ, Treves ST, Diller L, Greenbaum N, Mauch P, Lipshultz SE. Cardiovascular status in long-term survivors of Hodgkin's disease treated with chest radiotherapy. *J Clin Oncol* 2004;22:3139−3148.
28. Pein F, Sakiroglu O, Dahan M, Lebidois J, Merlet P, Shamsaldin A, Villain E, de Vathaire F, Sidi D, Hartmann O. Cardiac abnormalities 15 years and more after adriamycin therapy in 229 childhood survivors of a solid tumour at the Institut Gustave Roussy. *Br J Cancer* 2004;91:37−44.
29. van der Pal HJ, van Dalen EC, van Delden E, van Dijk IW, Kok WE, Geskus RB, Sieswerda E, Oldenburger F, Koning CC, van Leeuwen FE, Caron HN, Kremer LC. High risk of symptomatic cardiac events in childhood cancer survivors. *J Clin Oncol* 2012;30:1429−1437.
30. Veinot JP, Edwards WD. Pathology of radiation-induced heart disease: a surgical and autopsy study of 27 cases. *Hum Pathol* 1996;27:766−773.
31. Flett AS, Hayward MP, Ashworth MT, Hansen MS, Taylor AM, Elliott PM, McGregor C, Moon JC. Equilibrium contrast cardiovascular magnetic resonance for the measurement of diffuse myocardial fibrosis: preliminary validation in humans. *Circulation* 2010;122:138−144.

ACTA PÆDIATRICA
NURTURING THE CHILD

Acta Pædiatrica ISSN 0803-5253

REGULAR ARTICLE

Cardiac biomarkers indicate a need for sensitive cardiac imaging among long-term childhood cancer survivors exposed to anthracyclines

Kaisa Ylänen (kaisa@ylanen.fi)[1,2], Tuija Poutanen[1,2], Tanja Savukoski[3], Anneli Eerola[1], Kim Vettenranta[4,5]

1.Department of Paediatrics, Tampere University Hospital, Tampere, Finland
2.University of Tampere, Tampere, Finland
3.Department of Biotechnology, University of Turku, Turku, Finland
4.Hospital for Children and Adolescents, Helsinki, Finland
5.University of Helsinki, Helsinki, Finland

Keywords
Autoantibodies to cardiac troponin, Cardiac function, Malignancy, Natriuretic peptide, Troponin

Correspondence
Kaisa Ylänen, MD, Department of Paediatrics, Tampere University Hospital, PO Box 2000, Tampere FI-33521, Finland.
Tel: +358 3 31164058|
Fax: +358 3 31165511|
Email: kaisa@ylanen.fi

Received
25 September 2014; revised 26 October 2014; accepted 10 November 2014.

DOI:10.1111/apa.12862

ABSTRACT

Aim: The role that plasma N-terminal pro-brain natriuretic peptide (NT-proBNP) and cardiac troponins T (cTnT) and I (cTnI) play in supplementing imaging to screen for cardiac late effects remains controversial and the impact of high-sensitivity cTnT and troponin-specific autoantibodies (cTnAAbs) remains unexplored. We studied the role of cardiac biomarkers as indicators of the late effects of anthracyclines among childhood cancer survivors.

Methods: We measured NT-proBNP, cTnT, high-sensitivity cTnT, cTnI and cTnAAbs in 76 childhood cancer survivors at a median of 9 years after primary diagnosis. The survivors underwent conventional and real-time three-dimensional echocardiography and 62 underwent cardiac magnetic resonance imaging (MRI).

Results: Of the survivors, four (5.3%) without risk factors for cardiotoxicity were cTnAAb-positive with an impaired cardiac function in MRI. Another four (5.3%) had an abnormal NT-proBNP level associated with an abnormal cardiac function and risk factors for cardiotoxicity. None showed measurable cardiac troponins, determined by the three different methods, with even the high-sensitivity cTnT-levels remaining normal.

Conclusion: Elevated plasma NT-proBNP or cTnAAbs indicated that childhood cancer survivors benefitted from being evaluated with modern imaging, despite normal function in conventional echocardiography. However, troponins did not seem to provide additional information on the late cardiotoxicity of anthracyclines.

INTRODUCTION

The number of anthracycline-exposed childhood cancer survivors with potentially significant cardiac side effects is increasing. The use of biomarkers has been explored for the screening of anthracycline-induced cardiotoxicity, mainly during chemotherapy, and to a lesser extent in the late follow-up of the survivors. Among adult cancer patients, increased plasma N-terminal pro-brain natriuretic peptide (NT-proBNP) (1) and increased cardiac troponin I (cTnI) (2) during and soon after the completion of chemotherapy have been associated with late cardiac events. Yet, the use of the biomarkers in the screening of the late cardiac effects of anthracyclines among childhood cancer survivors remains investigational.

Novel, high-sensitivity methods in the analysis of cardiac troponin T (cTnT) in plasma enable the detection of even subclinical myocardial damage (3,4). Published studies on cardiac troponin among childhood cancer survivors have

Abbreviations
cTnAAbs, Troponin-specific autoantibodies; cTnI, Cardiac troponin I; cTnT, Cardiac troponin T; MRI, Magnetic resonance imaging; NT-proBNP, N-terminal pro-brain natriuretic peptide; RT3DE, Real-time three-dimensional echocardiography; SD, Standard deviation.

Key notes
- This study explored the role of cardiac biomarkers as indicators of the late effects of anthracyclines among childhood cancer survivors.
- We found that elevated plasma N-terminal pro-brain natriuretic peptide or troponin-specific autoantibodies indicated that childhood cancer survivors benefitted from being evaluated with modern imaging, despite normal function in conventional echocardiography.
- However, troponins measured in the follow-up did not seem to provide additional information on the late cardiotoxicity of anthracyclines.

used the troponin methods of the previous generation. Factors resulting in the release of cardiac troponin may also trigger the formation of autoantibodies to cardiac troponin (cTnAAbs). With these possibly resulting in false-negative results in the evaluation of the troponin levels, a focused assay for cTnI and minimally susceptible to the presence of cTnAAbs has been designed (5). The combined use of these modern assays maximises the chance to detect even minute amounts of troponins. The prevalence of cTnAAbs among anthracycline-exposed cancer survivors has not been previously reported on.

NT-proBNP is an inactive fragment of brain natriuretic peptide secreted by the cardiac ventricles in response to cardiomyocyte stretch. Elevated levels are being detected in many cardiac diseases.

In this study, NT-proBNP, cTnI, cTnT and high-sensitivity cTnT, as well as cTnAAbs, were assessed and related to the cardiac function among anthracycline-exposed, long-term survivors of childhood cancer in a prospective, cross-sectional setting. The focus of this study was on late cardiotoxicity.

PATIENTS AND METHODS

We prospectively enrolled all consecutive long-term survivors of childhood cancer with anthracyclines as part of their primary chemotherapy, who attended the population-based paediatric haematology–oncology service of Tampere University Hospital in Finland between February 2010 and June 2011. Survivors with a follow-up time from the end of primary therapy of <5 years, with an active malignancy or congenital heart disease, were excluded. Of the 86 patients initially recruited, 76 agreed to participate and these comprised 42 females and 34 males (Fig. 1). Their total cumulative anthracycline doses were calculated and conversion to doxorubicin isotoxic equivalents performed according to the Children's Oncology Group recommendations (www.survivorshipguidelines.org). The key characteristics of the survivors are presented in Table 1.

This study complied with the Declaration of Helsinki, and the Institutional Review Board of the Tampere University Hospital approved the study. All patients and their

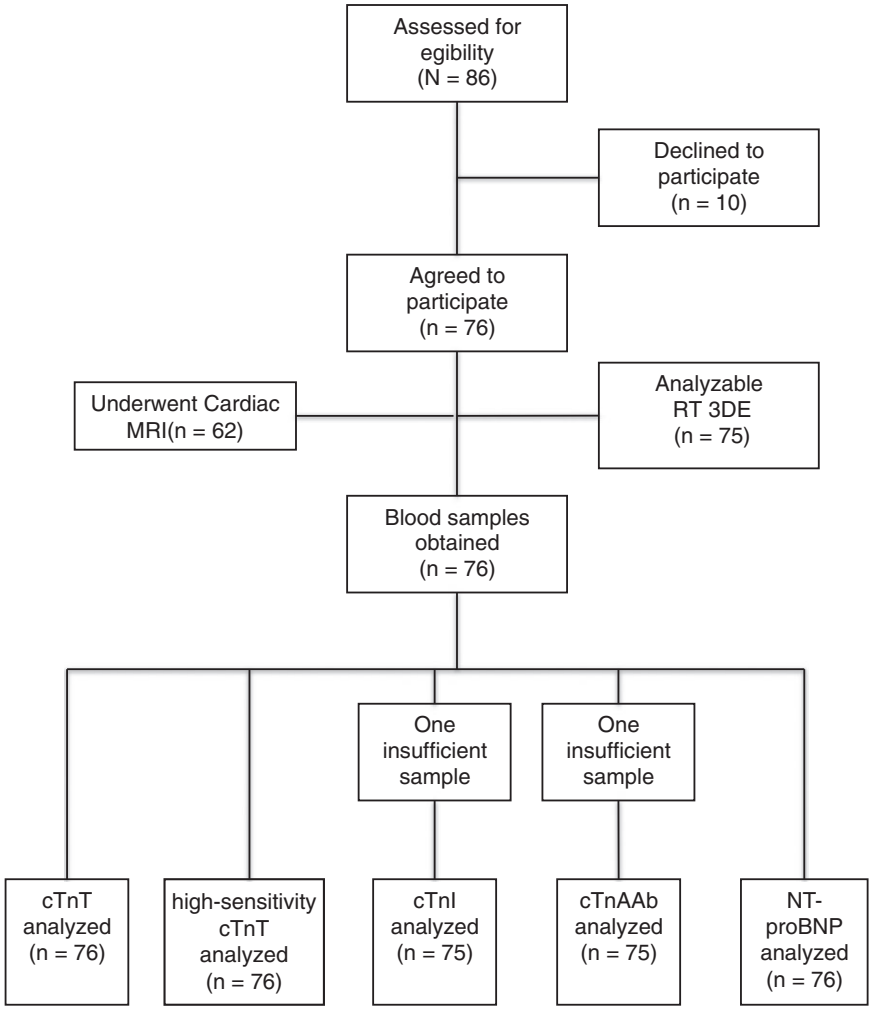

Figure 1 Study recruitment flow chart. The number of study patients with different imaging methods used and cardiac biomarkers obtained. cTnAAb, troponin-specific autoantibodies; cTnI, cardiac troponin I; cTnT, cardiac troponin T; MRI, magnetic resonance imaging; NT-proBNP, N-terminal pro-brain natriuretic peptide; RT3DE, real-time three-dimensional echocardiography.

Table 1 The clinical characteristics of the survivors

Variable	Survivors (n = 76)
Female	42 (55)
Male	34 (45)
Age at study (years)	14.3 ± 3.1 (7.2–20.0)
Age at primary diagnosis (years)	3.8 (0.0–13.8)
Time from primary diagnosis (years)	9.0 (5.4–18.4)
Time from end of primary therapy (years)	7.1 (5.0–18.0)
Cumulative anthracycline dose (mg/m^2)	224 (80–454)
Height (cm)	159.7 ± 15.6
Weight (kg)	54.6 ± 16.9
Body surface area (m^2)	1.55 ± 0.31
Leukaemia	42 (55)
Solid tumour	34 (45)
Relapse	6 (8)
Allogeneic stem cell transplantation	7 (9)
Cardiac irradiation	10 (13)

Values are n (%), mean ± SD or median (range).

legal guardian(s) gave their written, informed consent. The blood samples were taken and imaging performed at the time of enrolment.

Plasma NT-proBNP was determined using an electrochemiluminescence immunoassay method with a Cobas 6000 immunoanalyzer, an e601 module (Roche Diagnostics, Mannheim, Germany) and the proBNP II kit (Roche Diagnostics, Mannheim, Germany) with a detection limit of 5 pg/mL. Reference values for adults under 45 years of age were <63 pg/mL for males and <116 pg/mL for females. Age-related reference values were used for those younger than 19 years of age and those <160 pg/mL between the ages of six and 18 were considered normal (6).

cTnT measurements were performed with two different electrochemiluminescence immunoassay methods. The fourth-generation assay was performed with a Cobas 6000 immunoanalyzer, an e601 module (Roche Diagnostics, Mannheim, Germany) and the Elecsys Troponin T Cardiac T kit (Roche Diagnostics, Mannheim, Germany) with a detection limit of 0.01 μg/L and upper normal limit of 0.03 μg/L. The fifth-generation high-sensitivity cTnT assay was performed with an Elecsys 2010 immunoanalyzer (Roche Diagnostics, Mannheim, Germany) using the Elecsys Troponin T hs kit (Roche Diagnostics, Mannheim, Germany) with a detection limit of 5 ng/L and upper normal limit of 14 ng/L. Our laboratory reported normal high-sensitivity cTnT values as below 14 ng/L.

Concentrations of cTnI were measured with an Innotrac Aio!TM immunoanalyzer (Radiometer/Innotrac Diagnostics, Turku, Finland) using the Radiometer TnI Test (detection limit 0.0095 μg/L) minimally susceptible to the interference by cTnI-specific cTnAAbs (7) a problem in many commercial assays (8). The results were calculated using the MultiCalc Software (Perkin-Elmer/Wallac, Turku, Finland).

The measurement of human cTnAAbs was performed as previously described (5). Autoantibody positivity was defined as 100 counts or higher after a background correction (no troponin complex added) ($p < 0.05$, *t*-test).

Conventional and real-time three-dimensional echocardiography (RT3DE) was performed on the 76 survivors (9), but one RT3DE study failed due to a poor acoustic window. Of the 76 survivors, 62 agreed to undergo cardiac magnetic resonance imaging (MRI) as previously described (10). Fractional shortening values ≥28.0%, left ventricular ejection fraction ≥50.0% as assessed by RT3DE (11) and ≥55.0% by cardiac MRI (12) were considered normal. A detailed analysis on the imaging parameters has been previously reported by us (9,10) leaving this article to focus on the cardiac biomarkers.

We defined anthracycline-induced cardiotoxicity as one including fractional shortening <28.0%, left ventricular ejection fraction <50.0% by RT3DE or <55.0% by MRI, or MRI-derived left ventricular end-diastolic or end-systolic volumes exceeding 2 SD (12).

The statistical analysis was performed using the IBM® SPSS® Statistics (version 21) software (IBM Corp., Armonk, New York, USA). The data are presented as frequencies and percentages, and 95% confidence intervals for categorical data, and the mean and SD or median and range in case of continuous variables.

RESULTS

The complete survivor group

None of survivors had renal insufficiency or other established cause for increased NT-proBNP. However, four [5.3%, (2.1–12.8)] were on medication for late anthracycline-induced cardiomyopathy diagnosed more than 1 year after cancer diagnosis.

The echocardiographic and MRI data of the survivors are presented in Table 2. Of the survivors, 2/76 [2.6%, (0.7–9.1)] had an abnormal fractional shortening, but their NT-proBNP levels were normal and cTnAAbs negative. An abnormal left ventricular ejection fraction by RT3DE was detected in 10/75 [13.3%, (7.4–22.8)] with all being cTnAAb-negative and 2/10 [20.0%, (5.7–51.0)] having an abnormal NT-proBNP level. Of the 62 imaged with cardiac MRI, 49 [79.0%, (67.4–87.3)] had an abnormal left ventricular ejection fraction with 4/49 [8.2% (3.2–19.2)] also having an abnormal NT-proBNP and 3/49 [6.1%, (2.1–16.5)] being cTnAAb-positive.

Abnormal NT-proBNP

Of the 76 survivors, four [5.3%, (2.1–12.8)] had an abnormal plasma NT-proBNP (Table 3). None of them had a previously diagnosed anthracycline-induced cardiomyopathy. All had a normal fractional shortening. None had cardiac symptoms or an impaired subjective exercise tolerance. Yet, 2/4 had an abnormal left ventricular ejection fraction by RT3DE and all by MRI.

Cardiac troponins

All cTnT-levels were below 0.03 μg/L and those of high-sensitivity cTnT below 14 ng/L. The cTnI analysis was performed on 75/76 (one insufficient sample) and all had it unmeasurable (below 0.01 μg/L). Yet, 51/76 [67.1%, (55.9–

Table 2 Echocardiographic and cardiac magnetic resonance imaging parameters

Variable	Median (range)	Number of patients with abnormal values
M-mode (n = 76)		
FS (%)	32.7 (24.8–42.2)	2/76
RT 3DE (n = 75)		
LV EF (%)	56.4 (40.2–68.1)	10/75
Cardiac MRI (n = 62)		
LV EDV (mL/m^2)	86.8 (58.7–131.3)	18/34
LV ESV (mL/m^2)	43.5 (28.9–71.9)	56/62
LV EF (%)	50.1 (33.7–61.8)	49/62

EDV, End-diastolic volume; EF, Ejection fraction; ESV, End-systolic volume; FS, Fractional shortening; LV, Left ventricular; MRI, magnetic resonance imaging; RT 3DE, Real-time three-dimensional echocardiography.

76.6)] had an abnormal left ventricular ejection fraction by either RT3DE or MRI. Of the troponin-negative survivors, 8/76 [10.5%, (5.4–19.4)] had an abnormal left ventricular ejection fraction with both imaging methods (RT3DE and MRI).

Autoantibodies to cardiac troponin

cTnAAbs were detected in 4/75 [5.3%, (2.1–12.9)] (one insufficient sample) (Table 4). All were cTnT-, high-sensitivity cTnT- and cTnI-negative and had normal NT-proBNP levels. The cTnAAb-positive survivors had a normal fractional shortening and left ventricular ejection fraction by RT3DE. Yet, all three cTnAAb-positive survivors with MRI showed an abnormal left ventricular ejection fraction, with two having increased left ventricular end-diastolic and three of three having increased end-systolic volumes. All with cTnAAbs experienced a normal exercise tolerance.

Previously diagnosed anthracycline-induced cardiomyopathy

In Table 5, we summarise our data on patients with a previously diagnosed late-onset anthracycline-induced cardiomyopathy, all on enalapril and one also on carvedilol. The cumulative anthracycline dose was >300 mg/m^2 in three and the fourth had a primary diagnosis below 1 year of age. At the time of study, two of the four had an abnormal fractional shortening and three of the four had an abnormal left ventricular ejection fraction by RT3DE and three of three by MRI. An abnormal NT-proBNP level had previously been detected in three, all after the diagnosis of cardiomyopathy. Yet, at the time of study, all had their NT-proBNP within the normal range and were cTnAAb-negative.

DISCUSSION

Late, elevated NT-proBNP levels were shown to be linked to abnormalities detectable in the cardiac imaging. The presence of cTnAAbs could be established among anthracycline-exposed childhood cancer survivors being seemingly associated with enlarged left ventricular volumes in cardiac MRI. Ours is the first group to report on the simultaneous use of three state-of-the-art methods for the cardiac troponins in the screening of late, anthracycline-induced cardiotoxicity among the survivors of paediatric cancer.

All of our four patients with an elevated NT-proBNP had at least one known risk factor for anthracycline-induced cardiomyopathy: exposure below 1 year of age, cardiac irradiation or female gender. Despite a normal fractional shortening in echocardiography, the more detailed imaging methods (RT3DE, MRI) revealed abnormalities in all four with an enlargement of the left ventricular end-systolic volumes in MRI as an early sign.

Studies later during the follow-up have documented an association between an elevated NT-proBNP and echocardiographic left ventricular abnormalities (13,14), whereas another (15) documented abnormal NT-proBNP in 13% of the subjects in the absence of left ventricular dysfunction. In our data, the prevalence of abnormal NT-proBNP levels

Table 3 Characteristics of the patients with an abnormal NT-proBNP (all with normal troponins and cTnAAb-negative)

Variable	Pt 1	Pt 2	Pt 3	Pt 4
Gender	Male	Male	Female	Female
Age (years)	8.1	12.0	17.1	17.2
Age at diagnosis (years)	0.0	6.1	9.5	11.3
Diagnosis	Neuroblastoma	AML	AML	Osteosarcoma
Cumulative anthracycline dose (mg/m^2)	108	416	265	301
Cardiac irradiation	No	Yes	No	No
Allogeneic SCT	No	Yes	No	No
NT-proBNP (pg/mL)	328*	200*	190*	265*
FS (%)	30.5	33.1	31.4	29.8
RT 3DE LV EF (%)	43.8*	58.3	56.7	48.2*
Cardiac MRI LV EF (%)	44.0*	48.8*	44.4*	51.0*
Cardiac MRI LV EDV >2 SD	No	No	No	No
Cardiac MRI LV ESV >2 SD	Yes	Yes	Yes	No

AML, Acute myeloid leukaemia; cTnAAb, Troponin-specific autoantibodies; NT-proBNP, N-terminal pro-brain natriuretic peptide; SCT, Stem cell transplantation; SD, Standard deviation; other abbreviations as in Table 2.
*Abnormal value.

Table 4 Characteristics of the patients with autoantibodies to cardiac troponin (all with normal troponins and NT-proBNP)

Variable	Pt 5	Pt 6	Pt 7	Pt 8
Gender	Female	Female	Male	Male
Age (years)	11.0	13.7	14.2	16.2
Age at diagnosis (years)	3.4	5.1	3.7	5.7
Diagnosis	ALL	ALL	ALL	ALL
Cumulative anthracycline dose (mg/m^2)	180	151	123	120
Cardiac irradiation	No	No	No	No
Allogeneic SCT	No	No	No	No
cTnAAb (specific counts)	1996*	209*	41287*	8110*
FS (%)	35.5	32.3	30.2	29.0
RT 3DE LV EF (%)	67.2	53.3	54.7	50.4
Cardiac MRI LV EF (%)	47.5*	NA	40.2*	42.6*
Cardiac MRI LV EDV >2 SD	Yes	NA	Yes	No
Cardiac MRI LV ESV >2 SD	Yes	NA	Yes	Yes

ALL, Acute lymphoblastic leukaemia; NA, Not available; other abbreviations as shown in Tables 2 and 3.
*Abnormal value.

Table 5 Characteristics of the patients with an anthracycline-induced cardiomyopathy (all with normal troponins and cTnAAb-negative)

Variable	Pt 9	Pt 10	Pt 11	Pt 12
Gender	Female	Female	Female	Female
Age (years)	7.9	14.1	15.0	18.3
Age at malignancy diagnosis (years)	0.7	1.8	3.4	3.8
Diagnosis	Neuroblastoma	ALL	ALL	Infantile fibrosarcoma
Cum. anthracycline dose (mg/m^2)	113	339	360	355
Cardiac irradiation	No	Yes	No	No
Allogeneic SCT	No	Yes	No	No
Time from diagnosis to cardiomyopathy (years)	3.9	11.1	8.4	1.2
Lowest FS (%)	26*	27*	21*	21*
Peak NT-proBNP (pg/mL)	53	190*	253*	233*
NT-proBNP at study (pg/mL)	49	133	80	65
FS (%)	33.4	28.3	25.5*	24.8*
RT 3DE LV EF (%)	51.0	40.6*	40.2*	45.5*
Cardiac MRI LV EF (%)	51.3*	NA	46.4*	49.4*
Cardiac MRI LV EDV >2 SD	No	NA	No	Yes
Cardiac MRI LV ESV >2 SD	Yes	NA	Yes	Yes

Abbreviations as in Tables 2–4.
*Abnormal value.

lied at 5.3% with all having an abnormal left ventricular ejection fraction in MRI.

With the abnormal levels being linked to an abnormal left ventricular ejection fraction by MRI and those with a previously diagnosed anthracycline-induced cardiomyopathy having a history of abnormal levels, we postulate an elevated NT-proBNP to indicate left ventricular pathology among long-term childhood cancer survivors. In particular, those with elevated levels and defined risk factors in our study appeared in the need of close follow-up with modern imaging. Yet, normal NT-proBNP levels did not exclude cardiotoxicity and thus cannot be used as the sole screening method.

Among paediatric cancer patients, an elevated cTnT during treatment has predicted later echocardiographic left ventricular abnormalities (16,17). Other studies have shown a low-level elevation in a few patients without a correlation between the cTnT level and left ventricular function (15,18). Of our patients, 67% had an abnormal cardiac function by RT3DE and, or, MRI despite normal cardiac troponin with the sensitive methods.

Our cut-off value for the high-sensitivity cTnT (<14 ng/L) was the adult 99th percentile (19). Gender-specific reference values for the paediatric age group remain unavailable. Cheung et al. (4) recently reported on elevated high-sensitivity cTnT in 19% of the adult survivors associating with an impaired left ventricular function. Despite the fact that they used gender-specific reference values, all their survivors had levels below 14 ng/L, like the patients in our study.

The use of several cTnI assay methods with different cut-off values and lack of standardisation make comparison between studies difficult. Few studies have reported on paediatric patients during malignancy treatment (20,21) and only one during later follow-up (13). One reported that

cTnI was not useful in the detection of an early stage anthracycline-associated cardiotoxicity (20). El-Shitany et al. (21) showed an elevation during treatment to be associated with an impaired systolic function and pretreatment with carvedilol seemingly protective. The single study during later follow-up failed to show an increase in cTnI, but documented a 13% rate of cardiac dysfunction (13).

Late-onset cardiotoxicity appears to develop no earlier than 1 year after anthracycline treatment, but in many cases, it can occur later. Yet, the triggering event appears to occur during treatment. This is in accordance with an elevated cardiac troponin during rather than years after anthracycline therapy (2,16). The suggested mechanisms of the troponin release in heart failure, in addition to coronary ischaemia, include a cellular supply and demand imbalance of oxygen, injury due to oxidative stress and neurohumoral factors, myocardial apoptosis and proteolysis of contractile proteins (22) possibly also contributing to cardiac troponin leakage later during follow-up.

We could not demonstrate delayed troponin leakage among our 76 late survivors. As later follow-up on cTnT, high-sensitivity cTnT or cTnI failed to give additional information on cardiotoxicity over imaging, additional data are clearly needed on high-sensitivity cTnT during cardiotoxic treatment, its association with cardiac dysfunction and impact on long-term prognosis.

The mechanisms behind the generation of cTnAAbs and their clinical impact are not fully understood (23). An autoimmune reaction can be triggered by any release of cardiac troponin such as myocardial infarction or cardiotoxic treatments. Yet, exposure does not always lead to the formation of cTnAAbs suggestive of polymorphic responses (24). cTnAAbs have been detected in the serum of individuals with cardiac disease (25) and to a lesser extent among healthy adults (26). Ours is the first study to report on cTnAAbs among anthracycline-exposed cancer survivors. The number of antibody positive patients exceeded the previously reported prevalence of cTnAAb-positivity among children with congenital heart defects (0.7%) or healthy children (0%) (27).

The ability of circulating cTnAAbs to cause false-negative troponin results has been acknowledged (8) using a variety of techniques with some detecting anti-cTnI and others anti-cTnT autoantibodies (28,29).

Several studies have documented cTnAAbs among patients with dilating cardiomyopathy (28,29), while their role in the pathogenesis of heart disease and prognostic impact remains controversial. Some suggest an active role for the cTnAAbs in the process (30). Even though oxidative stress is the most plausible mechanism behind anthracycline-induced cardiotoxicity, other putative mechanisms do exist. Our four cTnAAb-positive survivors had no other risk factors for anthracycline-induced cardiomyopathy, except for female gender in two. Interestingly, the three with cardiac MRI had an abnormal left ventricular ejection fraction and increase in either left ventricular end-diastolic or end-systolic volumes or both. Further follow-up is required on the possible development of a symptomatic cardiomyopathy and prognostic impact of the cTnAAbs.

Study limitations

Our ethical permission did not allow for plasma analyses on the healthy controls and published values were employed (6,19,27). Due to the limited number of patients, we were not able to compare the imaging parameters between those with normal and abnormal biomarker levels.

CONCLUSION

Among survivors of childhood cancer screened with conventional echocardiography, an elevated plasma NT-proBNP appeared to indicate the need for more sensitive cardiac imaging with RT3DE or MRI. Furthermore, our data suggest that cTnAAbs play a role in the pathogenesis of anthracycline-induced cardiomyopathy. Despite this, and regardless of the analytical method used, our data clearly indicate cardiac troponins measured years after cancer chemotherapy do not appear to provide key additional information on the late cardiotoxicity of anthracyclines.

ACKNOWLEDGEMENT

We would like to thank Satu Ranta, RN, for practical assistance during the project.

CONFLICT OF INTEREST

None declared.

FUNDING

This study was supported by the following Finnish Foundations: the Blood Disease Research Foundation, the Competitive Research Funding of the Tampere University Hospital [9L114 and 9N084], the Emil Aaltonen Foundation, the Finnish Association of Haematology, the EVO funds of the Tampere University Hospital, the Finnish Cancer Foundation, the Finnish Cultural Foundation, the Finnish Cultural Foundation Pirkanmaa Regional Fund, the Foundation for Paediatric Research, the National Graduate School of Clinical Investigation, the Päivikki and Sakari Sohlberg Foundation, the Scientific Foundation of the City of Tampere and the Väre Foundation for Paediatric Cancer.

References

1. Sandri MT, Salvatici M, Cardinale D, Zorzino L, Passerini R, Lentati P, et al. N-terminal pro-B-type natriuretic peptide after high-dose chemotherapy: a marker predictive of cardiac dysfunction? *Clin Chem* 2005; 51: 1405–10.
2. Cardinale D, Sandri MT, Colombo A, Colombo N, Boeri M, Lamantia G, et al. Prognostic value of troponin I in cardiac risk stratification of cancer patients undergoing high-dose chemotherapy. *Circulation* 2004; 109: 2749–54.
3. Twerenbold R, Jaffe A, Reichlin T, Reiter M, Mueller C. High-sensitive troponin T measurements: what do we gain and what are the challenges? *Eur Heart J* 2012; 33: 579–86.
4. Cheung YF, Yu W, Cheuk DK, Cheng FW, Yang JY, Yau JP, et al. Plasma high sensitivity troponin T levels in adult survivors

of childhood leukaemias: determinants and associations with cardiac function. *PLoS ONE* 2013; 8: e77063.
5. Eriksson S, Halenius H, Pulkki K, Hellman J, Pettersson K. Negative interference in cardiac troponin I immunoassays by circulating troponin autoantibodies. *Clin Chem* 2005; 51: 839–47.
6. Nir A, Lindinger A, Rauh M, Bar-Oz B, Laer S, Schwachtgen L, et al. NT-pro-B-type natriuretic peptide in infants and children: reference values based on combined data from four studies. *Pediatr Cardiol* 2009; 30: 3–8.
7. Eriksson S, Ilva T, Becker C, Lund J, Porela P, Pulkki K, et al. Comparison of cardiac troponin I immunoassays variably affected by circulating autoantibodies. *Clin Chem* 2005; 51: 848–55.
8. Savukoski T, Engstrom E, Engblom J, Ristiniemi N, Wittfooth S, Lindahl B, et al. Troponin-specific autoantibody interference in different cardiac troponin I assay configurations. *Clin Chem* 2012; 58: 1040–8.
9. Ylänen K, Eerola A, Vettenranta K, Poutanen T. Three-dimensional echocardiography and cardiac magnetic resonance imaging in the screening of long-term survivors of childhood cancer after cardiotoxic therapy. *Am J Cardiol* 2014; 113: 1886–92.
10. Ylänen K, Poutanen T, Savikurki-Heikkilä P, Rinta-Kiikka I, Eerola A, Vettenranta K. Cardiac magnetic resonance imaging in the evaluation of the late effects of anthracyclines among long-term survivors of childhood cancer. *J Am Coll Cardiol* 2013; 61: 1539–47.
11. Poutanen T, Jokinen E, Sairanen H, Tikanoja T. Left atrial and left ventricular function in healthy children and young adults assessed by three dimensional echocardiography. *Heart* 2003; 89: 544–9.
12. Robbers-Visser D, Boersma E, Helbing WA. Normal biventricular function, volumes, and mass in children aged 8 to 17 years. *J Magn Reson Imaging* 2009; 29: 552–9.
13. Soker M, Kervancioglu M. Plasma concentrations of NT-pro-BNP and cardiac troponin-I in relation to doxorubicin-induced cardiomyopathy and cardiac function in childhood malignancy. *Saudi Med J* 2005; 26: 1197–202.
14. Lipshultz SE, Landy DC, Lopez-Mitnik G, Lipsitz SR, Hinkle AS, Constine LS, et al. Cardiovascular status of childhood cancer survivors exposed and unexposed to cardiotoxic therapy. *J Clin Oncol* 2012; 30: 1050–7.
15. Mavinkurve-Groothuis AM, Groot-Loonen J, Bellersen L, Pourier MS, Feuth T, Bokkerink JP, et al. Abnormal NT-pro-BNP levels in asymptomatic long-term survivors of childhood cancer treated with anthracyclines. *Pediatr Blood Cancer* 2009; 52: 631–6.
16. Lipshultz SE, Rifai N, Sallan SE, Lipsitz SR, Dalton V, Sacks DB, et al. Predictive value of cardiac troponin T in pediatric patients at risk for myocardial injury. *Circulation* 1997; 96: 2641–8.
17. Lipshultz SE, Scully RE, Lipsitz SR, Sallan SE, Silverman LB, Miller TL, et al. Assessment of dexrazoxane as a cardioprotectant in doxorubicin-treated children with high-risk acute lymphoblastic leukaemia: long-term follow-up of a prospective, randomised, multicentre trial. *Lancet Oncol* 2010; 11: 950–61.
18. Kismet E, Varan A, Ayabakan C, Alehan D, Portakal O, Buyukpamukcu M. Serum troponin T levels and echocardiographic evaluation in children treated with doxorubicin. *Pediatr Blood Cancer* 2004; 42: 220–4.
19. Saenger AK, Beyrau R, Braun S, Cooray R, Dolci A, Freidank H, et al. Multicenter analytical evaluation of a high-sensitivity troponin T assay. *Clin Chim Acta* 2011; 412: 748–54.
20. Oztarhan K, Guler S, Aktas B, Arslan M, Salcioglu Z, Aydogan G. The value of echocardiography versus cardiac troponin I levels in the early detection of anthracycline cardiotoxicity in childhood acute leukemia: prospective evaluation of a 7-year-long clinical follow-up. *Pediatr Hematol Oncol* 2011; 28: 380–94.
21. El-Shitany NA, Tolba OA, El-Shanshory MR, El-Hawary EE. Protective effect of carvedilol on adriamycin-induced left ventricular dysfunction in children with acute lymphoblastic leukemia. *J Card Fail* 2012; 18: 607–13.
22. Januzzi JL Jr, Filippatos G, Nieminen M, Gheorghiade M. Troponin elevation in patients with heart failure: on behalf of the third universal definition of myocardial infarction global task force: heart failure section. *Eur Heart J* 2012; 33: 2265–71.
23. Jahns R. Autoantibodies against cardiac troponin I: friend or foe? *Eur J Heart Fail* 2010; 12: 645–8.
24. Savukoski T, Ilva T, Lund J, Porela P, Ristiniemi N, Wittfooth S, et al. Autoantibody prevalence with an improved immunoassay for detecting cardiac troponin-specific autoantibodies. *Clin Chem Lab Med* 2013; 2: 1–7.
25. Nussinovitch U, Shoenfeld Y. Anti-troponin autoantibodies and the cardiovascular system. *Heart* 2010; 96: 1518–24.
26. Adamczyk M, Brashear RJ, Mattingly PG. Circulating cardiac troponin-I autoantibodies in human plasma and serum. *Ann N Y Acad Sci* 2009; 1173: 67–74.
27. Eerola A, Jokinen E, Savukoski T, Pettersson K, Poutanen T, Pihkala J. Cardiac troponin I in congenital heart defects with pressure or volume overload. *Scand Cardiovasc J* 2013; 47: 154–9.
28. Leuschner F, Li J, Goser S, Reinhardt L, Ottl R, Bride P, et al. Absence of auto-antibodies against cardiac troponin I predicts improvement of left ventricular function after acute myocardial infarction. *Eur Heart J* 2008; 29: 1949–55.
29. Shmilovich H, Danon A, Binah O, Roth A, Chen G, Wexler D, et al. Autoantibodies to cardiac troponin I in patients with idiopathic dilated and ischemic cardiomyopathy. *Int J Cardiol* 2007; 117: 198–203.
30. Okazaki T, Tanaka Y, Nishio R, Mitsuiye T, Mizoguchi A, Wang J, et al. Autoantibodies against cardiac troponin I are responsible for dilated cardiomyopathy in PD-1-deficient mice. *Nat Med* 2003; 9: 1477–83.